GAS-TO-PARTICLE CONVERSION:

SULFUR DIOXIDE IN A PHOTOCHEMICALLY REACTIVE SYSTEM

Thesis by

Paul Thomas Roberts

In Partial Fulfillment of the Requirements

for the Degree of

Doctor of Philosophy

California Institute of Technology

Pasadena, California

1975

(Submitted May 2, 1975)

to Lynn

ACKNOWLEDGEMENTS

In completing this dissertation, I have incurred a great many debts to people in the Caltech community. Foremost, I would like to thank my advisor Sheldon K. Friedlander for his guidance and patience. Professors James J. Morgan and John H. Seinfeld also contributed advice and guidance during the course of this research.

James J. Huntzicker was extremely helpful during all phases of the research and Warren H. White contributed greatly to the data analysis section of this work. Daniel Grosjean, George M. Hidy, and Rudolf B. Husar also provided helpful suggestions.

I thank all of the members of the Friedlander research group - Karl A. Bell, Daniel P. Y. Chang, Cliff Davidson, Greg Gartrell, Jr., Steve L. Heisler, Susanne V. Hering, Pamela S. McMurry, Peter H. McMurry, and Sadie S. Salim - all of whom were consistently interested and made valuable suggestions.

Elton Daley's, Joe Fontana's, and Eric W. Siegel's help in designing and constructing the various experimental apparatus was indispensible in carrying out this work. Bob Shultz did an excellent job in preparing the graphs and drawings for the dissertation. I thank Dwight Landis and Larry McClellan for their technical assistance. Katie Foley's aid, as Keck Reference Librarian, was also greatly appreicated.

For typing this thesis I thank the patient Sharon Hage and the very patient Lynn Roberts. I also appreciated the efforts of the secretaries of the department: Marjorie Connely, Elaine Granger, Helen Baldridge, Carla Willard, and Janet Yeager.

The National Institute of Environmental Health Sciences (grant no. 5 T01 ES 00004-14) and the U. S. Environmental Protection Agency (grant no. K802160-02-0) provided financial assistance during this research.

Finally, none of my work would have been possible without the constant love and encouragement of my wife, Lynn Dumenil Roberts.

ABSTRACT

Particulate phase sulfur compounds are suspected to be major contributors to human health effects and visibility reduction. The formation of such aerosol sulfur compounds in a photochemically reactive system was studied, in both the laboratory and the field.

An aerosol vaporization technique was developed capable of measuring both total filter and cascade impactor aerosol samples for nanogram levels of sulfur compounds. This method measures the total aerosol sulfur species concentration.

Model calculations using measured aerosol and gas phase sulfur concentrations and air trajectory analysis provided estimated conversion rates for sulfur dioxide to aerosol sulfur compounds. For afternoon periods in Los Angeles, the pseudo-first order rate constant for SO_2 oxidation was from 1 to 15% hr^{-1}. The estimated rates were higher at higher levels of photochemical activity. In the atmosphere and in smog chamber studies, this rate is dependent upon the presence of O_3 and olefins, as well as SO_2. In smog chamber experiments with 1-heptene, NO_x, and SO_2, the formation of the aerosol organic and sulfur compounds is consistent with the major aerosol producing step being a reaction between SO_2 and a reactive intermediate of the O_3-1-heptene reaction.

The size distribution of aerosol sulfur species was measured at various locations in the Los Angeles Basin. The sulfur was concentrated in the less than 0.5 μm size range during periods of high photochemical activity and in the 0.25-1.0 μm size range during other daylight hours.

Measurements of the size distribution of aerosol sulfur species were taken during smog chamber experiments with 1-heptene, NO_x, and SO_2 added to unfiltered ambient air, and irradiated with sunlight. A bimodal distribution developed with 2/3 of the sulfur in a mode below 0.1 μm and 1/3 in a mode above 0.2 μm in diameter.

The present and future effects of automobile emissions on aerosol sulfur compounds were estimated. The present contribution of motor vehicles to aerosol sulfur air quality at Pasadena is minimal. The introduction of the catalytic converter on new automobiles is estimated to produce a small increase in aerosol sulfur concentrations at receptor sites; however, the catalytic converter is estimated to produce dramatic increases in aerosol sulfur concentrations near roadways.

TABLE OF CONTENTS

LIST OF TABLES

LIST OF FIGURES

CHAPTER 1

INTRODUCTION

Air pollution is a question of considerable significance because it produces a measurable and detrimental effect upon man, animals, plants, and material. Although nature does introduce some contaminants into the atmosphere, a substantial part of air pollution is associated with anthropogenic emissions of gases, liquids, and solids. It is the interaction of these emissions, coupled with natural sunlight and with the transport and mixing properties of the atmosphere, which produces measurable damage effects. These complex interactions produce new gas phase and particulate phase substances (secondary pollutants) which add to the originally emitted and naturally occurring substances (primary pollutants). It has been determined that secondary materials produce major receptor damage in areas such as the Los Angeles Basin. Recognition of such secondary materials began with the work on gas phase oxidant or ozone (Haagen-Smit, 1952), and has proceeded to the work on specific chemical species in atmospheric particulate matter (for example, Hidy, et al., 1975). Recently, with the passage of the 1970 Clean Air Act by the United States Congress, increased emphasis has been placed upon the health related effects of air pollution.

Although present at much lower mass concentrations than most gaseous pollutants, particulate matter is very important in determining health related effects. The particle size range where most of the aerosol mass is found coincides with that particle size which penetrates deepest

into the human lung, as well as that which scatters visible light most effectively. Thus, visibility reduction is not only aesthetically displeasing, but also an indication of a possible health threat.

Formation of secondary particulate matter in the atmosphere has been shown to produce a major portion of the measured aerosol mass concentration in areas such as Los Angeles (Miller, et al., 1972; Hidy, et al., 1975). In fact, the secondary materials in atmospheric aerosols present in highest mass concentrations (nitrates, sulfates, and organics) have been shown to be the major overall contributors to visibility reduction due to light scattering in Los Angeles (White and Roberts, 1975).

Sulfur was first recognized as a possible air pollution problem in England during the reigns of Edward I and Edward II (1272-1327), due to the irritation and odor from burning sulfur-rich sea coal. J. S. Haldane (1935, p. 415) recognized the unpleasant irritant effects of sulfuric acid formed from sulfur in coal and badly purified lighting gas. More recently, attention has been focused on sulfur because of its presence at high concentration during three major air pollution episodes: the Meuse Valley in Belgium (1930), the Monongahela River Valley, Donora, Pennsylvania (1948), and London, England (1952). Although these situations occurred in what was probably a reducing-type atmosphere, sulfate is also important in an oxidizing atmosphere such as Los Angeles. In fact, although emissions and atmospheric concentrations of sulfur dioxide gas are much lower in Los Angeles than in many eastern U.S. cities, concentrations of sulfate aerosol are approximately the same. More recently, the CHESS study has indicted particulate sulfate to be a major

contributor to short- and long-term health problems (Finklea, et al., 1974). The recent trend toward burning high sulfur fuel in power plants indicates that air pollution problems associated with sulfur will continue to be of significance. Automobiles which are equipped with an oxidation catalyst may pose a serious threat to human health. These catalysts convert not only carbon monoxide and unburned hydrocarbons to less damaging pollutants, but also gaseous sulfur dioxide to sulfuric acid.

1.1 DESCRIPTION OF THE LOS ANGELES BASIN SULFUR SYSTEM

As an introduction to the problem of conversion of gaseous sulfur dioxide to particulate matter sulfur, a sulfur mass balance for the Los Angeles Basin was developed. Comparison of the Los Angeles Basin sulfur cycle with the global sulfur cycle demonstrates that man's activities totally dominate the sulfur cycle in Los Angeles. A discussion of sulfur emission quantities and locations within the Basin provides a better understanding of the roles of the various sulfur emission sources in determining atmospheric concentrations. The diurnal atmospheric sulfur concentration patterns at Pasadena demonstrate the interplay of emission location, meteorology, and concentrations of other chemical species in the determination of sulfur concentrations.

1.11 Global and Los Angeles Basin Sulfur Balances

Sulfur compounds enter the atmosphere mainly as gaseous species: SO_2, H_2S, and organic sulfides. Sulfur compounds existing as aerosol particles are primarily formed in the atmosphere from gaseous sulfur species, but some are associated with airborne soil dust, marine aerosols, and industrial operations.

Figure 1.1 shows the global circulation of sulfur as estimated by Friend (1973). As a global average sulfur cycle, it is designed to illustrate the different processes and their relative overall magnitude rather than a detailed example of what might be occurring in any given region.

On a global basis, natural sources combine to emit approximately 152×10^6 metric tons of sulfur per year - most of this consisting of sulfides released from decay of terrestrial and marine organic matter. Aerosol sulfur emitted as sea spray also plays an important role in the sulfur cycle. The annual output of SO_2 from anthropogenic sources amount to approximately 65×10^6 metric tons of sulfur per year; this is less than one-third of the total global sulfur emissions. The major mechanism of removal of sulfur from the atmosphere is precipitation. However, large amounts are also removed from the atmosphere by deposition of gases at surfaces, including soil, water, and vegetation. Although Figure 1.1 is essentially the same as that reported by various investigators using different assumptions (Eriksson, 1960; Junge, 1963; Robinson and Robbins, 1968; and Kellogg, et al., 1972*), the numbers used are limited due to the lack of data that fully describe the global chemical circulations. The natural phase of the cycle involving H_2S and other biological emissions is especially weak.

---

* The anthropogenic SO_2 emission quantities used by Kellogg, et al., (1972) were calculated improperly using SCEP (1970) data. Total U.S. energy use and SO_2 emissions were used for scale-up to global energy use, rather than scaling each fuel category (coal and fuel oil) separately. This separate scaling is necessary because of the large difference between the sulfur content of coal and fuel oil and the U.S. and global mix of fuels burned.

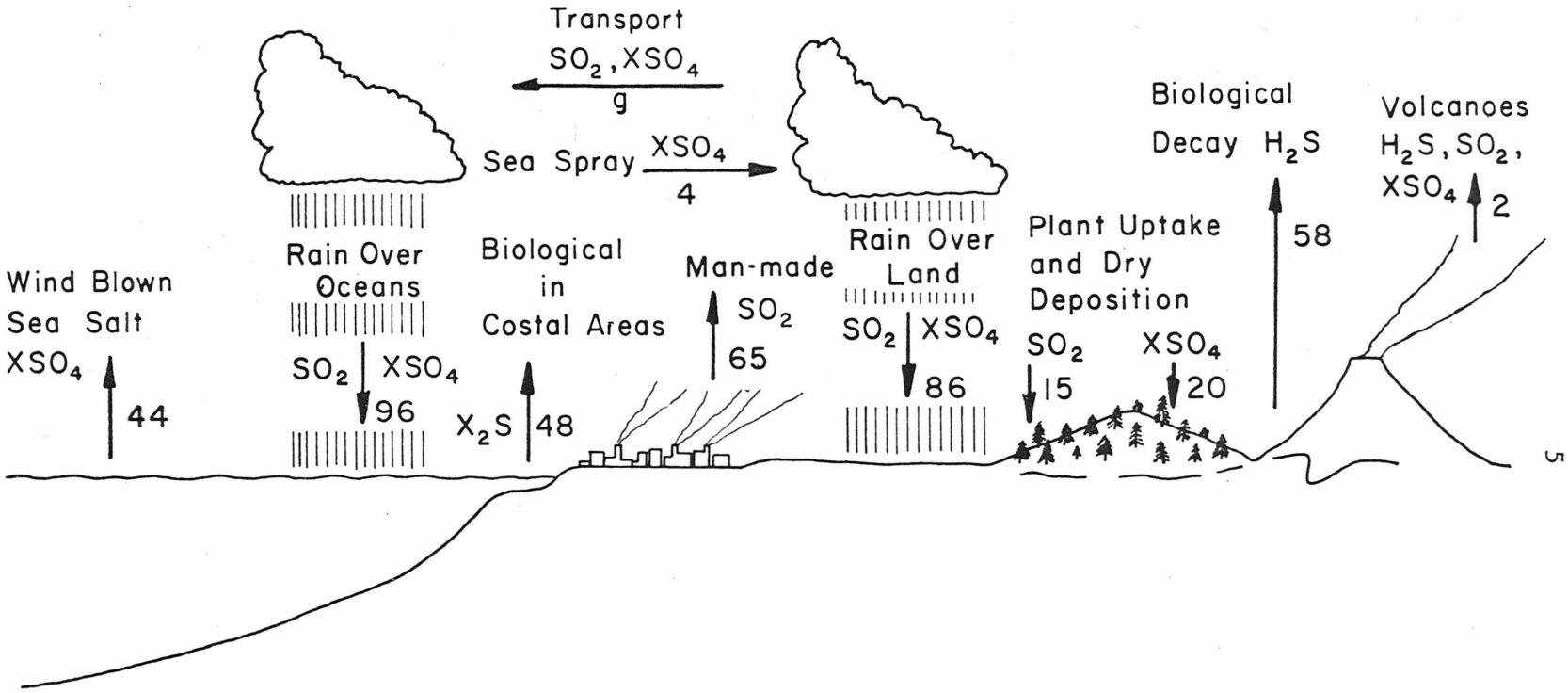

Figure 1.1 The Global Sulfur Cycle (from Friend, 1973)

Figure 1.1 provides a good overall picture of the global sulfur cycle, but it is important to view this system on a smaller scale in order to be able to understand the sulfur cycle in an urban basin such as Los Angeles. Table 1.1 shows the large geographical imbalance of the global circulation of sulfur. Over land areas in the northern hemisphere, anthropogenic emissions dominate natural sulfur emissions. This is especially true in the case of the Los Angeles Basin. However, even on a global basis, man's activities are becoming a substantial part of sulfur emissions as the use of high sulfur content fuels becomes increasingly necessary.

Manmade emissions of SO_2 come predominantly from stationary sources, including both power plants and chemical plant-refinery operations. Fuel combustion in Los Angeles involves natural gas and fuel oil, but not coal. Additional SO_2 is emitted by mobile sources (mainly the automobile) throughout the Basin. Los Angeles area gasoline has contained approximately 0.047 weight percent sulfur in recent years, compared with the national average of 0.030 weight percent sulfur (U.S. Bureau of Mines, 1974).

An average SO_2 emission inventory for Los Angeles County in 1973, arranged according to source category, is shown in Table 1.2. This shows that approximately 88% of the SO_2 emissions come from stationary sources. A rearrangement of this SO_2 inventory by source location is shown in Table 1.3. Stationary sources in coastal areas include 77% of total SO_2 emissions, with an additional 12% of SO_2 emissions being spread out over the basin. Only a small amount of SO_2 emissions (11%) is emitted by non-coastline stationary sources.

TABLE 1.1

The Relative Importance of Various Emission Sources to the Global Sulfur Balance

Sulfur Emission Quantities	Ratio	Calculated using Reference
global anthropogenic/total global	0.29	1
land anthropogenic/total land	0.52	1
northern hemisphere anthropogenic/total global anthropogenic	0.93	2,3
northern hemisphere natural/total global natural	0.46	1
northern hemisphere anthropogenic/northern hemisphere land	0.60	1
L.A. basin anthropogenic/L.A. basin total	0.98	4

[1]Friend (1973)

[2]Robinson and Robbins (1968)

[3]SCEP (1970)

[4]This work

TABLE 1.2

1973 Average SO_2 Emissions for Los Angeles County*

	SO_2 Emissions (metric tons/day)
Stationary Sources (Total)	319
Industrial Total	165
Chemical	88
Metals	9
Minerals	13
Petroleum Refining Total	51
Catalytic Cracking	43
Combustion	8
Oil Wells	0
Petroleum Marketing	0
Other Combustion	4
Power Plants	154
Commercial	0
Residential	0
Transportation Sources (Total)	45
Automobiles-Gasoline	31
Diesel	2
Aircraft	4
Ships and Railroad	9
Total Emissions	365

*Average data for 1973, from the Los Angeles Air Pollution Control District (1974).

TABLE 1.3

Average SO_2 Emissions in Los Angeles County by Source Location *

Source Location	SO_2 Emissions (metric tons/day)
Coastline Sources	252
El Segundo	35
Redondo Beach	9
Wilmington-Torrance	142
Alamitos Bay	51
Ships in Los Angeles Harbor	11
Aircraft	4
Inland Point Sources	36
Power Plants	11
Other	25
Area Sources	40
Total	328

*Average data for 1973, from the Los Angeles Air Pollution Control District (1974).

Although Table 1.2 and 1.3 provide a good picture of the average SO_2 emissions, large variations occur on a daily and even hourly basis. Sulfur emissions from fuel combustion can vary due to changes in electrical usage, sulfur content of the fuel, and availability of natural gas and fuel oil. Tabulations of sulfur emissions on a daily basis for combustion sources is available from the Los Angeles Air Pollution Control District. However, SO_2 emissions data from other industrial sources are available for average conditions only.

Other chemical species are emitted besides SO_2; however, no estimate of emission quantities of H_2S, H_2SO_4, SO_3 or organic sulfur compounds has been made by the Los Angeles APCD. In the case of fuel combustion emissions, more than 97% of the sulfur contained in the fuel is emitted as SO_2; the remainder is emitted as SO_3 gas. The direct emission of sulfuric acid, H_2S, and organic sulfur compounds has been ignored in the sulfur mass balance due to insufficient information. The quantities of such emissions are expected to be quite small. Average concentrations of H_2S in the Los Angeles Basin are about 6 ppb (Hidy, et al., 1975). No reliable measurements of H_2SO_4 or organic sulfur compound emission or ambient concentration levels presently exist for Los Angeles. However, some sulfur species concentration data exist for Japan. The concentration of methyl mercaptan in a residential area surrounded by oil refineries and chemical plants in Japan was about 3 ppb and of dimethyl sulfide in residential areas near Kraft pulp mills, about 0.4 ppb (Okita, 1970). Thus, even if these concentrations existed in Los Angeles, the sulfur mass ratio of each of these compounds to SO_2 would be 0.09 for H_2S, 0.04 for methyl mercaptan, and 0.01 for

dimethyl sulfide (using 0.07 ppm for the average SO_2 concentration near industrial source areas).

Figure 1.2 is the estimated sulfur mass balance for the Los Angeles Basin for July 25, 1973. The quantities shown were estimated using: SO_2 emissions data for Los Angeles (LAAPCD, 1974), SO_2 and CO concentrations measured by the Los Angeles Air Pollution Control District (1973), and the deposition velocity for SO_2 as reported by Shepherd (1974). The total sulfur concentration remaining airborne was estimated by scaling the CO concentration (assuming no CO is lost to the ground via absorption) by the CO and SO_2 emissions on that day. This is only an approximation, since CO is emitted mostly from area sources, while SO_2 is emitted mostly from point sources. However, the automobile has a dominant effect on total sulfur concentrations at a receptor site such as Pasadena (see section 3.5). Figure 1.2 shows that all of the emitted sulfur can be accounted for by this procedure. Such balances for three days in July, 1973 indicate that sulfur losses (by the paths noted in Figure 1.2) account for an average of 20 metric tons of SO_2 per day more than sulfur emissions (an average of 315 metric tons of SO_2 per day total emissions). This indicates that all important removal mechanisms have been accounted for in Figure 1.2. These mechanisms are: loss of both aerosol sulfur and SO_2 to the ground, reaction of SO_2 to form aerosol sulfur, and transport out of the Los Angeles area.

1.12 Diurnal Sulfur Concentration Patterns

The measured diurnal concentration pattern of a chemical species is affected by many parameters. For an unreactive species (CO for example), meteorology and emission strength and location relative to

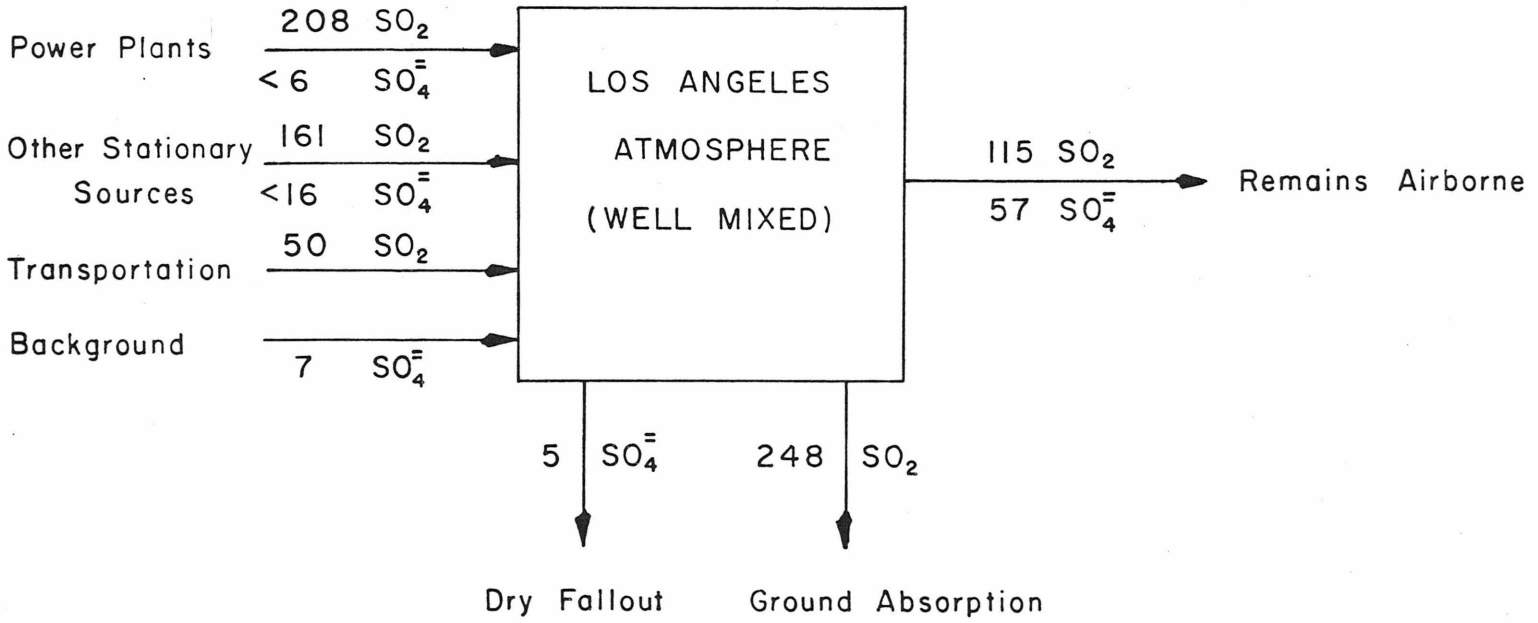

units are metric tons SO_2 per day

Figure 1.2 The Los Angeles Basin Sulfur Cycle for July 25, 1973 (in-out = 1 metric ton SO_2/day)

the sampling site have the most important effects on measured atmospheric concentrations. Atmospheric mixing height and wind speed and direction are especially important. However, for reactive components such as the various sulfur species, additional parameters also play a major role in determining measured concentrations. Conditions that have existed in the atmosphere during transport from the source to the sampling site are important. In the sulfur system, these reaction conditions determine the rate of SO_2 oxidation, the ability of the aerosol to contain oxidized sulfur, and the ability of the ground and vegetation to serve as a sink for gaseous SO_2 and sulfur aerosol. Sampling sites can be classified by their source-site relationship into three categories: background sites, near-source sites, and receptor sites. A good receptor site should have little influence from localized emissions and be representative of the general area. However, compounds emitted early in the time-location history of the sampled air parcel have been diluted relatively more than later emissions. Thus, measurements taken at any sampling site will be weighted toward the more recent emissions among all emissions into that air parcel. However, this is not the case if all of the emissions of the particular chemical species are from area sources of equal strength and emissions become well-mixed vertically in a very short time. Thus, measurements of CO should show no bias, while the differences in SO_2 emission sources (point source at the coast vs. area automobile emission sources) results in a bias at the sampling site toward later emissions.

Section 1.11 has shown that the major stationary sources of SO_2 in the Los Angeles Basin are the power plants and refinery-chemical

plant complexes located along the coast. The average summer and fall diurnal wind pattern involves winds of low velocity and fluctuating direction in the morning, then the establishment of a sea breeze from the west and the south in the late morning and continuing most of the afternoon, and then a reverse-flow wind system in the evening that tends to flush out the Basin (see Neiburger and Edinger, 1954). Once the marine wind stabilizes in the late morning, sulfur oxides are transported from coastal stationary sources to downwind receptor sites along a direct, definable pathway. Additional quantities of sulfur oxides are emitted into the air from industrial and automobile sources during the transport of an air parcel from source to receptor. A temperature inversion normally confines emitted pollutants to a volume fixed by the ground, the mountains, and the inversion base.

Figure 1.3 shows the daytime variations of SO_2, aerosol sulfur, and other measured parameters at Pasadena on July 25, 1973. Aerosol sulfur refers to the various sulfur species present in the particulate phase (including H_2SO_4, $(NH_4)_2SO_4$, sulfides, and sulfur containing organic compounds.) This sampling site in the Keck Laboratories of the California Institute of Technology is a receptor site with no influence of local stationary source SO_2 emissions. The concentrations of O_3, aerosol sulfur, and b_{scat}, as well as secondary organic aerosol (Grosjean and Friedlander, 1974), peak at about 1400 PST. Then as the sea breeze reaches Pasadena, the concentrations of these secondary pollutants drop dramatically. However, the sea breeze transports fresh SO_2 emissions from the coast to Pasadena. This pattern occurs most summer and fall days in the Los Angeles Basin.

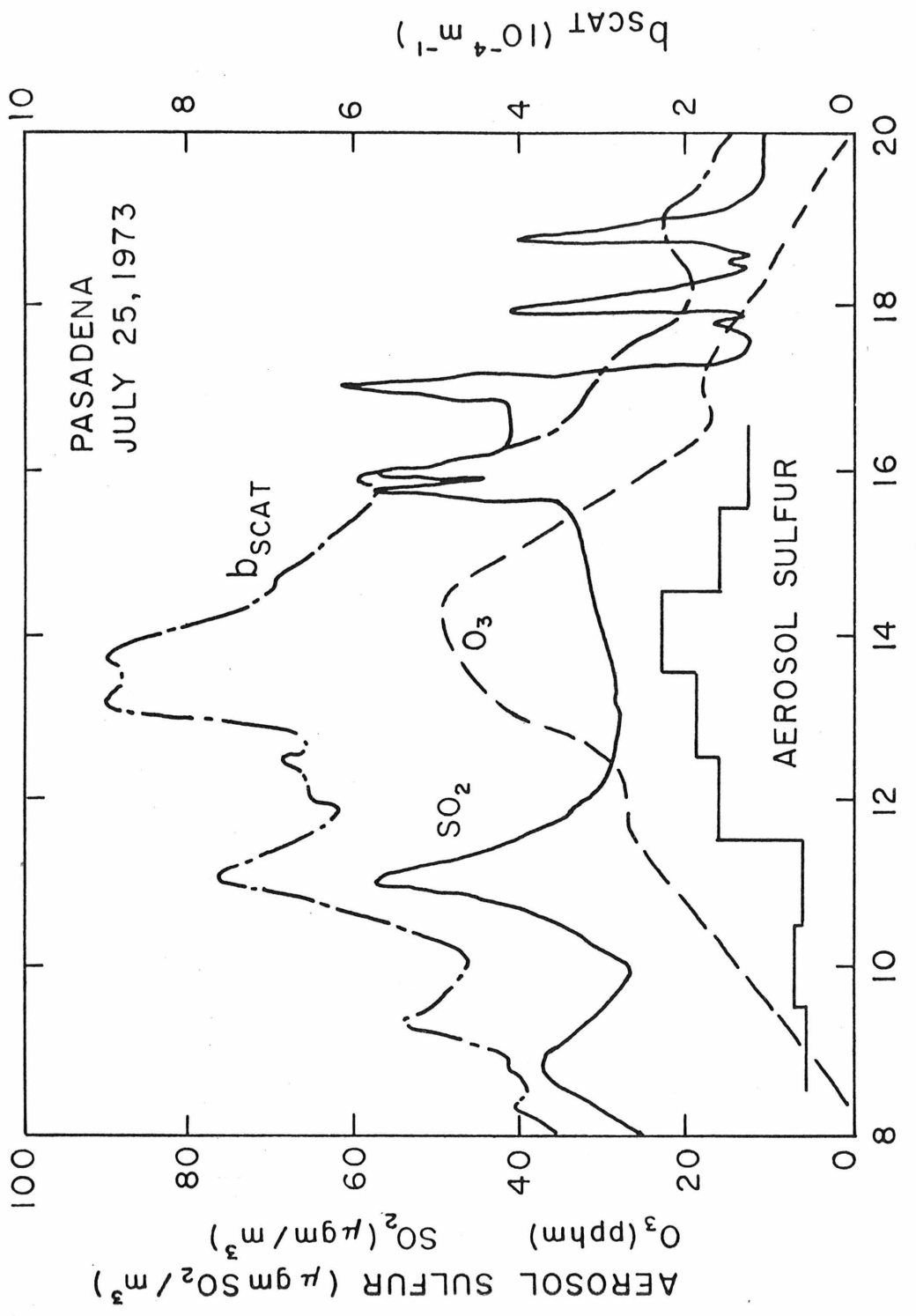

Figure 1.3 Daytime Concentration Profiles at Pasadena on July 25, 1973

1.2 LITERATURE REVIEW

A brief review of the voluminous literature on sulfur dioxide and aerosol sulfur will be presented. A discussion of atmospheric sulfur conversion studies will be followed by a brief discussion of smog chamber studies with SO_2 and the possible SO_2 oxidation mechanisms. Emphasis will be placed on results which are relevant to sulfur aerosol formation in a polluted atmosphere such as Los Angeles. General reviews of photochemical reactions in the atmosphere have been written by Alshuller and Bufalini (1965, 1971). Urone and Schroeder (1969), Bufalini (1971), and Calvert (1973) have written reviews specifically on sulfur reactions in polluted atmospheres.

Field studies have been conducted to determine the rate of loss of SO_2 from the gas phase; however, each was conducted within the direct influence of large stationary source emissions of SO_2. Katz (1950) measured sulfur dioxide and "total sulfur contaminants" (assumed to be SO_2, SO_3, and H_2SO_4) in the Sudbury, Ontario nickel-smelting area. His data showed that SO_2 accounted for about 85% of the total sulfur concentration. For average residence times, a pseudo-first order rate constant of SO_2 loss of 2.1% hr^{-1} was calculated (Katz, 1970). Katz found that this rate of oxidation was the same for both day and night. His estimated rate actually includes SO_2 loss by absorption, as well as oxidation. Weber (1970) used measurements of the CO_2 and SO_2 concentrations in Frankfurt am Main to estimate the residence time of SO_2 under the direct influence of power plant emissions (about 5 km away). He determined that almost 50% of the sulfur dioxide was lost (via reaction

or absorption) in a period of 20 to 60 minutes, assuming that CO_2 was inert. Gartrell, Thomas, and Carpenter (1963) measured SO_2 and soluble sulfates at various downwind distances (up to 10 miles) in a coal-fired power plant plume using an instrumented helicopter. They estimated average oxidation rates of up to 108% hr^{-1} in fog or mist, 60 to 120% hr^{-1} in conditions of about 75% relative humidity, and rates of 3 to 10% hr^{-1} at low relative humidities. Thus, the oxidation of SO_2 in power plant plumes can be fast, especially at high relative humidities. It is suspected that these high oxidation rates are the result of the catalytic qualities of the particulate matter present. No field measurements of the SO_2 oxidation rate have been conducted in a photochemical atmosphere such as Los Angeles or in an area downwind of a major stationary source.

There have been relatively few smog chamber studies of irradiated mixtures of hydrocarbons, NO_x, and SO_2 (Renzetti and Doyle, 1959; Prager, et al., 1960; Harkins and Nicksic, 1965; Wilson, et al., 1970, 1972; Groblicki and Nebel, 1971; Stephens and Price, 1972; and Smith and Urone, 1974). Although SO_2 oxidation rates are calculated from such data, none of the investigations reported mass balances for sulfur. It is important to obtain a sulfur mass balance because oxidation rates determined from gas phase concentrations may include losses to the walls rather than just reaction to form sulfur aerosol. Also, no studies have been conducted with natural sunlight or ambient particulate matter. Such considerations are important because indoor lamps with intensity and/or spectrum differences from natural sunlight may promote one particular reaction mechanism over another. The presence of ambient particulate matter allows heterogeneous mechanisms to proceed at rates

similar to those in the real atmosphere. Of the aerosol parameters, only condensation nuclei and light scattering have been measured in hydrocarbon, NO_x, SO_2 smog chamber studies; no measurement of the sulfur size distribution has been made. Measurements have been made of the total size distribution, as a function of time, in experiments with SO_2 in air (Clark, 1972) and with SO_2, propylene, and O_3 (McNelis, 1974). These measurements were made using an electrical mobility analyzer.

Previous measurements of the aerosol sulfur size distribution, have been made in urban areas (Roesler, et al., 1965; Wagman, et al., 1967; Ludwig and Robinson, 1968; and Hidy, et al., 1975). All investigators found that the sulfate is concentrated in the small particle sizes (less than 0.5 μm). However, only Hidy, et al. (1975) took samples as short as 2 hours in duration and only Ludwig and Robinson (1968) obtained size discrimination below about 0.5 μm in diameter.

There are many diverse views regarding the relative importance in a polluted atmosphere of various SO_2 oxidation paths. The relatively slow rates of photo-oxidation of SO_2 in air exposed to light (Gerhard and Johnstone, 1955; and Cox and Penkett, 1970) and the demonstrated catalytic influence of some solids and moisture on the rate of SO_2 oxidation (Johnstone, et al., 1958, 1960; Junge and Ryan, 1958; Cheng, et al., 1971; and others) have convinced many scientists that the heterogeneous oxidation paths are probably dominant over homogeneous ones. However, in a photochemical atmosphere such as Los Angeles, the presence of many gas phase oxidants might contribute to high SO_2 oxidation rates. Calvert (1973) recently has reviewed the possible homogeneous SO_2 oxidation paths.

The major pathways considered to be important in a photochemical atmosphere are:

(1) Metal aided catalysis of the oxidation in liquid droplets.

(2) Catalysis of SO_2 oxidation on the surface of soot particles (Novakov, et al., 1974).

(3) Homogeneous gas phase oxidation of SO_2 by OH (Wood, et al., 1974).

(4) Homogeneous gas phase oxidation of SO_2 by an intermediate of the O_3, olefin reaction (Cox and Penkett, 1972; McNelis, 1974).

(5) Homogeneous gas phase oxidation of SO_2 by other reactive intermediates (such as HO_2, RO_2, and RO).

Computer simulations of the 1-butene, NO_x, SO_2 system indicate that (3) and (4) play a dominant role in the oxidation of SO_2 in a system without particles (Demerjian, et al., 1974).

1.3 DESIGN OF THE STUDY

This study was designed to answer the following questions:

(1) How fast is sulfur dioxide converted to aerosol sulfur in the Los Angeles atmosphere?

(2) What mechanisms control this conversion of sulfur dioxide to aerosol sulfur?

(3) Where, with respect to particle size, does the sulfur aerosol appear?

A program of coordinated laboratory and field measurements was undertaken in conjunction with sufficient modeling work to understand the measurements (Figure 1.4). An aerosol vaporization technique was

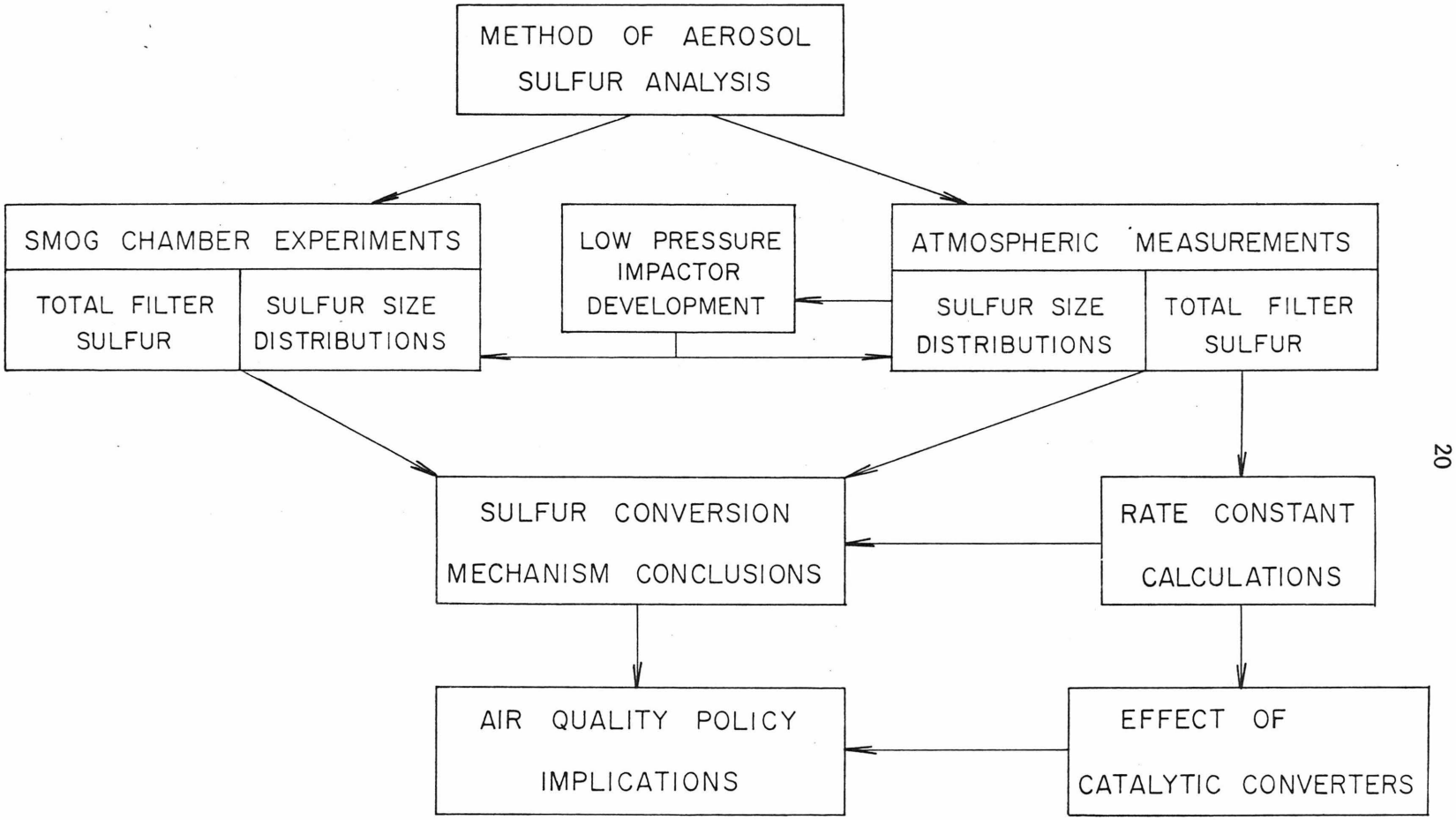

Figure 1.4 Research Flow Chart

developed (Chapter 2) capable of measuring both total filter and cascade impactor aerosol samples for nanogram levels of sulfur. This corresponds to sampling times of 1/3 to 1 hour for normal ambient concentrations. Measurements were then made of gas and aerosol phase sulfur at both a source-dominated site and a representative receptor site in the Los Angeles Basin. Model calculations using this data, along with air trajectory analysis, provided estimated conversion rates for sulfur dioxide to aerosol sulfur (Chapter 3). The estimated rates were higher at higher levels of photochemical activity. Sulfur size distributions taken at these sites indicated that a major portion of the aerosol sulfur mass was below 0.25 μm in diameter and thus collected on the after filter of the cascade impactor. The necessity of obtaining more detailed information about this small particle size sulfur aerosol required design and construction of a low-pressure cascade impactor (Appendix C). The aerosol sulfur measurement techniques were then used in smog chamber studies with various hydrocarbons, NO, NO_2, and SO_2 added to ambient air and irradiated with natural sunlight (Chapter 4). The mechanism of formation of aerosol sulfur and carbon in the 1-heptene-NO-NO_2-SO_2 system was analyzed by a kinetic scheme.

The results of the chemical (conversion mechanism) and physical (sulfur size distribution) insights gained in the work into the sulfur problem in Los Angeles, combined with the interaction of the meteorology, gives a better understanding of the formation of aerosol phase sulfur compounds and thus of the possible controls available for such compounds.

CHAPTER 2

METHOD OF AEROSOL SULFUR ANALYSIS

This chapter describes an aerosol vaporization method that measures sulfur at the nanogram level directly from the collection substrate. This method has the advantages of small sample size requirements, speed of analysis, minimization of sample handling (and thus possible contamination), and high absolute sensitivity and reproducibility. Samples collected on stainless steel strips in a cascade impactor or on glass fiber filters can be analyzed for aerosol sulfur by this method. Heating of the aerosol to approximately 1200° C is accomplished by resistance heating of the collection substrate (in the case of the steel strips) or of two stainless steel strips with a disk from the glass fiber filter placed between them. The sulfur is evolved into a flowing clean-air stream which then passes into a sulfur flame photometric detector. The resulting signal is integrated electronically to obtain the sulfur mass vaporized from the collected aerosol sample.

This method is a variation of Gas Evolution Analysis (GEA) which involves practically instantaneous heating to approximately 1200°C. In this way all sulfur compounds that either evaporate (e.g., H_2SO_4) or decompose to vapor products [e.g., $(NH_4)_2SO_4$] below 1200°C are measured. Others have discussed GEA methods that involve sample handling to measure sulfuric acid at microgram sulfur levels (Scaringelli and Rehme, 1969; Maddalone, et al., 1975). Knights (1973) has obtained

qualitative determination of some sulfate compounds using temperature programmed mass spectrum analysis. Otherwise, wet chemical techniques involving extraction have been employed to determine aerosol sulfur concentrations at the microgram level (Tokiwa, et al., 1974).

2.1 METHOD BACKGROUND

The technique described here is essentially a modification of Gas Evolution Analysis (GEA). Gas Evolution Analysis is a thermal analytical technique where a non-gaseous sample is heated at a specified rate in a carrier gas stream and the gaseous products of decomposition and vaporization are measured by a suitable detector. The trace of the detector response as a function of the sample temperature is the effluent gas thermogram. Since the decomposition of a chemical compound is dependent upon its chemical nature and its physical and chemical environment, specific compounds in the sample can be identified when the heating conditions and detector are carefully selected.

Gas evolution analysis using a thermal conductivity detector was first used as a companion technique to differential thermal analysis, thermogravimetric analysis and other thermal techniques. However, these applications yield no specific species identification. GEA has recently been combined with gas chromatography (Wendlandt and Southern, 1965) and mass spectrometric analysis (Schutzle, 1972 and Knights, 1973) to identify the evolved gases. Although Knights was able to identify sulfur species to some extent in atmospheric aerosol samples, the results were qualitative in nature and involved many unresolved identification problems. Some of these problems also occured with the experimental

systems used in these investigations: the loss of the evolved sulfur species to the walls of the heating chamber, the wide range over which some sulfur compounds decomposed, the interconversion of various sulfur species as they were heated, and the change in detector response due to a change in carrier gas flow characteristics produced by the increasing temperature. To avoid these problems, practically instantaneous heating of the aerosol sample to approximately 1200°C has been used. This procedure evolves all the sulfur species that either vaporize or decompose below this temperature at the same time and thus provides a measure of the total sulfur in the aerosol, rather than a measure of the individual sulfur species existing in that sample.

Scaringelli and Rehme (1969) described an oven heating technique that was developed to measure sulfuric acid concentrations in aerosol samples. Ammonium sulfate also is determined quantitatively with sulfuric acid at the temperature used (500°C), with partial decomposition and measurement of Hg_2SO_4 and $Fe_2(SO_4)_3(NH_4)_2SO_4$. Incomplete recovery of standard sulfate solutions (80 to 85%) was assumed to apply to atmospheric samples as well. Although a lower limit of detection of 3 nanograms of H_2SO_4 is claimed, no standards were analyzed below about 1.5 µgm H_2SO_4.

Maddalone, et al. (1975) have developed a technique to determine sulfate by the thermal reduction of Perimidylammonium sulfate, formed by precipitation from a sulfate solution. Measurement of the evolved SO_2 is performed using the West-Gaeke procedure. The method is free of interferences and is quite precise. However, although the lower limit of detection is listed as 100 ngm of sulfate, standards were not run below about 1.5 µgm of sulfate.

Recently, Leahy, et al. (1975) have been able to separate various sulfates by a combination of solvent extraction and selective volitalization at concentration levels above 100 μgm $SO_4^=$. Also, Mudgett, et al. (1974) have investigated the use of warm, dry air (about 150°C) to vaporize H_2SO_4 from Fluoropore filters at concentration levels above 0.3 μgm H_2SO_4. However, neither method has been tested extensively in the field.

2.2 APPARATUS

A diagram of the glass vaporization apparatus and the associated circuitry is shown in Figure 2.1. A stainless steel strip is mounted on the tungsten posts using stainless steel nuts and washers. Clean air flows in the top of the cell, across the stainless steel strip into a cone placed just above the strip and then directly into the flame of the photometric detector. The power supply continuously charges the capacitors. When the switch is closed, the capacitors are discharged through the strip. A sample or standard of sulfur in purified water can be analyzed by placing a 1 to 5 μℓ aliquot on a stainless steel strip or in a tungsten boat and heating by capacitor discharge. Atmospheric particles collected on a glass fiber filter can be vaporized directly in the same apparatus by clamping a small disk cut from the filter between two stainless steel strips and discharging the capacitors through the strips. The capacitance and voltage used for steel strip and glass fiber filter disk analyses are 0.285 Farads at 11.5 volts and 0.387 Farads at 15.0 volts, respectively. These values are for a strip size of 0.21 inch by 0.80 inch and would be different for another system with different strip size or connecting resistances.

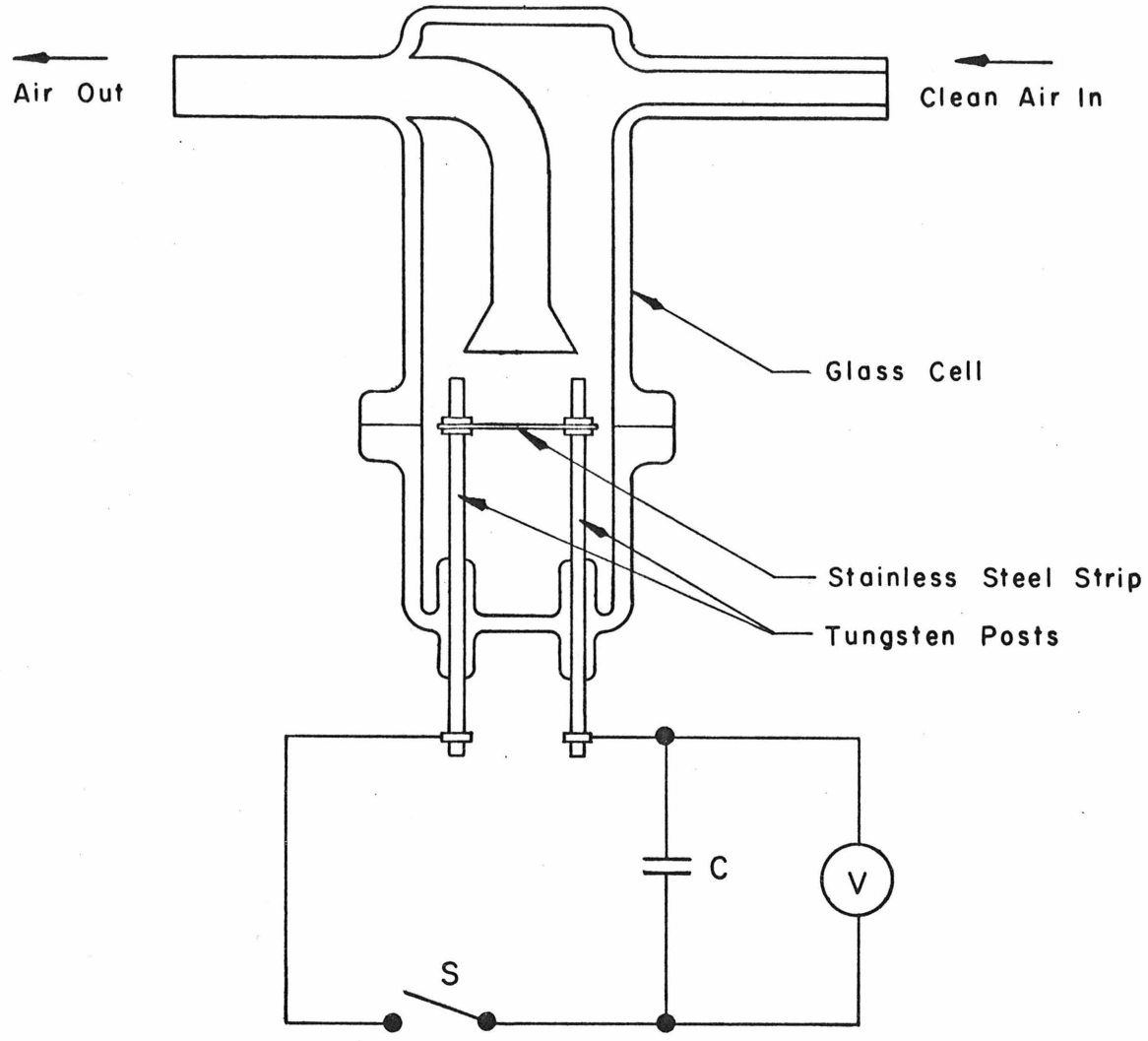

Figure 2.1 Aerosol Vaporization Apparatus and Associated Circuitry

The linear sulfur concentration signal of a Meloy Laboratories Model SA 160-2 Sulfur Analyzer is integrated by a Varian Aerograph Model 477 Electronic Integrator during each analysis. Release of sulfur from a sample produces a sharp increase in detector response with a slowly decaying tail (a total integration time of about 1 min. for a 25 ng S standard). At a constant air flow rate, the sulfur concentration can be expressed as mass of sulfur per time. Thus, the integration with respect to time yields the mass of sulfur evolved from the sample.

The metal strips are cut from 0.001 inch thick stainless steel shim stock, type 302 full hard. The holes, 0.1 inch diameter to fit the tungsten posts, are punched in the strip using a two-piece die and a metal rod. The strips are wiped clean with a cotton cloth and heated in a furnace for 2 hours at 900^{o}C. This pretreatment procedure produces stainless steel strips with low sulfur background values.

Gelman A glass fiber filters (47 mm in diameter) are used for total filter sample collection. These filters must be pretreated to remove the background sulfur. However, with glass fiber filters, there is an additional source of contamination: during sampling the conversion of gaseous sulfur compounds, especially SO_2, to a sulfur species that remains on the filter and then is measured as aerosol sulfur (Lee and Wagman, 1966). Both of these problems are overcome by a treatment procedure used by the Brookhaven Analytical Group (Forrest and Newman, 1974). This procedure involves washing the filters with purified water, heating them to 450^{o}C

for 2 hours, rewashing them with water, soaking them in 0.5 N HCl for 2 minutes and removing the excess acid by suction, and then drying them at 110°C. Filters treated in this manner show no increase in the sulfur filter blank on the second of two filters in series when used to sample air with up to 1.0 ppm SO_2.

Purified water extractions of most filter materials can be made in order to determine the water-soluble sulfur aerosol concentration. Membrane filter materials, such as Gelman GA series filters or Millipore MF series filters, have reasonably low extractable sulfur blanks and thus are good for this type of analysis. However, because it takes at least 3 ml of water to extract a 47 mm diameter filter and a maximum of 5 μℓ of that extract can be used per analysis, this technique cannot measure sulfur concentrations as low as the direct analysis techniques without going through an evaporation and redissolving procedure.

2.3 ANALYSIS AND CALIBRATION PROCEDURE

Aerosol samples collected directly on metal strips (as in a single jet cascade impactor) are mounted directly in the glass cell and heated by capacitor discharge two times in succession. This is necessary because not all of the sample vaporizes the first time. An average of 4.3% of the sulfur in the sample was vaporized by the second heating of 68 cascade impactor samples on stainless steel strips. Extraction samples and standard solutions are placed on a clean (by prior capacitor discharge) metal strip using a microsyringe. Volumes up to 5 μℓ can be handled. Care must be taken not to allow any of the solution droplet to spread under the washers that hold the

metal strip in place, because it will not be heated there. The air flowing to the detector evaporates the sample solvent. The sample can then be heated twice to 1200°C by capacitor discharge to recover all of the sulfur in the sample. Continual analysis of extraction samples is best done using a tungsten boat (Ernest F. Fullam, Inc., Schenectady, N. Y. 12301, catalog no. 1213) in place of a metal strip. This allows more analysis to be performed without changing the metal strip. This procedure with glass fiber filter extraction aliquots had been used by J. D. Husar, et al. (1975) with an apparatus originally set up by the author.

Aerosol samples collected on pretreated glass fiber filters can be analyzed directly by cutting out small disks of the filter using a hole punch and then placing the disk between two stainless steel strips. Different disk areas (from 0.03 to 0.20 cm^2) can be obtained by choosing one of the six sizes available on the hole punch. The good, consistent thermal contact between the two strips and the filter disk required for complete heating of the collected aerosol was achieved by squeezing the strips together with a pair of pliers while tightening the strip-retaining nuts. Stress caused by excessive bending of the strips must be avoided because it produces incomplete heating of the filter disk. Analysis of the first disk conditions a new pair of strips; then subsequent disks from the same sample filter provide replicate analyses (up to four per pair of strips) for the mass of aerosol sulfur. Each analysis must involve three successive heatings to vaporize all of the sulfur from the sample.

Other methods of directly heating a total filter aerosol sample were attempted without success. Filter materials other than glass fiber (Millipore MF, Gelman GA, Nuclepore, and paper filters) extinguished the flame of the sulfur detector when heated to the temperature necessary to evolve all of the sulfur compounds. Silver membrane filters evolved excessive amounts of sulfur when heated directly by capacitor discharge. Also, the filtration efficiency of such material is low (Appel and Wesolowski, 1972). Graphite filters absorbed significant amounts of SO_2 from the air. Non-conducting materials were tried as substitutes for one of the stainless steel strips. However, in order to tightly hold a filter disc in place, they had to be of fairly large mass in comparison to either a steel strip or a filter disk. Thus, they acted as heat sinks, making it impossible to heat the collected aerosol to a sufficient temperature to evolve all of the sulfur compounds.

2.4 CALIBRATION RESULTS

Because the aerosol sulfur analysis method described here involves heating the sample to about 1200°C in a very short time, it is not specific for any one sulfur compound. Instead, any sulfur compound which either evaporates (e.g., H_2SO_4) or decomposes completely to gas phase sulfur species [e.g., $(NH_4)_2SO_4$] at temperatures below 1200°C will be measured by the method. Pure (98.3%) H_2SO_4 has a boiling point of 338°C, while 25% H_2SO_4 in water boils at 106°C. Although there remains a controversy concerning the exact decomposition temperatures of the various ammonium salts (Knights, 1973), it is agreed that NH_4HSO_4, NH_4HSO_3 and $(NH_4)_2SO_4$ all decompose completely at atmospheric

pressure to gas phase sulfur products for temperatures above 500°C. Ostroff and Sanderson (1959) found the decomposition temperatures at atmospheric pressure of the metal sulfates $MnSO_4$, $FeSO_4$, $CoSO_4$, $NiSO_4$, $CuSO_4$, $ZnSO_4$, $CdSO_4$, $PbSO_4$, and $MgSO_4$ to be between 537 and 895°C. $CaSO_4$ was found to decompose at 1149°C. The final non-volatile product in every case was a metal oxide. Analysis of standard solutions of Na_2SO_4 and $CaSO_4$ resulted in equivalent sulfur responses when compared with other standard solutions. Thus, all the compounds mentioned above should be measured in the vaporization method. In addition, organic sulfur compounds such as thiophene and benzene thiols will also be measured by the described vaporization method.

The background sulfur value for each of the substrates is shown in Table 2.1. The low values show that the pretreatment procedures described previously are effective in reducing the sulfur background to acceptable levels. The glass fiber filter blank corresponds to 19 ng sulfur per cm^2.

The reproducibility of the method is illustrated in Table 2.2. The net integrated area (after subtracting the blank for the purified water) per ng sulfur is constant for H_2SO_4 standard solutions of 20 to 260 ng sulfur with a coefficient of variance of 7.3%. The lower limit of detection of the vaporization method (estimated by 2.5 times the standard deviation of the blank) is 0.8 ng sulfur for the purified water solutions, 1.0 ng sulfur for the pretreated metal strips, and 1.2 ng sulfur for the glass fiber filter disks (area of 0.199 cm^2). Cross-calibration of the sulfur analyzer with an SO_2 permeation tube indicates 100% recovery of the standard solutions used for Table 2.2.

TABLE 2.1

Sulfur Blank Values for the Various Substrates

Blank Analyzed	Sulfur Mass Per Sample (ng S)	No. of Samples
pretreated metal strip, unused	0.9 ± 0.4	22
no. 6 glass fiber filter disk, pretreated (area of 0.199 cm^2)	3.8 ± 0.5	10
1.0 μℓ purified water on clean strip	0.8 ± 0.3	13
1.0 μℓ purified water extract of Gelman GA-1 membrane filter (47 mm filter extracted with 3 ml water)	1.2 ± 0.2	9

TABLE 2.2

Accuracy of the Vaporization Method for H_2SO_4 on a Stainless Steel Strip

Mass of Sulfur in the Standard (ng S as H_2SO_4)	Net Integrated Area Per Mass of Sulfur (1/ng S)
21.8	1148.
21.8	1060.
21.8	1023.
43.6	1274.
43.6	1188.
43.6	1222.
43.6	1032.
65.4	1032.
65.4	1135.
87.1	1088.
87.1	1143.
87.1	1094.
261.5	1011.
261.5	1055.
average	1107.
standard deviation	80.
coefficient of variance	7.3%

A calibration curve constructed by vaporization of standard solutions of H_2SO_4, $(NH_4)_2SO_4$ and Na_2SO_4 from stainless steel strips is shown in Figure 2.2. The net integrated area (after subtracting the blank for purified water) is plotted vs. the mass of sulfur in the standard solution. The error bars represent the standard deviation for three to five replicates of that standard. An error weighted, least squares fit of the data results in a correlation coefficient of 0.9996 and a χ^2 of 2.24. The slope is 1110. per ng sulfur. The net area intercept of 20. is one-tenth the standard deviation of the purified water blank. Figure 2.2 also shows that standard solutions of H_2SO_4, $(NH_4)_2SO_4$, and Na_2SO_4 yield equivalent responses when vaporized from stainless steel strips.

Complete recovery of $(NH_4)_2SO_4$ standards from glass fiber filter disks was achieved. However, attempted calibration of the glass fiber filter disks by addition of H_2SO_4 standard solutions was unsuccessful. This incomplete vaporization may be the result of binding of H_2SO_4 to the glass surface when heated or when a large volume of acidic solution is placed on a filter disk. Leahy, et al. (1975) also had this problem with glass fiber filters.

2.5 INTERMETHOD COMPARISON

The aerosol vaporization method discussed in this chapter has been used to measure aerosol sulfur concentrations in smog chamber studies (see Chapter 3). Figure 2.3 shows a comparison of the measured aerosol

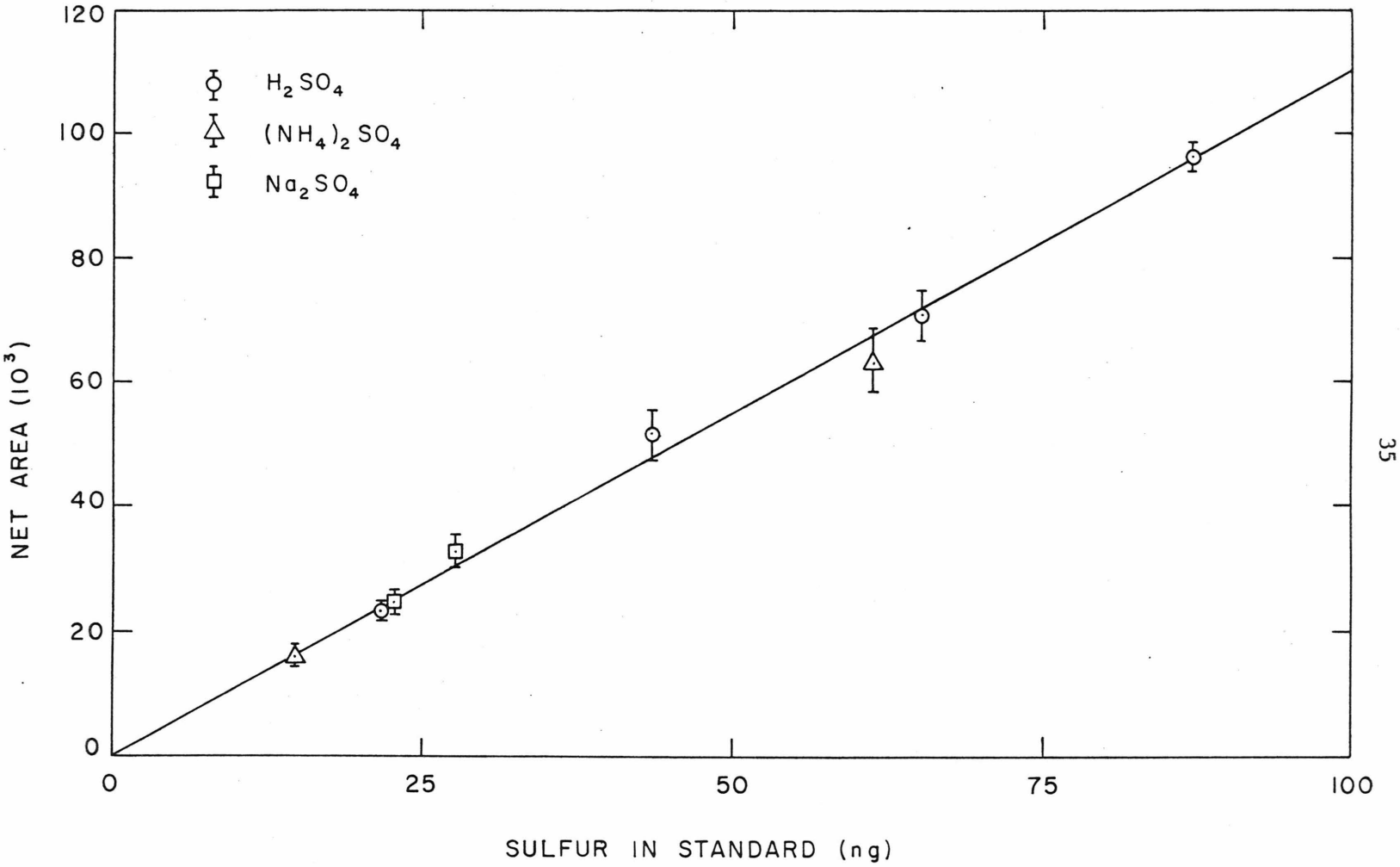

Figure 2.2 Calibration Curve for Various Sulfur Standards

sulfur concentration using the method described here with the calculated aerosol sulfur concentration, employing the initial and subsequent continuous measurements of the SO_2 concentration (see also Figures 4.2 and 4.3). For five samples during each of five smog chamber experiments with SO_2 and 1 heptene, the recovered sulfur (gas plus aerosol phase) to beginning sulfur ratio was 0.98 ± 0.09. This indicates that the aerosol sulfur vaporization method described here measures all of the aerosol sulfur formed in such experiments.

A comparison of this method with a wet chemical procedure was possible when samples were taken at California State University at Dominguez Hills at the same time as the ACHEX study (Hidy, et al., 1975). Figure 2.4 shows this comparison for the two days, October 5 and October 11, 1973. Good agreement was obtained for the samples taken October 5, 1973; however, the wet chemical procedure yields results higher by as much as a factor of two on October 11, 1973. It is possible that either of the procedures may have interferences at the low concentration values found on October 11, 1973 (this wet chemical method is presently being evaluated under an Environmental Protection Agency contract to the State of California). Good agreement between the two methods was obtained on October 5, 1973, when the winds were directly from the local sulfuric acid plant, indicating that the aerosol vaporization method does measure sulfuric acid.

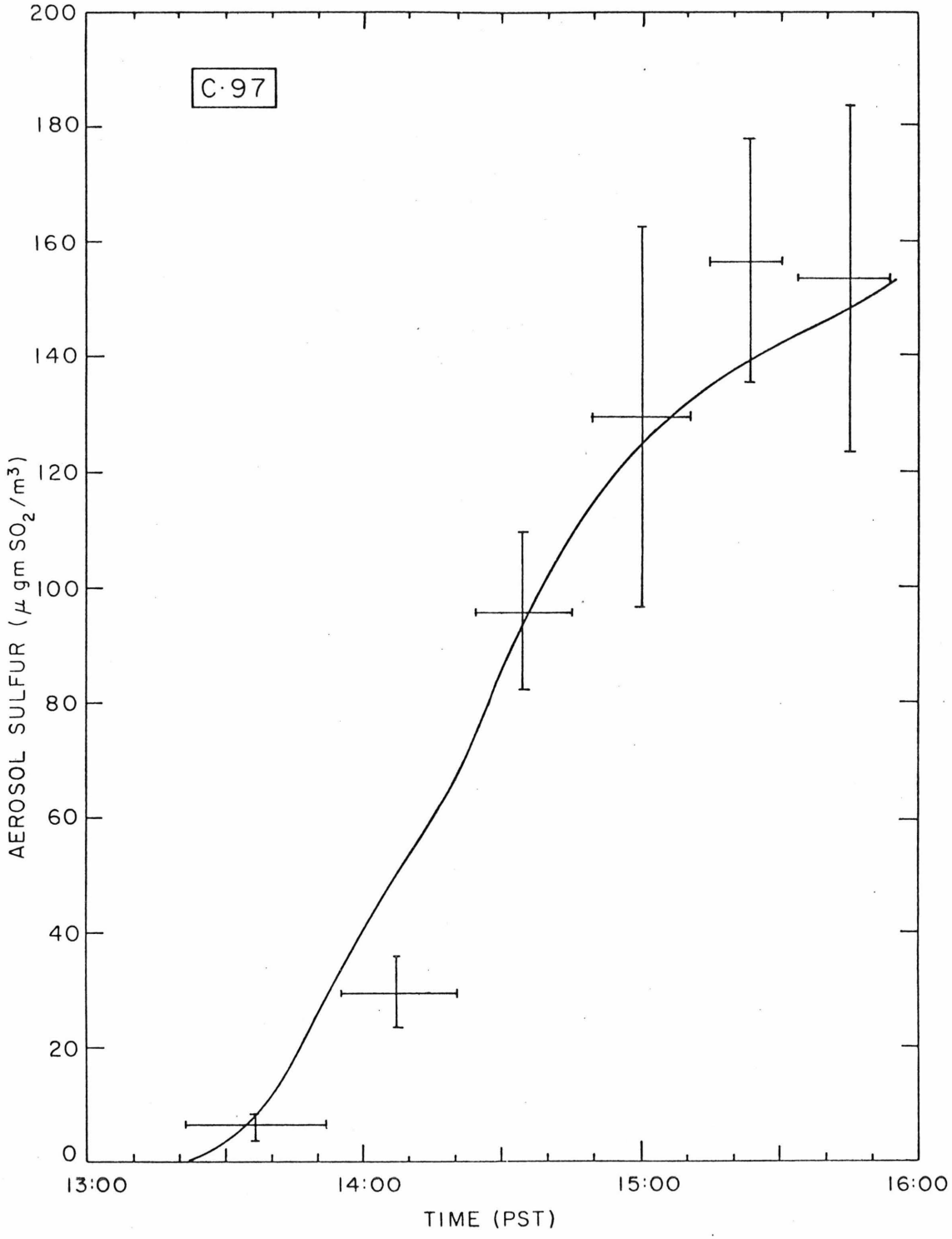

Figure 2.3 Comparison of the Measured and Calculated Aerosol Sulfur Concentrations for Experiment C.97. The Calculated Values (solid line) Were Obtained by Difference from Continuous Readings of the SO_2 Concentration.

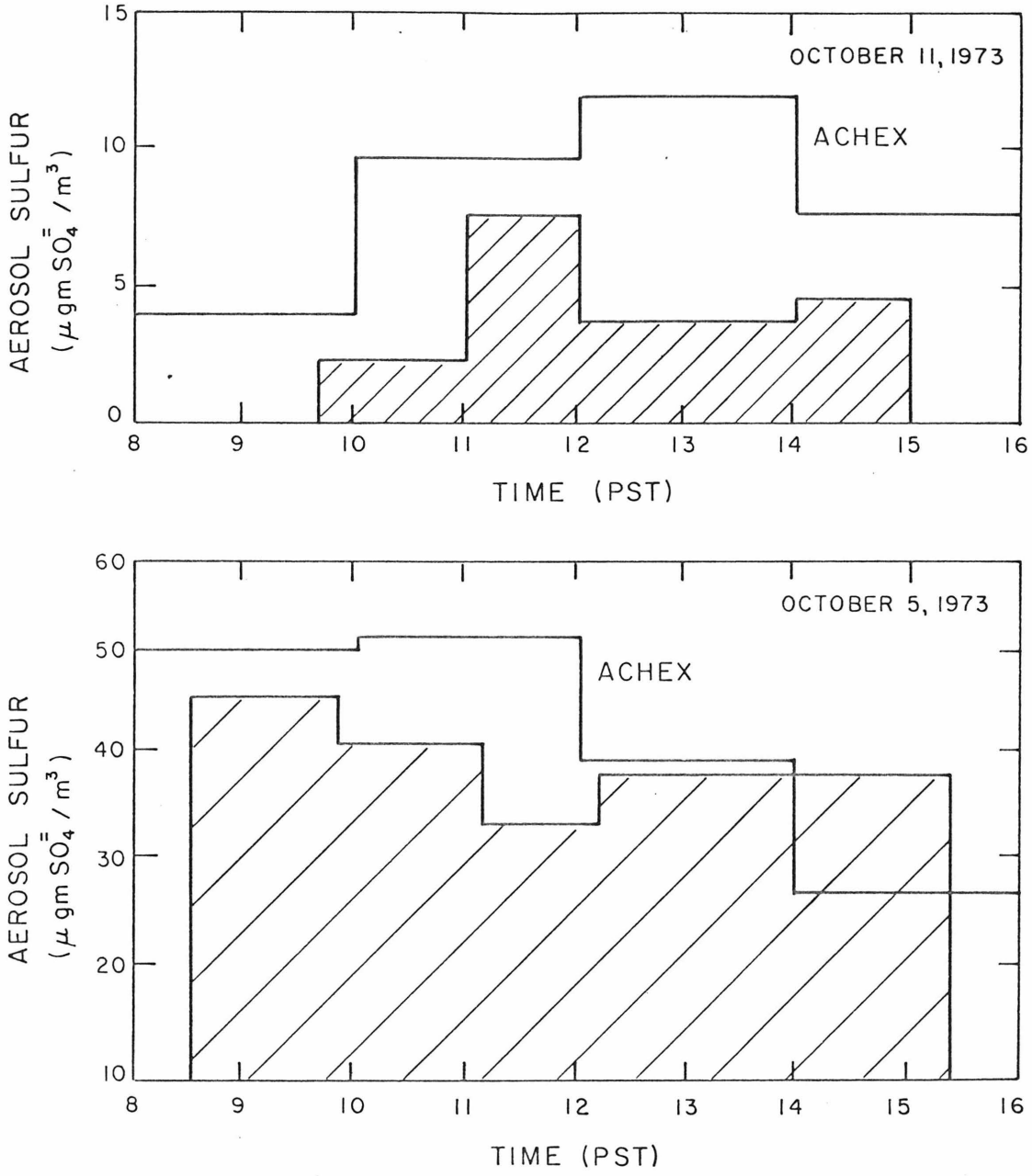

Figure 2.4 Comparison of Measurements Using the Aerosol Vaporization Technique (hatched area) with ACHEX Sulfate Concentrations for Dominguez Hills (samples for vaporization analysis only taken from 0837 to 1525 PST on October 5, 1973, and from 0939 to 1510 PST on October 11, 1973).

2.6 SUMMARY AND RECOMMENDATIONS

An aerosol vaporization method that measures sulfur at the nanogram level directly from the collection substrate using a flame photometric detector has been described. Calibration shows the method to have a coefficient of variance of 7.3% and a lower limit of detection of 1 ng sulfur. The method will respond to any sulfur compound that either evaporates or decomposes below 1200°C.

There are many additional applications for the aerosol vaporization method described here. The ability to measure ng level quantities of aerosol sulfur will be extremely useful when a short sampling time is required, such as samples taken from aircraft. The maximum mass of sulfur that can be analyzed is limited by the non-linearity of the photometric detector at high sulfur masses (normally about 250 ng S). However, this maximum can be raised by moving the cone of the glass cell away from the strip position or eliminating the cone completely. Eliminating the cone produced a maximum mass of about 600 ng S. A temperature-programmed heating procedure could provide some sulfur species identification, although efforts in this direction have so far been unsuccessful. Also, the same vaporization apparatus coupled in the appropriate way with a chemilumenscence NO_x analyzer or a flame ionization detector (with or without a chromatographic column) should allow aerosol nitrogen and carbon concentrations to be determined directly from the collection substrate.

CHAPTER 3

FIELD STUDIES: ATMOSPHERIC SULFUR CONVERSION RATES

There have been many laboratory studies of sulfur dioxide to aerosol sulfur conversion (see reviews by Urone and Schroeder, 1969; Bufalini, 1971), but there are little data on the actual rate and conversion mechanism in an urban atmosphere. Most of the atmospheric studies have been performed in power plant plumes or other source-dominated areas (see, for example, Gartrell, et al., 1963; Weber, 1970; Katz, 1970). This chapter contains the results of calculations of the pseudo-first order decay rate of sulfur dioxide in the photochemically involved atmosphere of the Los Angeles basin. A sulfur conversion model is developed that requires the aerosol-to-gas phase sulfur ratio near the coast and at a downwind receptor site, the time-location history of the particular air parcel that is sampled at the receptor site, and a knowledge of the introduction and removal of sulfur from that air parcel as it is transported across the basin. The applicability of this model to sulfur conversion in Los Angeles is discussed in the context of the assumptions made in the model derivation and the data available for calculations. The sensitivity of the determined rate to the measured and estimated parameters is tested by varying each of them individually in the model. The rate determination is significantly more sensitive to the measured quantities than to the estimated ones. A pseudo-second order rate law (first order in both SO_2 and O_3 concentrations) is tested which reduces the scatter in the rate constant determination. Thus, the oxidation of SO_2 in the Los Angeles atmosphere is promoted by the photochemistry.

The model was used to determine the effect of the automobile upon sulfur concentrations at receptor sites such as Pasadena. The present automobile contribution to aerosol sulfur, as well as the projected contribution due to the introduction of the catalytic converter on new cars, is estimated. Also, an estimate of the pseudo-first order decay rate of sulfur dioxide for St. Louis, Missouri is made using data taken at Washington University.

3.1 MODEL DEVELOPMENT

In Los Angeles, the major stationary sources of SO_2 are power plant and refinery areas located along the coast. When a stable marine wind is established during the late morning, sulfur oxides are transported from these sources to downwind receptor sites. Additional quantities of sulfur oxides are emitted from industrial and automobile sources along the transport path.

For a detailed understanding of the time and emission history of aerosol samples taken at a receptor site, it is convenient to use an air trajectory technique such as that suggested by White, Husar and Friedlander (1973). From such an analysis, it is possible to determine the average position-time history of that air parcel and to calculate pollutant inputs during movements of the air from major source to receptor site. Once this has been done, such data can be used in the eulerian diffusion model which will be developed next.

Equation 3.1 is the semi-empirical equation of atmospheric diffusion in an eulerian system for the average concentration of component C; assuming that there is a steady wind in the x direction and zero

wind in the y (horizontal) and z (vertical) directions, that molecular diffusion can be neglected with respect to turbulent diffusion and that the turbulent diffusion term in the x direction, $\frac{\partial}{\partial x}\left[K_x \frac{\partial \bar{C}}{\partial x}\right]$ can be neglected with respect to the convective diffusion term in the x direction, $\bar{u} \frac{\partial \bar{C}}{\partial x}$.

$$\frac{\partial \bar{C}}{\partial t} + \bar{u} \frac{\partial \bar{C}}{\partial x} = \frac{\partial}{\partial y}\left[K_y \frac{\partial \bar{C}}{\partial y}\right] + \frac{\partial}{\partial z}\left[K_z \frac{\partial \bar{C}}{\partial z}\right] + R + S \qquad (3.1)$$

K_y and K_z are the eddy diffusivities in the y and z directions, respectively. The last two terms on the right hand side of this equation characterize chemical and physical changes which modify the existing species concentration: R is the rate of change of species C due to chemical reactions involving C, and S is the rate of change of species C due to sources and sinks. Note that $\bar{C}$, K_y, K_z, R, and S are all functions of x, y, z, and t.

A number of assumptions have been made just by writing Equation 3.1 in place of the exact equation (see Lamb, 1973); the time scale of chemical reactions must be "slow" with respect to the time scale of turbulence and the distribution of sinks and sources must be "smooth." Also, for the atmosphere, $k \ll 60$ hour^{-1} for a first order rate equation and spatial variations in $\bar{C}$ and S must occur over distances of 600 meters or larger. This last requirement would be violated near strong point and line sources.

Under the limitations stated above, Equation 3.1 can be written for each of two components, sulfur dioxide (SO_2) and total sulfur (S_T). This additionally assumes that total sulfur is the sum of gaseous sulfur (SO_2) and aerosol sulfur and that the turbulent diffusion of

aerosol sulfur can be characterized by the same eddy diffusivities as for sulfur dioxide.

$$\frac{\partial SO_2}{\partial t} + \bar{u}\frac{\partial SO_2}{\partial x} = \frac{\partial}{\partial y}\left[K_y \frac{\partial SO_2}{\partial y}\right] + \frac{\partial}{\partial z}\left[K_z \frac{\partial SO_2}{\partial z}\right] - kSO_2 + \frac{W_{SO_2}}{H} - \frac{v_g SO_2}{H} \quad (3.2)$$

$$\frac{\partial S_T}{\partial t} + \bar{u}\frac{\partial S_T}{\partial x} = \frac{\partial}{\partial y}\left[K_y \frac{\partial S_T}{\partial y}\right] + \frac{\partial}{\partial z}\left[K_z \frac{\partial S_T}{\partial z}\right] + \frac{W_{S_T}}{H} - v_g \frac{SO_2}{H} - v_a \frac{(S_T - SO_2)}{H} \quad (3.3)$$

Both SO_2 and S_T are expressed as sulfur mass concentration. The gas to particle conversion is expressed as a pseudo-first order reaction with rate constant k. The area source terms W_{SO_2} and W_{S_T} are expressed as volume terms using the mixing height H. Thus, the sources are assumed to become mixed uniformly up to the mixing height in a short time. The ground loss terms (sinks) are shown as the product of the deposition velocity (v_a for aerosol, v_g for SO_2) and the average concentration, divided by the mixing height.

Now, the SO_2/S_T ratio is assumed to be a function of x only. Georgii (1970) has shown that the SO_2/S_T ratio is not a function of z at low altitudes. The SO_2/S_T ratio is not a strong function of y because SO_2 (and S_T at SO_2/S_T ratios above 0.70) is determined mainly by automobile emissions and such emissions are distributed fairly uniformly with respect to position in Los Angeles (Roberts, et al., 1971). With $SO_2/S_T = g(x)$, the following substitution is made:

$$\frac{\partial}{\partial y}\left[K_y \frac{\partial SO_2}{\partial y}\right] + \frac{\partial}{\partial z}\left[K_z \frac{\partial SO_2}{\partial z}\right] - \frac{\partial SO_2}{\partial t} = g(x)\left\{\frac{\partial}{\partial y}\left[K_y \frac{\partial S_T}{\partial y}\right] + \frac{\partial}{\partial z}\left[K_z \frac{\partial S_T}{\partial z}\right] - \frac{\partial S_T}{\partial t}\right\} \quad (3.4)$$

Substituting into Equations 3.2 and 3.3 and rearranging, the result is:

$$\bar{u}\frac{dg}{dx} = -kg + \frac{g}{H}\left[\frac{W_{SO_2}}{SO_2} - \frac{W_{S_T}}{S_T} + \frac{S_T - SO_2}{S_T}(v_a - v_g)\right] \qquad (3.5)$$

Setting the travel time $T = x/\bar{u}$ and integrating along a known trajectory yields:

$$k = \frac{1}{\Delta T}\left\{-\ell n \frac{SO_2}{S_T}\Big|_{start}^{end} + \int_{start}^{end}\left[\frac{1}{H}\frac{W_{SO_2}}{SO_2} - \frac{W_{S_T}}{S_T} + \frac{S_T - SO_2}{S_T}(v_a - v_g)\right]dT\right\} \qquad (3.6)$$

For area automobile emissions, let the aerosol sulfur to total sulfur ratio be $f = (W'_{S_T} - W'_{SO_2})/W'_{S_T}$ where W'_{S_T} and W'_{SO_2} are the area source terms for the automobile only. Then 3.6 can be rewritten, assuming no aerosol sulfur from other emission sources, as:

$$k = \frac{1}{\Delta T}\left\{-\ell n \frac{SO_2}{S_T}\Big|_{start}^{end} + \int_{start}^{end}\left[\left(1 - \frac{SO_2}{S_T}\right)\left(\frac{v_a - v_g}{H} + \frac{W_{S_T}}{H\,SO_2}\right) - \frac{f\,W'_{S_T}}{H\,SO_2}\right]dT\right\} \qquad (3.7)$$

Because we do not know the value of S_T along the trajectory, Equation 3.7 must be solved by an iterative process. A value of k is chosen and then, starting at the beginning of the trajectory and proceeding at 1/2 hour intervals along the trajectory, successive SO_2/S_T ratios are calculated from the following equation:

$$\frac{SO_2}{S_T}\Big|_{i+1} = \frac{SO_2}{S_T}\Big|_{i} \exp\left\{(\Delta T)\left[-k + \left(1 - \frac{SO_2}{S_T}\Big|_i\right)\left(\frac{v_a - v_g}{\bar{H}} + \frac{W_{S_T}}{\bar{H}\,\overline{SO_2}}\right) - \frac{f\,W'_{S_T}}{\bar{H}\,\overline{SO_2}}\right]\right\} \qquad (3.8)$$

where i and i+1 are the beginning and end of the interval, and $\bar{H}$ and $\overline{SO_2}$ are the average values for that interval. The value of k is adjusted

until the SO_2/S_T ratio at the end of the trajectory matches the measured value. Equation 3.8 states that the SO_2 to S_T ratio at the end of an interval is equal to the SO_2 to S_T ratio at the beginning of that interval, modified by chemical reaction and sources and sinks at the ground during that interval. The SO_2/S_T ratio at the beginning and end of the trajectory and the values of W_{SO_2}, W_{S_T}, H, and SO_2 as a function of time (distance) along the trajectory are necessary for solution of Equation 3.7.

In effect, this calculation process is analogous to that of allowing the transport and source and sink processes (including chemical reaction) to proceed for each half hour interval along a given eulerian axis, and then slightly realigning that axis for the beginning of the next half hour interval. This realignment, due to the curved pattern of the wind field, will produce little error in this simple model, since such angles are less than about 10 degrees for the trajectories used in the following calculations.

In the above development, it has been intrinsically assumed that the sources emit at steady state for approximately the time period of sampling (one hour). This is a reasonable assumption, except near the time of peak load at the power plants (6-8 A.M. and 5-8 P.M.). None of the trajectories include power plant emissions from these time periods.

3.2 APPLICATION OF THE MODEL TO LOS ANGELES

The procedure for calculating the pseudo-first order rate of SO_2 loss described in the last section will be applied to known trajectories

from the coast to Pasadena. Intervals of 1/2 hour along a given trajectory will be used, beginning approximately 1/2 hour downwind of the major coastal sources of SO_2 and ending at the receptor site. Only samples whose trajectory clearly shows direct transport from the coastline will be used in the calculations. This is done because a long residence time over land (greater than 5 or 6 hours) introduces large errors in the emissions into that air parcel. This is essentially due to the inability of an air trajectory analysis to predict the air parcel location as a function of time, since wind speeds and directions are so small and variable in the early morning hours (before 9 or 10 A.M.). The usual establishment of a sea breeze at the coast in the mid-morning hours (10 to 11 A.M.) and the subsequent transport to downwind receptor sites can thus provide the basic meteorological regime needed to apply the model developed in section 3.1.

The trajectories were calculated by Warren H. White using surface wind streamline maps drawn up from the hourly wind direction and wind speed data available from the Los Angeles County Air Pollution Control District (LAAPCD) and the National Weather Service, a total of 19 stations in the western Los Angeles Basin. The trajectory calculation procedure is similar to that used by Angell, et al. (1972). The calculated trajectory for the 1500 PST sample on July 25, 1973 is shown in Figure 3.1. The other trajectories are included in Appendix B. The trajectories showed wind transport patterns similar to those determined by Angell, et al. (1972).

The mixing height, as a function of time and location, was obtained from Meteorology Research, Inc. data that were determined by vertical

Figure 3.1 The Calculated Trajectory for 1500 PST Arrival at Caltech on July 25, 1973

aircraft spirals and pibal data at various locations throughout the basin on the required days (Blumenthal, et al., 1975). The average SO_2 concentration for each interval along a known trajectory was determined using Los Angeles Air Pollution Control District monitoring data. The automobile contribution to W_{SO_2} and W_{S_T} was calculated by updating (to summer 1973) the average miles driven as a function of time of day and position in the Los Angeles basin (Roberts, et al., 1971) and using the average values of 0.075 weight percent sulfur and 11.2 miles per gallon for the Los Angeles area (U.S. Bureau of Mines, 1974 and Roberts, et al., 1971). The few small industrial sources of SO_2 inland of the coastal area (emission data from LAAPCD, 1974) are treated as area sources over the 2 mile by 2 mile grid square in which they are located. This network of grid squares is the same as that used by Roberts, et al. (1971). The values of the deposition velocities for aerosol and gas phase sulfur, v_a and v_g, were obtained from the literature. According to the experimental results of Chamberlain (1966), the deposition velocity for particles with diameters from 0.08 μm to 1.0 μm is v_a = 0.03 ± .005 cm/sec. This is the size range of the major portion of the sulfur aerosol. The value of v_g = 0.8 cm/sec (Shepherd, 1974) has been used for the deposition velocity of gaseous SO_2.

Also needed in the model are the SO_2/S_T ratios at the beginning and end of the trajectory. Total aerosol sulfur samples of 1 hour duration were taken on the roof of the W. M. Keck Laboratories during the daylight hours on July and October 1973. Gas phase sulfur and other parameters were also measured at the same time. These aerosol and gas phase sulfur measurements determined the SO_2/S_T ratio at Pasadena for

each trajectory (see Appendix A for a full listing of the atmospheric sulfur concentrations). Because of the many possible trajectory starting locations, it is difficult to measure the SO_2/S_T ratio at both ends of the same trajectory. However, five days were spent at the California State University at Dominguez Hills in October, 1973, to determine the near-source SO_2/S_T ratio and its variability. The sampling was conducted atop the mobil van being used for the ACHEX study (Hidy, et al., 1975). This sampling location is within 2 to 4 miles of about 50% of the stationary source SO_2 emissions in Los Angeles County and, under most wind conditions, receives air transported directly from these sources. Shown in Table 3.1 are the results of these measurements. Wind direction readings indicate that for the samples taken on October 5, 1973 and the first sample on October 3, 1973, the air was being transported from the area of the local sulfuric acid plant. The first sample on October 4, 1973 appeared to be transported to the sampling site from the west at a very slow velocity (less than 5 km/hr), indicating the possibility of a long residence time in the air. For all of the other sampling periods, the SO_2 concentration was at typical source-enriched levels of 30 to 65 ppb and the winds were from the west around to the southeast at fairly high velocities (average about 15 km/hr). The power plant and refinery locations were distributed in these directions. Thus, for non-sulfuric acid emissions, a near source SO_2/S_T ratio of about 0.96 is obtained from this data (time averaged value for all non-starred time periods in Table 3.1). Support for such a ratio for power plant emissions can be obtained from the literature. Studies made by Brookhaven National Laboratory indicate an SO_2/S_T ratio in the flue gas

TABLE 3.1

Values of the SO_2/S_T Ratio, Measured at California State University at Dominguez Hills*

Date(1973)	Time	SO_2/S_T
October 3	0916 - 1016	*0.82
	1017 - 1148	0.92
	1150 - 1335	0.98
October 4	0910 - 1021	*0.82
	1026 - 1125	0.91
	1129 - 1400	0.94
October 5	0837 - 0939	*0.89
	0943 - 1107	*0.85
	1112 - 1217	*0.88
	1221 - 1525	*0.80
October 10	1203 - 1406	0.97
October 11	0939 - 1100	0.97
	1104 - 1204	0.97
	1210 - 1403	0.98
	1407 - 1510	0.96
Time weighted average (all samples)		0.91
Time weighted average (non-* values)		0.96

*This indicates that a sample is assumed to be not relevant to the calculation of the beginning SO_2/S_T ratio (see text).

of an oil-fired power plant of 0.99 (Forrest, et al., 1973) to 0.98 (Manowitz, et al., 1970). Values in a coal-fired power plant were about 0.99 (Manowitz, et al., 1973), although Caffe and Gerstle (1967) obtained values as low as 0.95 for the SO_2/S_T ratio in the emissions of a coal-fired power plant. Pierson, et al. (1974) determined that more than 99% of the emitted sulfur from an automobile without a catalytic converter is SO_2 ($SO_2/S_T > 0.99$). Therefore, a value of SO_2/S_T = 0.97 has been used for the beginning ratio, since none of the trajectories pass near the sulfuric acid plant.

A computer program was used to calculate the area source contribution of sulfur to the air parcel as it moved along the calculated trajectory (see GRACER, Appendix D). Then these data, along with the average values of SO_2 and H for each 1/2 hour interval and the beginning and ending SO_2/S_T ratios, are used by a second program (LYNN, Appendix D) to calculate the pseudo-first order rate constant, k, via Equation 3.8.

3.3 RESULTS

The calculated pseudo-first order rate constant for each of 14 samples taken at Pasadena in July and October, 1973, is given in Table 3.2. The error indicated for each rate constant is that due to errors in the measured and estimated parameters, calculated using:

$$\sigma_k^2 = \sum_i \left(\frac{\partial k}{\partial x_i}\right)^2 \sigma_{x_i}^2 \qquad (3.9)$$

where each $\partial k/\partial x_i$ was determined numerically by varying x_i (with all other x_j constant, $j \neq i$) and calculating the resulting effect on k.

TABLE 3.2

Pseudo-First Order Rate Constants
for the Los Angeles Atmosphere (Equation 3.7)

Date (1973)	Time of Arrival at Pasadena (PST)	k (% hr^{-1})	Starting location
July 10	1300	1.2 ± 0.9	El Segundo
	1400	3.0 ± 1.7	El Segundo
	1500	10.0 ± 5.7	El Segundo
	1600	14.6 ± 8.9	El Segundo
July 25	1400	12.1 ± 2.0	Alamitos Bay
	1500	8.6 ± 3.4	El Segundo
	1600	10.3 ± 2.9	El Segundo
July 26	1200	5.2 ± 4.2	Alamitos Bay
	1300	5.1 ± 3.0	Alamitos Bay
	1400	8.1 ± 8.1	Alamitos Bay
	1500	4.6 ± 1.7	Alamitos Bay
October 4	1430	3.7 ± 1.4	El Segundo
	1530	5.5 ± 2.0	El Segundo
	1630	4.7 ± 2.3	El Segundo
Range		1 to 15	

The weighted, average value is k = 9% $hour^{-1}$. These rate constant values are the net result of all conversion mechanisms which may be converting SO_2 to aerosol sulfur in the daytime hours. Also indicated in Table 3.2 is the general starting location of each air trajectory (the calculated air trajectories are in Appendix B). The Alamitos Bay source-area consists of two large power plants, the El Segundo area of two power plants, plus a refinery. A value of 0.97 was used for the SO_2/S_T ratio just downwind of these sources, since neither included the sulfuric acid plant.

The sensitivity of these calculations of the pseudo-first order rate constant to the various parameters is illustrated in Table 3.3 for the 1500 PST sample of July 25, 1973. For each parameter used in the calculation, the calculated partial derivative of k with respect to that parameter is indicated. However, to compare the sensitivity of k to the various parameters, these derivatives must be made non-dimensional. The average value along the trajectory of the given parameter is used for this purpose. Thus, the last column in Table 3.3 is an indication of the relative sensitivity of k to each of the parameters (units of % hr^{-1}). The SO_2/S_T ratios at the beginning and ending of the trajectory are by far the most important in determining k; next come the SO_2 concentration and the SO_2 ground loss term, followed by the area source terms, the mixing height, and the aerosol ground loss term. With the exception of the beginning SO_2/S_T ratio, this sensitivity order is exactly the same as a listing of the variables in decreasing order of the confidence in their values; e.g., we have a good measure of the SO_2/S_T ratio at Pasadena, measurement of the SO_2 concentration at quite

TABLE 3.3

Sensitivity of the Calculated Pseudo-First Order Rate Constant to the Measured and Estimated Parameters*

Variable (x_i)	$\left.\frac{\partial k}{\partial x_i}\right\|_{\bar{x}_i}$	$\bar{x}_i$	$\left.\frac{\partial k}{\partial x_i}\right\|_{\bar{x}_i} \cdot \bar{x}_i$
SO_2/S_T (0)	3.8×10^{1}	0.97	3.7×10^{1}
SO_2/S_T (Pasadena)	4.6×10^{1}	0.75	3.4×10^{1}
$v_{aerosol}$ (m/hr)	5.4×10^{-2}	1.0	5.4×10^{-2}
v_{SO_2} (m/hr)	5.7×10^{-2}	25.2	1.5
W_{auto} (μgm SO_2/m^2hr)	9.1×10^{-4}	453.	4.1×10^{-1}
$W_{industrial}$ (μgm SO_2/m^2hr)	1.2×10^{-3}	609.	6.1×10^{-1}
Mixing Height (m)	1.4×10^{-3}	227.	2.3×10^{-1}
$[SO_2]$ (μgm SO_2m^3)	1.6×10^{-2}	218.	4.4

*Data for the 1500 PST July 25, 1973, sample are shown ($k = 8.6 \pm 3.4\%$ hr^{-1}). The units for k are % hr^{-1}.

a number of points along a given trajectory, a good estimate of the SO_2 deposition velocity from many literature studies, and reasonably good estimates of the mixing heights from vertical aircraft spirals. The beginning SO_2/S_T ratio and its variability was discussed in section 3.2 and, for these trajectories, is fairly well known. Graphic illustration of the changes in the calculated k, due to changes in the values of the SO_2/S_T ratio at the beginning and ending of the trajectory, is shown in Figures 3.2 and 3.3, respectively. This is also for the 1500 PST sample on July 25, 1973. Much flatter curves would be obtained for the other, less important, variables.

Figure 3.4 shows the pseudo-first order rate constant for each of the 14 samples, as a function of the average O_3 concentration along each trajectory. This O_3 concentration is an indication of the average photochemical reaction conditions during the transport of that air parcel to Pasadena. A weighted, least squares fit of the data yields:

$$k = -.031 + 0.68\ \overline{O_3} \qquad r = 0.75,\ \chi^2 = 16.5 \qquad (3.10)$$

where the units of k are $hour^{-1}$, and of $\overline{O_3}$, ppm. This shows that the rate of SO_2 oxidation increases with higher photochemical activity, as indicated by higher average O_3 concentrations.

The findings of Equation 3.10 suggest that the scatter in the calculated rate constants might be reduced by using a more complicated SO_2 conversion rate form, such as the one postulated by Cox and Penkett (1972). This reaction involves the oxidation of SO_2 by an intermediate of the O_3-olefin reaction with a rate law of the form:

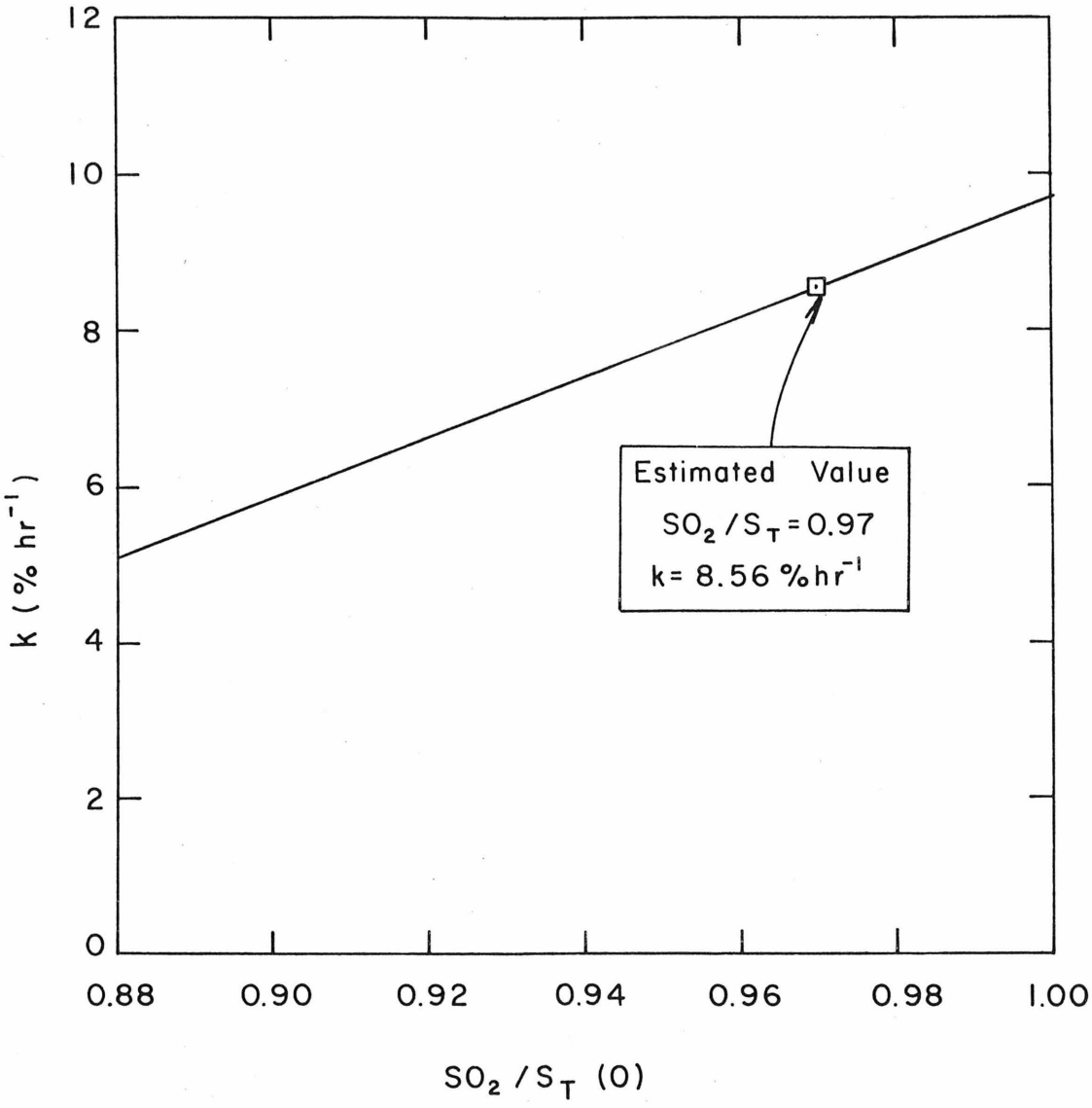

Figure 3.2 The Dependence of the Pseudo-First Order Rate Constant on the Beginning SO_2/S_T Ratio (1500 PST Arrival at Caltech on July 25, 1973)

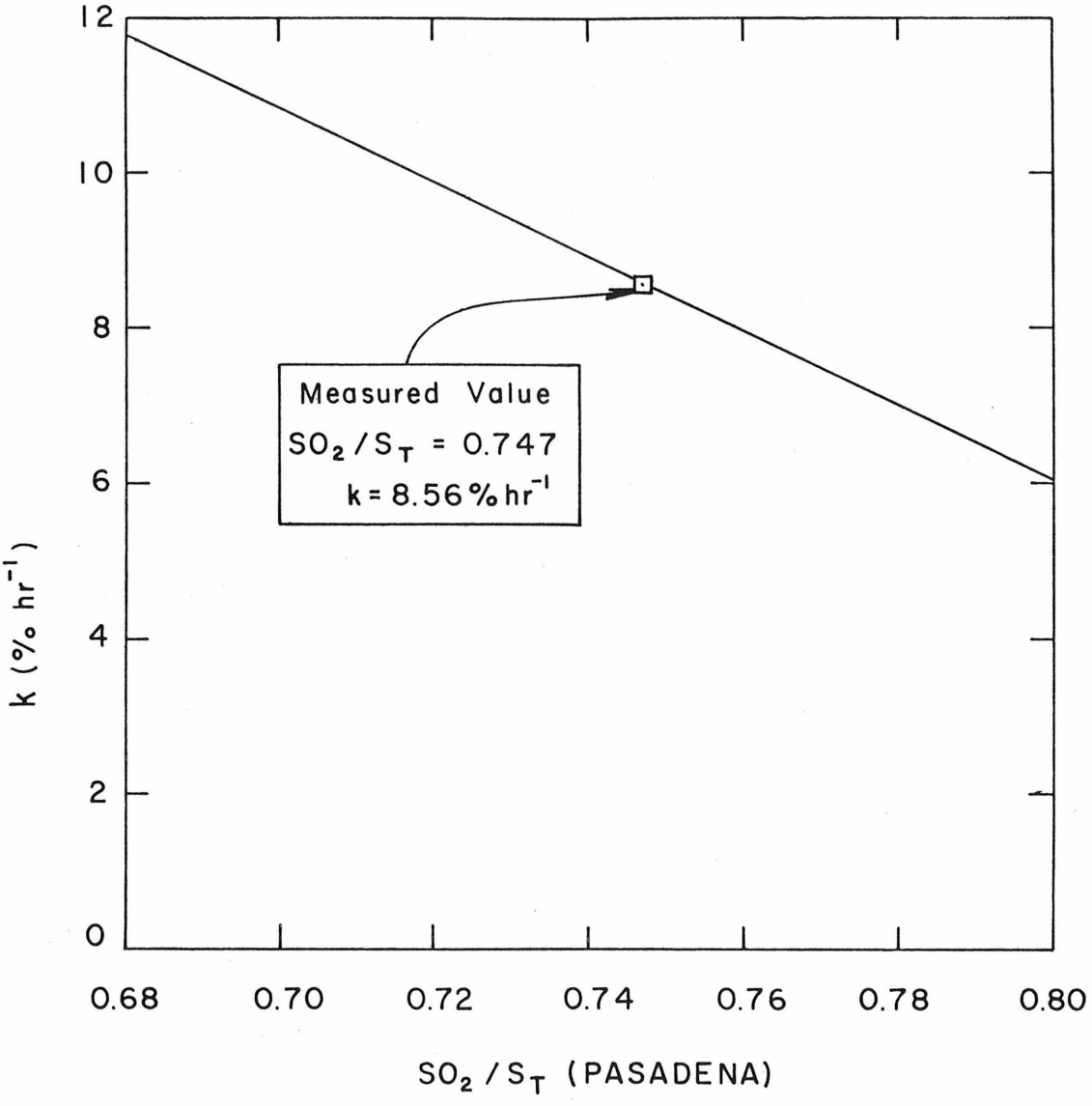

Figure 3.3 The Dependence of the Pseudo-First Order Rate Constant on the SO_2/S_T Ratio at Pasadena (1500 PST Arrival at Caltech on July 25, 1973)

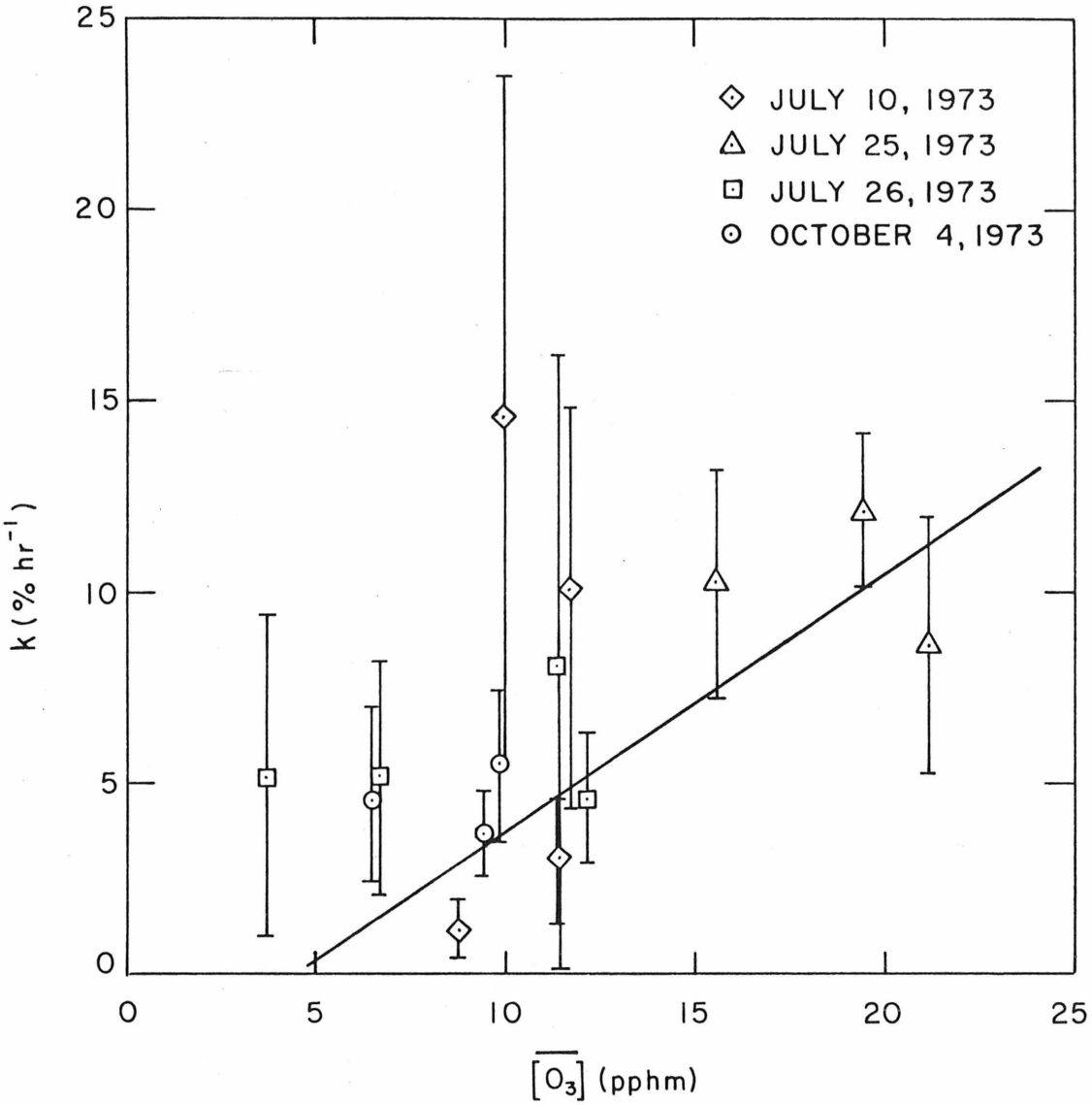

Figure 3.4 The Pseudo-First Order Rate Constant as a Function of the Average O_3 Concentration Along the Trajectory

$$\frac{d[SO_2]}{dt}_{\text{by reaction}} = -k_1 [O_3][\text{olefin}][SO_2] \qquad (3.11)$$

where $[SO_2] < 1.0$ ppm. Although good correlation for the Los Angeles atmosphere has been found between the total concentration of all C_3+ olefins and the total hydrocarbon concentration, the total hydrocarbon concentrations available along the trajectories (LAAPCD data) are just not sensitive enough for rate constant calculations. However, the olefin concentration can be lumped into the rate constant and the following rate law form tested:

$$\frac{d[SO_2]}{dt}_{\text{by reaction}} = -k_2 [O_3][SO_2] \qquad (3.12)$$

The results of putting this rate law form into Equation 3.2 and solving for k_2 are shown in Table 3.4. The weighted average value is $k_2 = 0.73$ ppm^{-1} hr^{-1}, very close to the value determined in Equation 3.10, using the pseudo-first order rate constant and the average O_3 concentration. The range of these pseudo-second order rate estimates is smaller than that of the pseudo-first order rate estimates shown in Table 3.2. This is an indication of the photochemically involved oxidation of SO_2 by a mechanism which would fit the rate law in Equation 3.12 (see section 4.5 for a discussion of this type of mechanism in a controlled smog chamber system). More than a single mechanism may be important in converting SO_2 to aerosol sulfur during the daylight hours. Thus, the following rate law form was tested, using a fixed k_c and calculating k_2':

TABLE 3.4

Pseudo-Second Order Rate Constants
for the Los Angeles Atmosphere (Equations 3.12 and 3.7)

Date (1973)	Time of Arrival at Pasadena (PST)	k_2 ($ppm^{-1}hr^{-1}$)	Starting Location
July 10	1300	0.17 ± 0.11	El Segundo
	1400	0.29 ± 0.14	El Segundo
	1500	0.94 ± 0.41	El Segundo
	1600	1.56 ± 0.71	El Segundo
July 25	1400	0.88 ± 0.17	Alamitos Bay
	1500	0.50 ± 0.16	El Segundo
	1600	0.82 ± 0.23	El Segundo
July 26	1200	1.45 ± 1.42	Alamitos Bay
	1300	0.82 ± 0.45	Alamitos Bay
	1400	0.77 ± 0.63	Alamitos Bay
	1500	0.41 ± 0.14	Alamitos Bay
October 4	1430	0.44 ± 0.15	El Segundo
	1530	0.61 ± 0.27	El Segundo
	1630	0.74 ± 0.40	El Segundo
Range		0.2 to 1.6	

$$\frac{d\,[SO_2]}{dt}_{\text{by reaction}} = -k_c - k_2' [O_3][SO_2] \qquad (3.13)$$

Changing k_c over the range 0.1 to 2.5 ppm/hr produced no improvement of the scatter of the calculated rate constant. Other plausible rate law forms involve concentrations of species not measurable or estimable along a trajectory and thus cannot be tested with this data.

3.4 RESULTS FOR ST. LOUIS, MISSOURI

Aerosol sulfur measurements were made at Washington University during September 1973 in cooperation with Regional Air Pollution Study (RAPS) preliminary investigations. The resulting SO_2/S_T ratios and trajectory measurements allow estimation of the maximum pseudo-first order rate constant for SO_2 in the St. Louis atmosphere. Sulfur concentrations in St. Louis are dominated by the major stationary sources outside the city. St. Louis is considered to have a non-photochemically involved air pollution problem, much like many U.S. cities other than Los Angeles. Assuming a SO_2/S_T ratio at the source of 0.97 and no sources or sinks along the transport path, the pseudo-first order rate constant is less than 2% per hour for the daylight samples on September 6, 1973 (SO_2/S_T ratios averaged 0.82). Figure 3.5 shows that the SO_2 and aerosol sulfur concentrations follow one another quite closely, indicating fairly consistent transport times from the source. The average O_3 concentration was below 0.08 ppm.

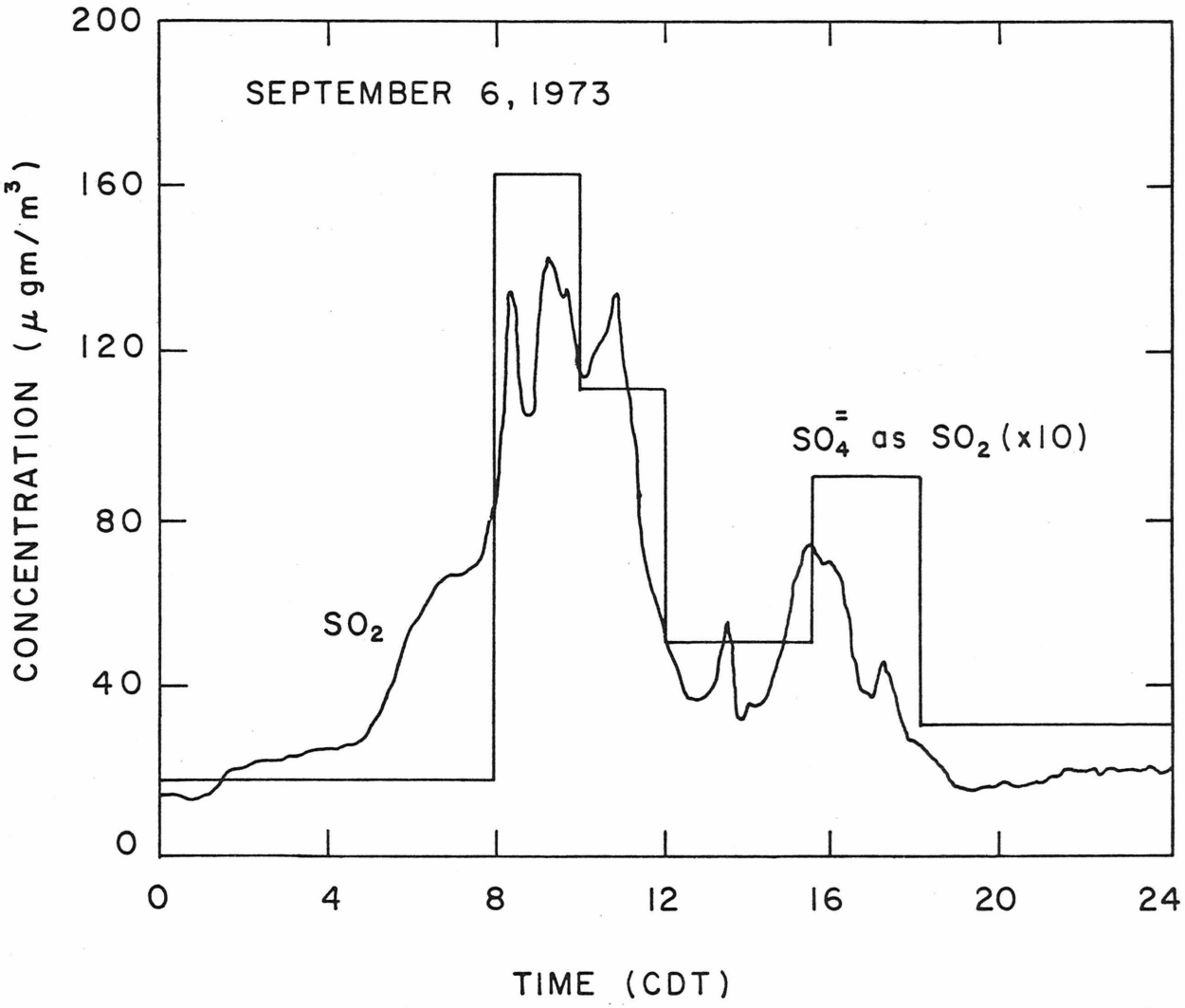

Figure 3.5 Diurnal Profile of SO_2 and Aerosol Sulfur at Washington University, St. Louis, Missouri on September 6, 1973

3.5 THE EFFECTS OF THE AUTOMOBILE ON AEROSOL SULFUR

The model developed in section 3.1 and the data used to calculate the pseudo-first order rate constants in section 3.3 can be used to estimate the present and future effects of the automobile upon aerosol sulfur concentrations (Roberts and Friedlander, 1975).

An estimate of the contribution of automobile emitted SO_2 to the aerosol sulfur at Pasadena can be made by substituting the rate constants shown in Table 3.2 into Equation 3.8 and eliminating the automobile area source term (i.e., use industrial area sources only). Comparison of the resulting SO_2/S_T ratio at Pasadena with the ratio actually measured determines the aerosol sulfur presently attributable to automotive origin. Such calculations for the same 14 samples indicate 2 to 11 percent of the measured aerosol sulfur at Pasadena resulted from conversion of auto-emitted SO_2. In contrast, 20 to 70 percent of the total sulfur at Pasadena came from automobile SO_2 emissions (estimated for the same 14 samples using the CO concentration as a tracer for automotive emissions). This is true, even though the automobile emits only about 15% of the total SO_2 in the Los Angeles basin, because such emissions are distributed fairly evenly throughout the basin. And because there is dilution, any SO_2 emitted late in a trajectory is given heavier weight than earlier emissions in determination of the total sulfur at the receptor site, but the shorter reaction time means a smaller weight in determination of the aerosol sulfur concentration.

Although the present contribution of automobile-emitted SO_2 to aerosol sulfur at a receptor site such as Pasadena is small, this effect

could be increased by the introduction of the catalytic converter on new automobiles. Besides oxidizing carbon monoxide and unburned hydrocarbons to less noxious gases, the catalytic converter has been found to promote the oxidation of SO_2 to SO_3 in the converter and emit sulfuric acid mist and sulfates directly. This could result in an increase in the sulfate concentrations both in areas of heavy traffic and at downwind receptor sites.

Figures 3.6 and 3.7 show the estimated increase in aerosol sulfur at Pasadena due to the conversion of SO_2 to H_2SO_4 in automobile catalytic converters. It is assumed that such vehicles use fuel that contains 0.03 wt. % sulfur, a quantity typical of present unleaded Los Angeles gasoline (United States Bureau of Mines, 1974). Figure 3.6 shows the increase in aerosol sulfur at Pasadena as a function of the fraction of the SO_2 converted to H_2SO_4 in the automobile converter, assuming all automobiles to have catalytic converters. This is calculated by adjusting the fraction converted (f) in Equation 3.7 for each of the 14 samples. The middle curve indicates the average response of the samples, while the shaded region shows the range of the response. The fraction converted is a complex function of driving speed and exhaust temperature (see California Air Resources Board Staff Report, 1975). It varies from about 35% for urban and 60 mph driving to 78% for 30 mph cruising. An average for Los Angeles driving patterns might be about 50%. At this level, the average calculations indicate an increase in the aerosol sulfur concentration at Pasadena of 1.5 μgm $SO_4^=/m^3$ or 8% over the average of 20 μgm $SO_4^=/m^3$. However, values up to twice this amount can be expected under some atmospheric conditions. Figure 3.7 shows

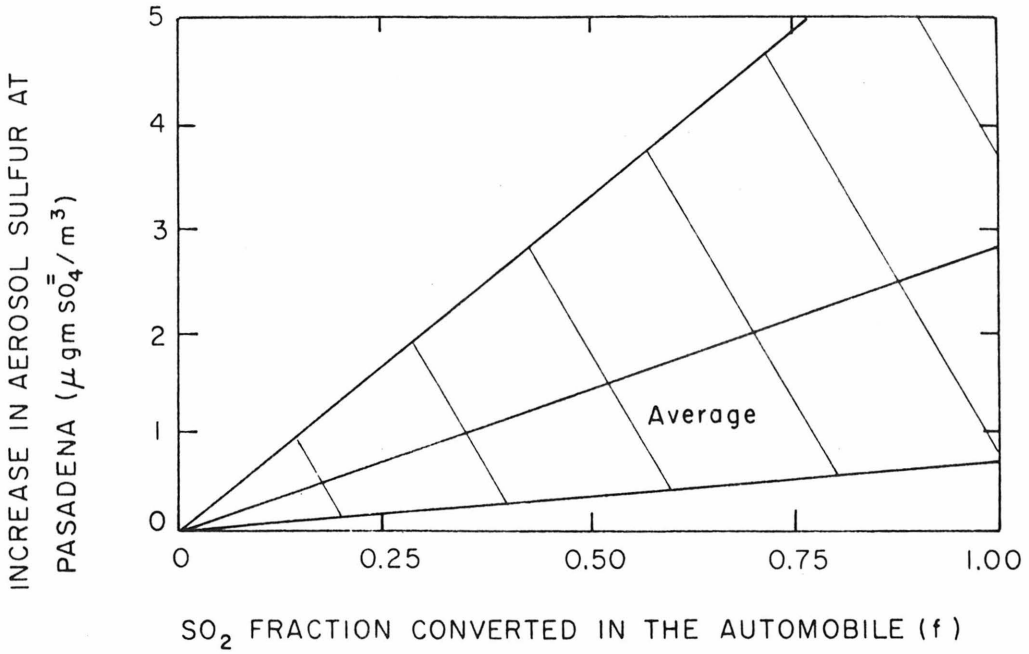

Figure 3.6 The Increase in Aerosol Sulfur at Pasadena as a Function of the Fraction of SO_2 Converted in Automobile Reactors. All Automobiles Assumed to be Equipped with Catalytic Converters. Gasoline Assumed to be 0.03 Weight Percent Sulfur.

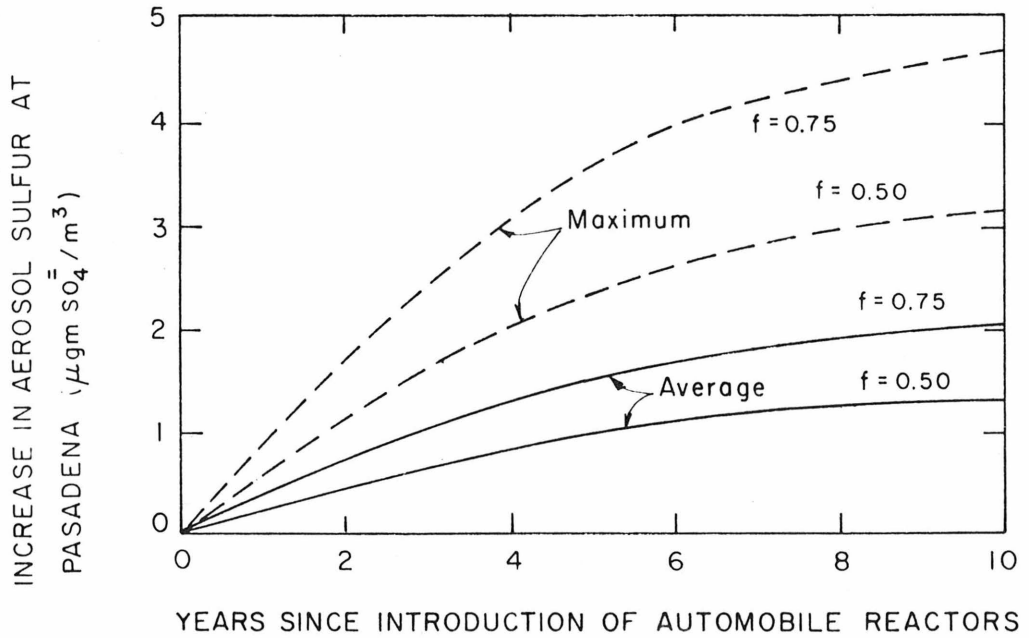

Figure 3.7 The Increase in Aerosol Sulfur at Pasadena as a Function of the Fraction of SO_2 Converted in Automobile Reactors with the Replacement Schedule Reported by Lees, et al., p. 128 (1972). Gasoline Assumed to be 0.03 Weight Percent Sulfur.

the dynamic effect of replacement of older automobiles without catalytic converters by those with such devices for the average and maximum curves in Figure 3.6 at two levels of the converted fraction (50% and 75%). This assumes the automobile birth-death schedule and average vehicle mileage as a function of age for Los Angeles County given by Lees, et al. (1972). This must be taken into account, since newer cars are driven more miles per year than older ones. Figure 3.7 indicates that, even in the worst conditions, introduction of catalytic converters will have little effect on the aerosol sulfur at downwind receptor sites such as Pasadena during the first few years. However, larger effects will occur as the system approaches that of all automobiles having catalytic converters.

Local receptor effects of the oxidation catalytic converters must be considered along with the downwind receptor effects estimated above. Table 3.5 shows estimated sulfate concentrations due to the conversion of SO_2 to H_2SO_4 in automobile reactors, using measured CO concentrations as a tracer for automobile emissions and assuming all automobiles to have such reactors. These concentrations are in addition to other sulfates already existing in the air. Although they show some variance in the estimated sulfate concentrations, both the 7-mode and CVS carbon monoxide emission factors result in a substantial addition to the aerosol sulfur burden close to high density automobile traffic. These high concentrations would pose a significant threat to human health and thus constitute the major problem due to the introduction of catalytic converters on new automobiles.

TABLE 3.5

Estimated Aerosol Sulfur Concentrations Near Roadways Due to 50% of the Automobile-Emitted SO_2 Being Converted to Aerosol in Automobile Reactors.*

Level of [CO]	[CO](ppm)	Estimated $[SO_4^=]$($\mu gm/m^3$)	
		(CO by 7-mode)	(CO by CVS)
L.A. average - summer 1973	4	5.	3.
L.A. average - winter 1972	6	7.	5.
L.A. daily max average - winter 1972	17	20.	13.
Average near freeway at rush hour	25	30.	19.
LAAPCD first stage alert	50	60.	39.

*All automobiles are assumed to be equipped with such reactors. Unleaded fuel is assumed to be 0.03 wt. % S.

3.6 SUMMARY

A simple diffusion model has been developed to determine the rate of oxidation of sulfur dioxide in the Los Angeles atmosphere. Air trajectory analysis provided time-location history information for air parcels sampled at Pasadena in July and October, 1973. The resulting pseudo-first order rate constant average for the fourteen one-hour samples was 9 percent per hour, with a range from 1 to 15 percent per hour. This rate was found to depend on the average ozone concentration along the trajectory. In fact, a pseudo-second order rate law (first order in both SO_2 and O_3 concentrations) was found to significantly reduce the scatter in the calculated rate constant. The pseudo-second order rate constant average was 0.7 $ppm^{-1}\ hr^{-1}$, with a range from 0.2 to 1.6 $ppm^{-1}\ hr^{-1}$. A lower pseudo-first order rate constant was estimated for the St. Louis, Missouri atmosphere: a maximum of 2 percent per hour for four samples taken September, 1973. These results indicate that sulfur dioxide is oxidized at a rate significantly higher in Los Angeles than in St. Louis, because there are higher levels of photochemical activity present in Los Angeles.

The present and future effects of the automobile on sulfur air quality also was examined. Presently, the automobile contributes little to the aerosol sulfur at a downwind receptor site such as Pasadena. An increase of about 8% in the aerosol sulfur concentration at Pasadena is estimated for average conditions after the introduction of the catalytic converter. However, a substantial increase in aerosol sulfur

concentrations near roadways is predicted due to the sulfuric acid emissions of catalytic converter-equipped automobiles.

CHAPTER 4

SMOG CHAMBER STUDIES

The particle size distribution of sulfur in atmospheric aerosol particles is important; both long- and short-term health hazards of aerosol sulfur (Finklea, et al., 1974) are dependent upon the sulfur size distribution. Visibility reduction by particulate matter, sulfate or otherwise, is dependent upon its size distribution (White and Roberts, 1975).

Smog chamber experiments were carried out to study the mechanism of aerosol sulfur formation and to determine the sulfur size distribution as a function of time. An olefin, NO, NO_2, and SO_2 were added to ambient air, resulting in the formation of organic and sulfur aerosol when irradiated with natural sunlight. The sulfur size distribution function was measured at five successive times during an experiment using a low pressure cascade impactor. Analysis of the collected samples was carried out using the aerosol vaporization technique discussed in Chapter 2.

A general reaction scheme for aerosol formation in the 1-heptene-NO_x-SO_2 system is presented. Analysis of data obtained in such a chemical system confirms that the aerosol sulfur and most of the aerosol carbon is formed in a reaction between a reactive photochemical intermediate and sulfur dioxide.

4.1 SYSTEM DESCRIPTION

The smog chamber experiments were conducted on the roof of the Keck Laboratories at Caltech in a Teflon bag (volume-to-surface ratio of 1. to 0.05 m). The roof is 52 feet above the street level. To make the bag, FEP Teflon film panels (10, each 54 in. x 28 ft. x 0.002 in.) were heat sealed together and the seams reinforced with mylar tape. Teflon was used because of its transparency to solar radiation (transmittance of greater than 75% of the ultraviolet, 92% of the visible, and 94% of the infrared) and its chemically inert nature (DuPont, 1966). The bag has the shape of a pillow sealed at both ends. The bag was filled with ambient Pasadena air through a hole in the end of the bag using an 11-inch diameter attic fan. The hole was then sealed with a plexiglass clamp. Pollutant addition and continuous sampling were accomplished through two identical Teflon ports at ground level on one side of the bag. Teflon was the only material that contacted the air inside the bag. Ropes across a wooden frame (held two feet off the ground by cinder blocks) supported the bag (see Figure 4.1). Air circulating under the bag kept the maximum temperature attained inside the bag below 42^{o}C. The bag was retained in place by a fishing net. Wind action on the bag and a slight temperature gradient(produced naturally within the bag) kept the contents mixed during an experiment.

Chemicals were injected into the bag through the injector port with an auxiliary pump adding additional air to speed mixing. Using the auxiliary pump, complete mixing of added pollutants was obtained in

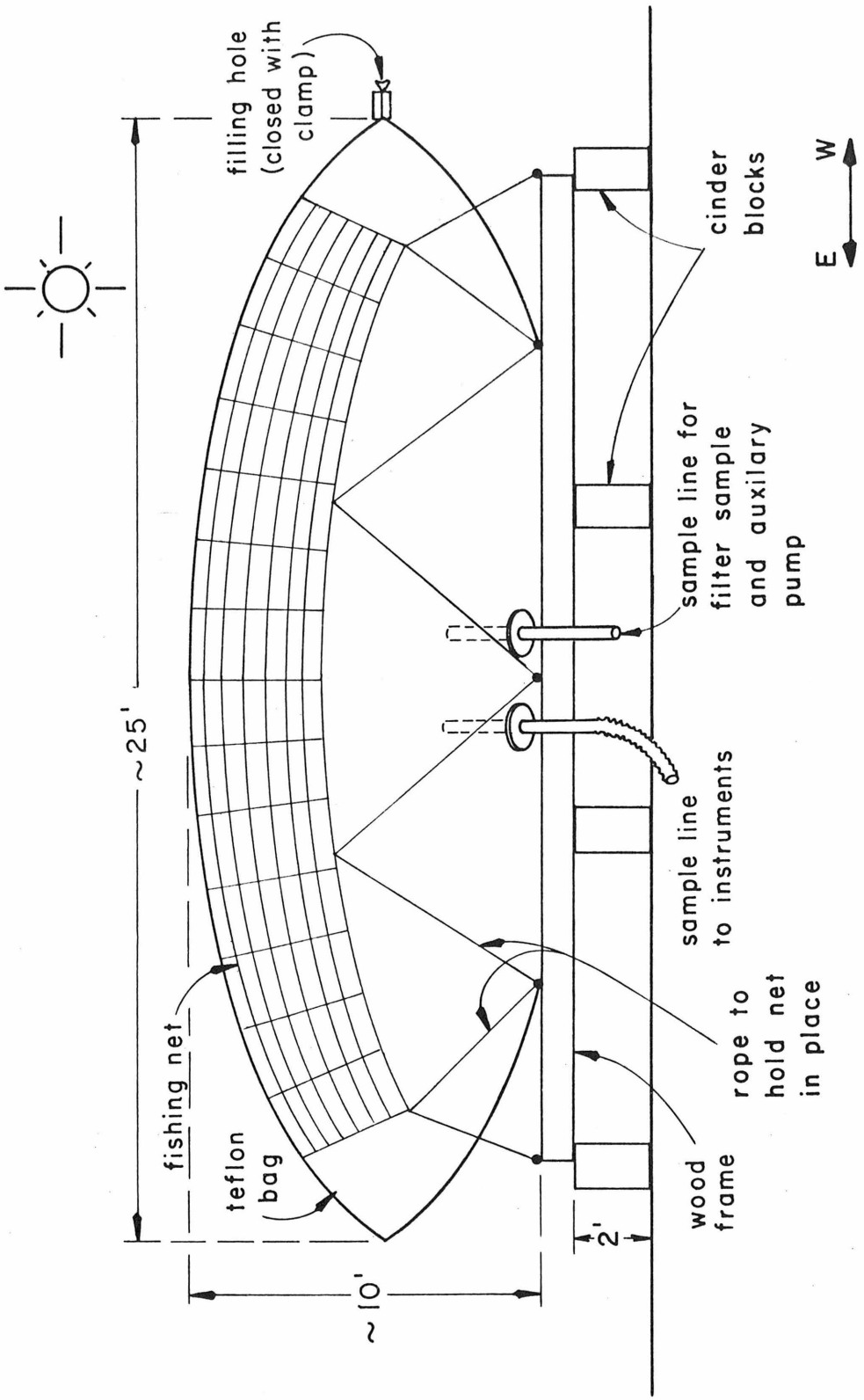

Figure 4.1 Diagram of the Smog Chamber and Supporting Apparatus

approximately five minutes. Air for measurements was withdrawn continuously through a Teflon sampling tube that reached four feet into the middle of the reaction vessel. A 20-foot section of flexible black Teflon tubing (1 inch I.D.) carried the air to a glass manifold from which each instrument could sample for analysis. The measured response time of this sampling system was 20 seconds.

Continuous measurements were made of the following parameters, recorded with a digital printer: ozone, sulfur dioxide, condensation nuclei, b_{scat}, temperature, dew point, and broad band solar radiation. Total hydrocarbons, methane, and carbon monoxide were also measured once every five minutes through an extra Teflon sampling tube at the end of the bag. Particles above 0.30 μm in diameter were measured as a function of time with an optical particle counter. A description of the instruments and their characteristics is provided in Table 4.1. Calibration of the gas phase instruments was performed before each series of experiments. A chemiluminescent NO_x monitor (Bendix Corp., Model 5513802 with a gold catalyst) also was used in the experiments, but both the NO and NO_x modes of the instrument showed interferences from other substances (see Winer, et al., 1974). Thus, no values are reported for NO_x concentrations.

The chemiluminescent O_3 monitor (REM, Inc.) was calibrated using the California Air Resources Board recommended procedure. However, in light of the recent findings of the Ad Hoc Oxidant Measurement Committee of the California Air Resources Board (Demore, et al., 1975), the instrument was cross-calibrated with a Dasibi UV photometer (Model 1003-AH) that had been calibrated against the committee's secondary O_3 standard. The 1:1 linear

TABLE 4.1

Description of the Instruments Used to Determine Concentrations in the Smog Chamber Experiments.

Measured Parameter	Measurement Principle (Calibration Method)	Instrument Make and Model
b_{scat}	extinction coefficient due to light scattering (Freon)	Meteorology Research Inc.,Model 1550. Integrating Nephelometer*
condensation nuclei	expansion cloud chamber-light scattering	Environment One Corp. Model Rich 100
particles $\geq$ .3 μm	optical light scattering (polystryene latex spheres)	Modified Climet Instruments Model CI-207 Particle Analyzer
O_3	chemiluminecence reaction with ethylene (neutrally buffered potassium iodide solution, later corrected to UV photometry standard)	REM, Inc. Model 612 Atmospheric Ozone Monitor
Total hydrocarbons, methane, CO	gas chromatography - flame ionization detector (certified gases)	Beckman Instruments Model 6800 Air Quality Chromatograph†
SO_2	flame photometry (SO_2 permeation tube)	Meloy Labs Model SA-120 Sulfur Gas Analyzer
temperature	thermocouple	YSI Tele-Thermoeter Model 43-TC
dew point	thermoelectric sensor	E G & G Model 880-CI Dew Point Hygrometer†
solar radiation	broad band pryoheliometer	Epply Pryoheliometer, No. 2977

*Loan courtesy of Meteorology Research, Inc.; †Loan courtesy of the California Air Resources Board.

relationships between each of the instruments result in the following:

$$[O_3]_{UV\ std.} = 0.73 + 0.765\ [O_3]_{REM} \qquad (4.1)$$

where the O_3 concentrations are in pphm. This relationship is consistent with the committee's findings with respect to the relationship of the absolute O_3 concentration to the O_3 concentration as measured by an instrument calibrated with a neutrally buffered KI solution. All O_3 concentrations in this thesis are corrected according to Equation 4.1.

The concentration of 1-heptene was determined using the total hydrocarbon mode of the gas chromatograph. The flame ionization detector does not respond to the oxygenated products expected from reactions of an olefin in photochemical smog (Scott, 1974). Therefore, all changes in total hydrocarbon response were assumed to be 1-heptene concentration changes.

Aerosol samples were taken at the injection port using both a 47-mm in-line filter holder and a cascade impactor. The vaporization technique described in Chapter 2 was used to measure the aerosol sulfur. A Dohrman model DC-50 Total Carbon Analyzer was used to measure the aerosol carbon collected on glass fiber filters by a technique described by Grosjean (1975). The term "aerosol carbon" is used to denote the concentration of carbon containing species in the aerosol (expressed as carbon), not the concentration of elemental carbon in the aerosol.

The procedure for a typical experiment was as follows: the bag was filled and emptied at least three times to remove residuals from the last experiment, filled about three-fourths full (all with the fan) and then the end filling-hole was sealed off. The auxiliary pump was then

used to fill the bag completely and mix the injected pollutant gases. NO was added first, in at least the concentration necessary to eliminate any ambient O_3 present; thus, any reactions of SO_2 or hydrocarbon with O_3 were prevented at the high concentrations present before complete mixing. NO_2 and SO_2 were added next and allowed to become mixed completely (about five minutes) before the hydrocarbon was added. After complete mixing of the hydrocarbon, the auxiliary pump was shut off and the aerosol sampling train was attached to that Teflon port. Monitoring of the progress of the bag run was continued until the bag volume had been reduced to about one-tenth of the initial volume. If the bag was sampled until the volume was exhausted, a drastic decrease in particle number caused by wall losses was evident when the volume was less than about 5 m^3.

4.2 SUMMARY OF THE EXPERIMENTS

Experiments were carried out in the Teflon bag with sulfur dioxide, nitric oxide, nitrogen dioxide, and the following olefins: cyclohexene, 2-methyl 2-butene, 1-heptene, 2,3 dimethyl 2-butene, and 1,7 octadiene. Also, a few experiments were run with the addition of SO_2 alone to ambient Pasadena air. A summary of the experiments, showing initial conditions and the resulting maximum O_3 concentration, change in b_{scat}, and range of the rate of SO_2 loss, is given in Table 4.2. The hydrocarbon 1-heptene was studied most extensively because it represents the middle range organics present in the atmosphere (it both forms organic aerosol and promotes formation of sulfur aerosol) and because it decays at a rate that allows study over a period of two to three

TABLE 4.2

SO_2 Smog Chamber Summary

Run No.	Hydrocarbon	$[HC]_o$ (ppm)	$[NO]_o$ (ppm)	$[NO_2]_o$ (ppm)	$[SO_2]_o$ (ppb)	Δb_{scat} ($10^{-4} m^{-1}$)	k^* ($\%hr^{-1}$)	$[O_3]_{max}$ (pphm)	%RH	T (^oC)
A.92	cyclohexene	0.72	0.23	0.12	46.	7.9	38	78	40	30
B.92	2-methyl 2-butene	0.08	0.17	0.	80.	0.	0	5	35	36
C.04	1-heptene	0.89	0.20	0.20	0.	2.4	0	53	45	31
C.91	1-heptene	0.91	0.10	0.	40.	6.3	25-56	37	20	38
C.93	1-heptene	1.10	0.21	0.10	41.	0.5	30	100	30	40
C.94	1-heptene	2.26	0.23	0.11	45.	9.0	24-90	65	29	35
C.95	1-heptene	1.85	0.19	0.10	39.	9.5	25-82	41	16	35
C.96	1-heptene	1.66	0.10	0.10	80.	14.5	21-99	33	14	38
C.97	1-heptene	1.47	0.20	0.11	86.	14.0	27-72	26	16	36
E.91	2,3 dimethyl 2-butene	0.67	0.25	0.13	50.	0.	90	81	35	35
F.91	1,7 octadiene	0.46	0.21	0.21	41.	> 27.2	17-35	138	20	38
Z.91	ambient air	0.	0.	0.	93.	-0.2	0	32	26	36
Z.92	ambient air	0.	0.	0.	103.	-1.0	7	46	20	38
Z.93	ambient air	0.	0.	0.	122.	-0.7	11	54	24	39

*pseudo-first order rate constant for SO_2 loss: $\frac{d[SO_2]}{dt} = -k[SO_2]$

hours. The concentrations of O_3, NO, NO_2, and SO_2 present in these experiments are comparable to ambient concentrations in Los Angeles. However, olefin concentrations are higher than those measured in the atmosphere. The 15-30% relative humidity values are typical of afternoon photochemical smog in Los Angeles. Total filter samples for aerosol chemical analysis were taken as a function of time during 1-heptene experiments C.93, C.94, C.95, C.96, and C.97. Impactor measurements were made at 15 to 20 minute intervals for experiments C.95, C.96, and C.97. A complete listing of the aerosol chemical data is given in Appendix A.

4.21 Bag Volume Calculations

Independent measurements of the bag volume can be made using the injected volume and measured initial concentration of either SO_2 or of 1-heptene. For the 13 experiments shown in Table 4.2, the average initial volume using the initial SO_2 concentration was 96 ± 11 cubic meters. Using the initial 1-heptene concentrations for C.93 through C.97, the average initial volume was 98 ± 18 cubic meters. The spread in the measurement resulted because the bag was not filled to exactly the same volume each time. The initial volume for each experiment (calculated using the initial SO_2 concentration) is used to calculate the initial concentrations of NO, NO_2, and the hydrocarbon (if the gas chromatograph was not in operation).

4.22 Sulfur Mass Balance in the Bag

The measurements of gas and aerosol phase sulfur during runs C.95 through C.97 were used to calculate sulfur recovery. Table 4.3 shows the overall sulfur recovery (the sum of SO_2 and particulate sulfur) to

be between 98 and 100% for the three experiments. Each is the average of five or six total filter samples and the corresponding gas phase SO_2 concentrations. The initial value is the SO_2 concentration just after the auxiliary filling pump has been turned off.

Another way to examine the measured sulfur mass balance is to compare the measured particulate sulfur with the calculated particulate sulfur concentration using the initial SO_2 concentration and the decaying SO_2 concentration values. This is done in Table 4.4 and in Figures 4.2, 4.3, and 4.4. Only the last two particulate sulfur values are used for Table 4.4, because the values actually include cumulative loss throughout the experiment. The aerosol sulfur recoveries of 104 to 107% for experiments C.95 to C.97 are excellent. Figures 4.2, 4.3, and 4.4 graphically show the particulate sulfur concentration as a function of time during experiments C.95, C.96, and C.97. There is excellent agreement between the values calculated from the continuous SO_2 concentration and the measured values.

4.3 EXPERIMENTS WITH 1-HEPTENE

A set of runs was made with 1-heptene because preliminary experiments showed that it promotes conversion of SO_2 to particulate phase sulfur, and is itself converted to organic aerosol, unlike smaller olefins (Harkins and Nicksic, 1965). The starting conditions and other pertinent information for the 1-heptene experiments C.04, C.91, and C.93 through C.97 are given in Table 4.2. Continuous concentration profiles of SO_2, 1-heptene, O_3, b_{scat}, and CNC (condensation nuclei count) are given in Figures 4.5 through 4.11 for these experiments. On

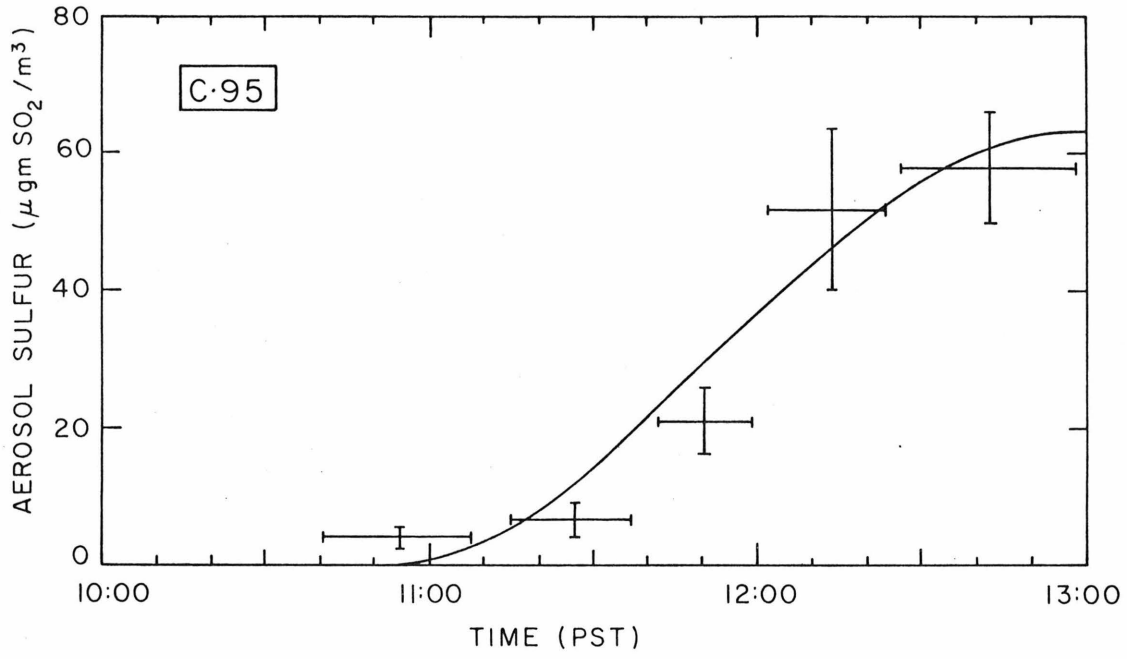

Figure 4.2 Comparison of Measured and Calculated Aerosol Sulfur Concentrations for Experiment C.95. The Calculated Values (solid line) Were Obtained by Difference from Continuous Readings of the SO_2 Concentration.

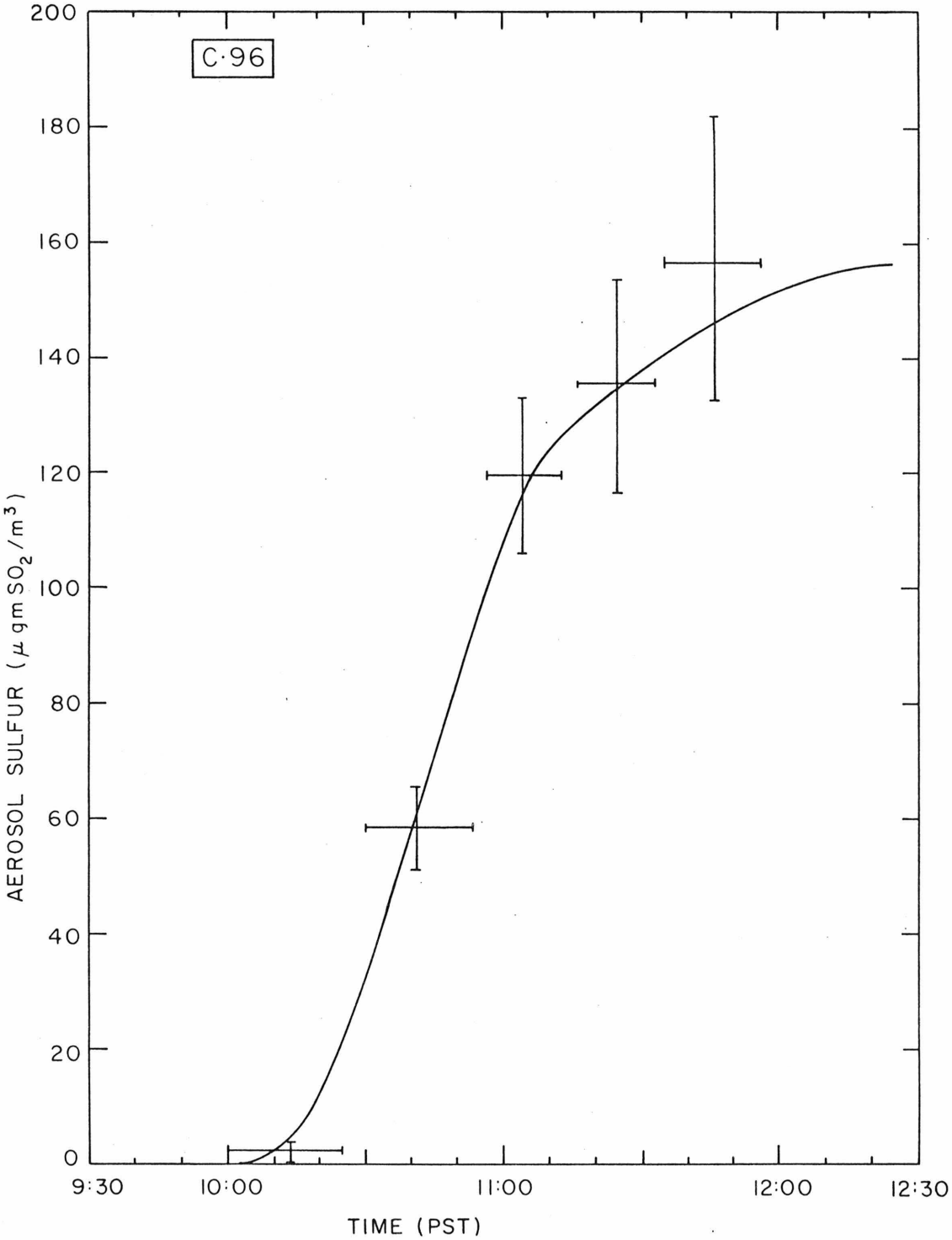

Figure 4.3 Comparison of Measured and Calculated Aerosol Sulfur Concentrations for Experiment C.96. The Calculated Values (solid line) Were Obtained by Difference from Continuous Readings of the SO_2 Concentration.

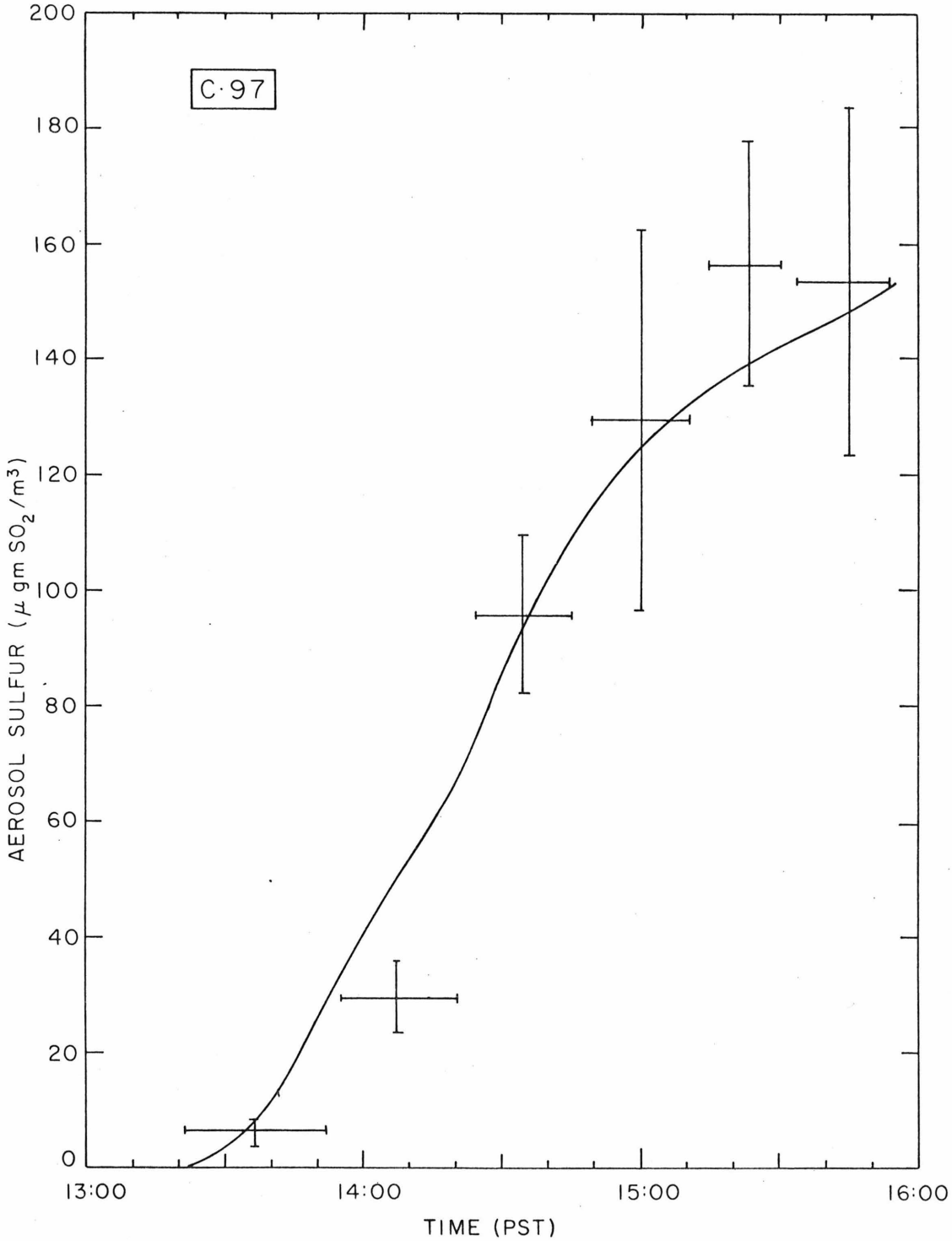

Figure 4.4 Comparison of Measured and Calculated Aerosol Sulfur Concentrations for Experiment C.97. The Calculated Values (solid line) Were Obtained by Difference from Continuous Readings of the SO_2 Concentration.

each figure is noted the time of injection of the NO, NO_2, SO_2 and 1-heptene.

A general discussion of the features of the 1-heptene experiments follows with C.95 as the major example (Figure 4.9). The initial decay in the SO_2 concentration, before the 1-heptene was added, was the result of dilution from the auxiliary filling pump. The SO_2 decay was slight until the O_3 concentration became larger than 5 pphm, at which point there was a sharp downward trend in the SO_2 concentration. This behavior was observed in each of the experiments with SO_2 and is indicative of the involvement of the photochemistry in the oxidation of SO_2. The variation of the condensation nuclei concentration in experiment C.95 was especially interesting. There were three regimes of new particle formation: first, the large increase in the nuclei concentration just after the introduction of SO_2; second, another large increase in nuclei after the introduction of the 1-heptene; and third, the sharp drop in nuclei concentration accompanying the increase in the SO_2 oxidation rate and the O_3 concentration rising above 5 pphm. All three regimes were not visible in all of the experiments because many times the 1-heptene was introduced shortly after the SO_2. However, all experiments show the sharp drop in the nuclei concentration when the O_3 is above 5 pphm. In fact, this also corresponds to the beginning of the 1-heptene decay by reaction. An increase in b_{scat} (decrease in visibility) usually began about 20 minutes after the O_3 concentration had gone above 5 pphm.

Thus, two major regimes were observed in these smog chamber experiments: first, SO_2, O_3, 1-heptene, and b_{scat} are constant as the NO is converted to NO_2; and second, O_3 induces decay of both SO_2 and 1-heptene

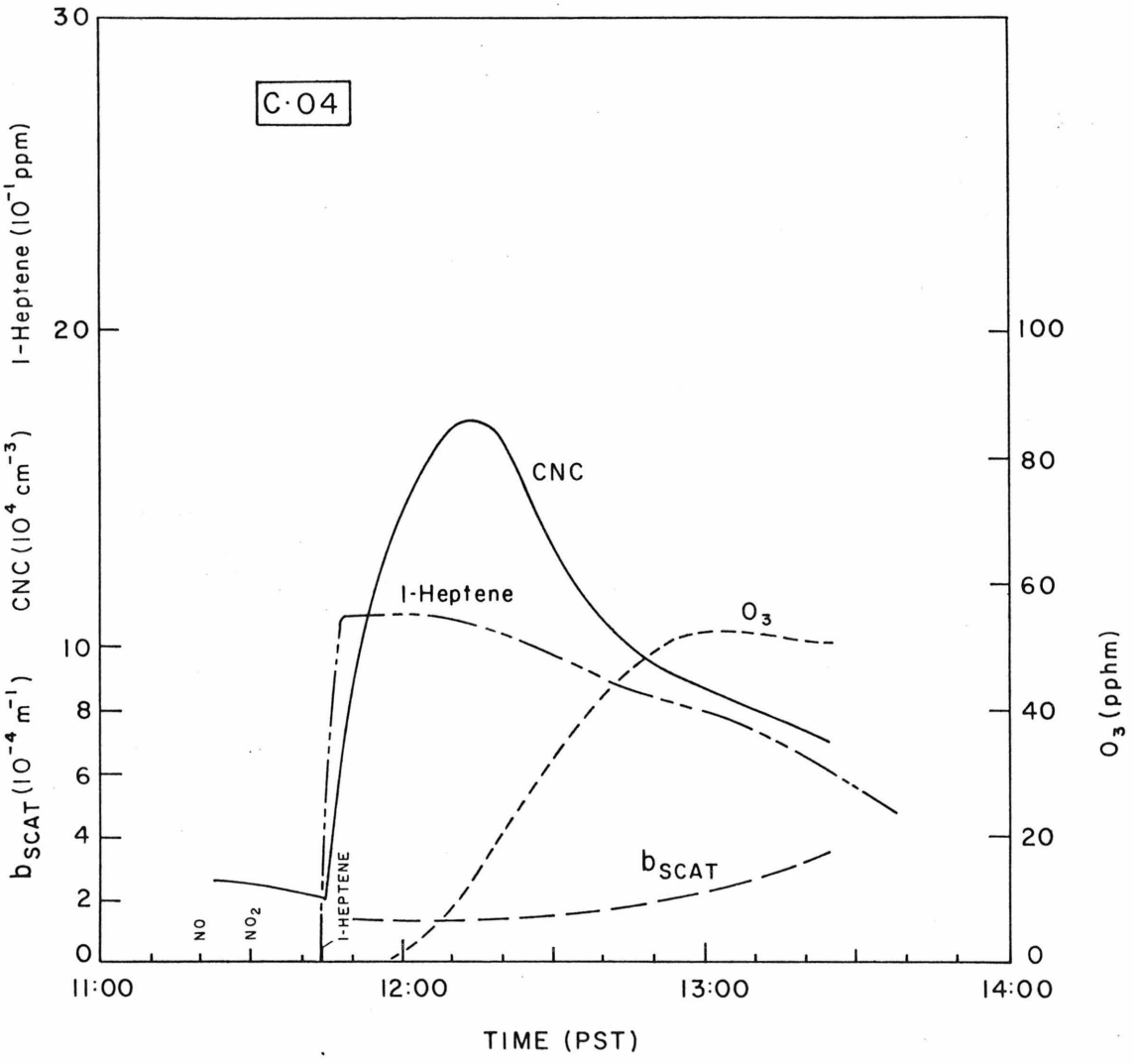

Figure 4.5 Concentration and Light Scattering Profiles for Experiment C.04. (Average of 45% RH and 31°C, no SO_2 added.)

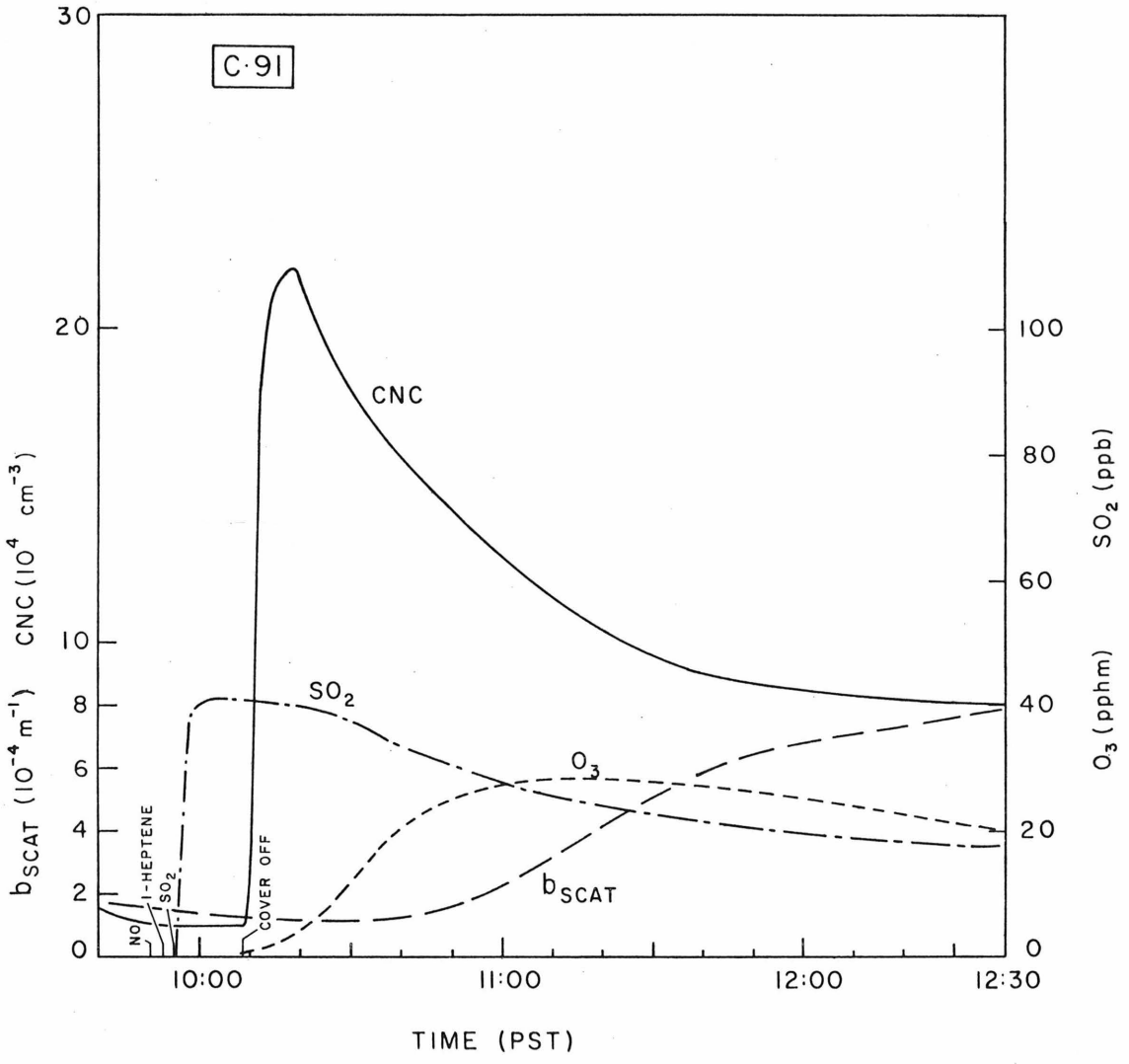

Figure 4.6 Concentration and Light Scattering Profiles for Experiment C.91. (Average of 20% RH and 38°C.)

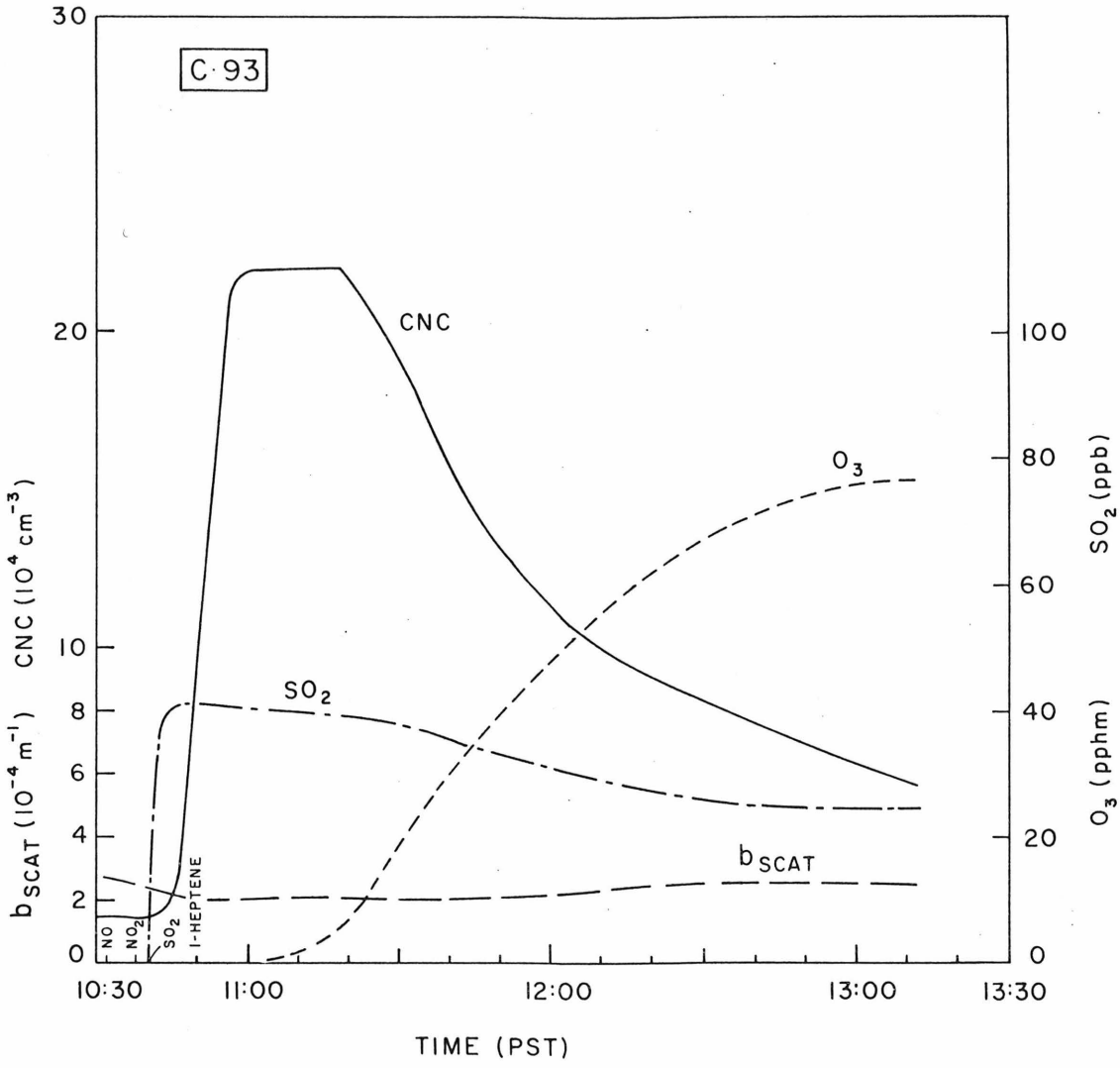

Figure 4.7 Concentration and Light Scattering Profiles for Experiment C.93. (Average of 30% RH and 40°C.)

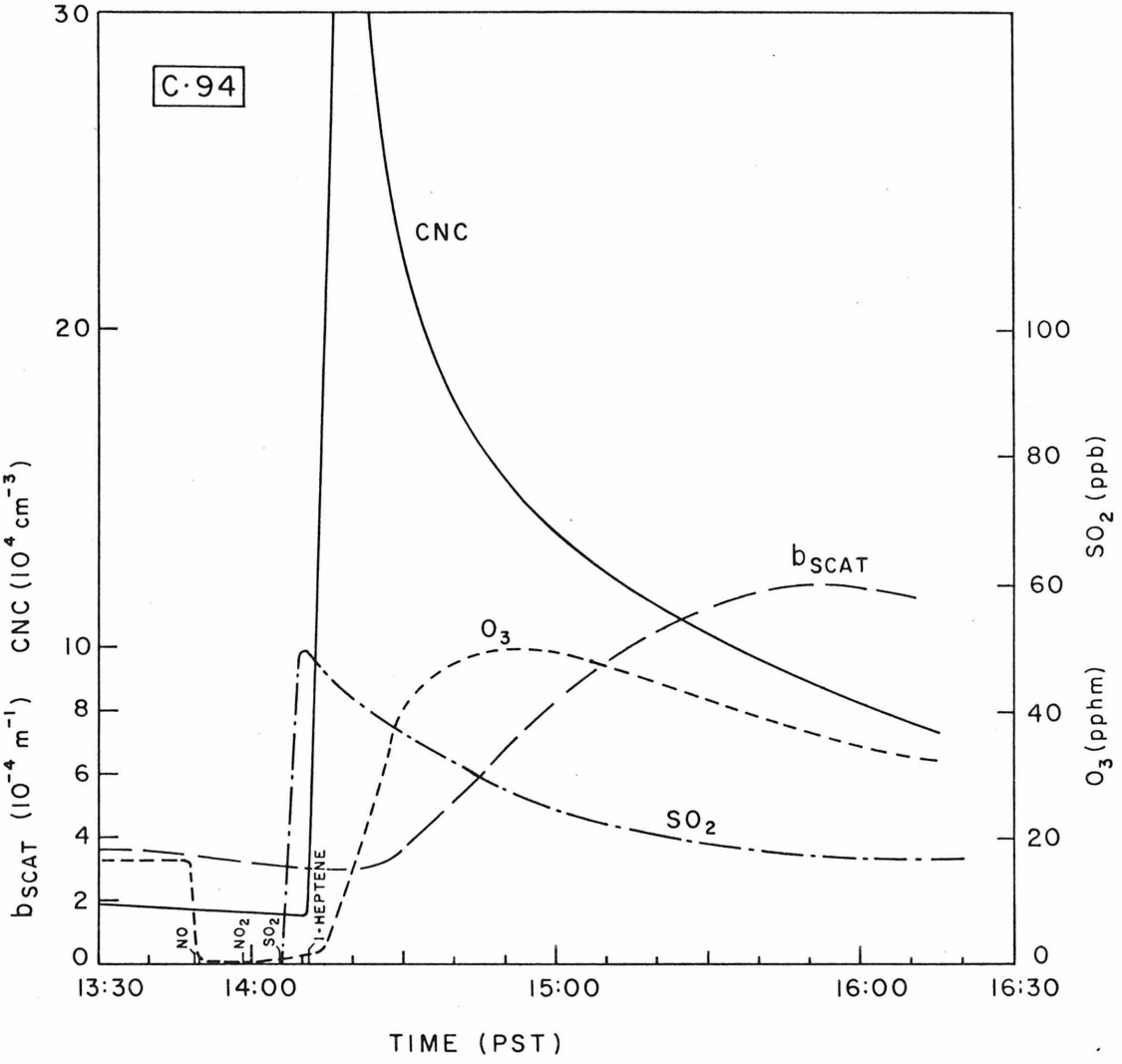

Figure 4.8 Concentrations and Light Scattering Profiles for Experiment C.94. (Average of 29% RH and 35°C.)

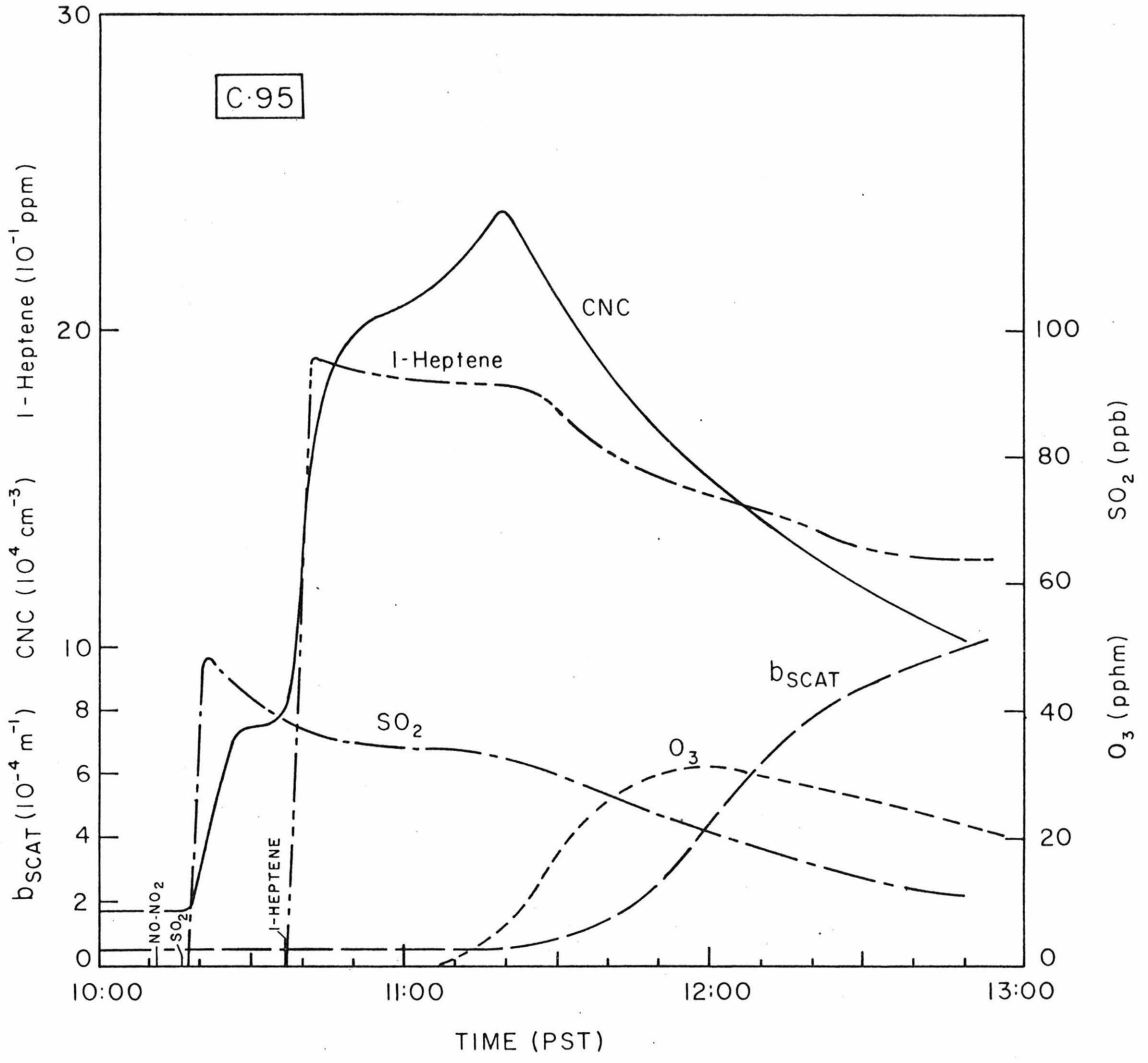

Figure 4.9 Concentration and Light Scattering Profiles for Experiment C.95. (Average of 16% RH and 35°C.)

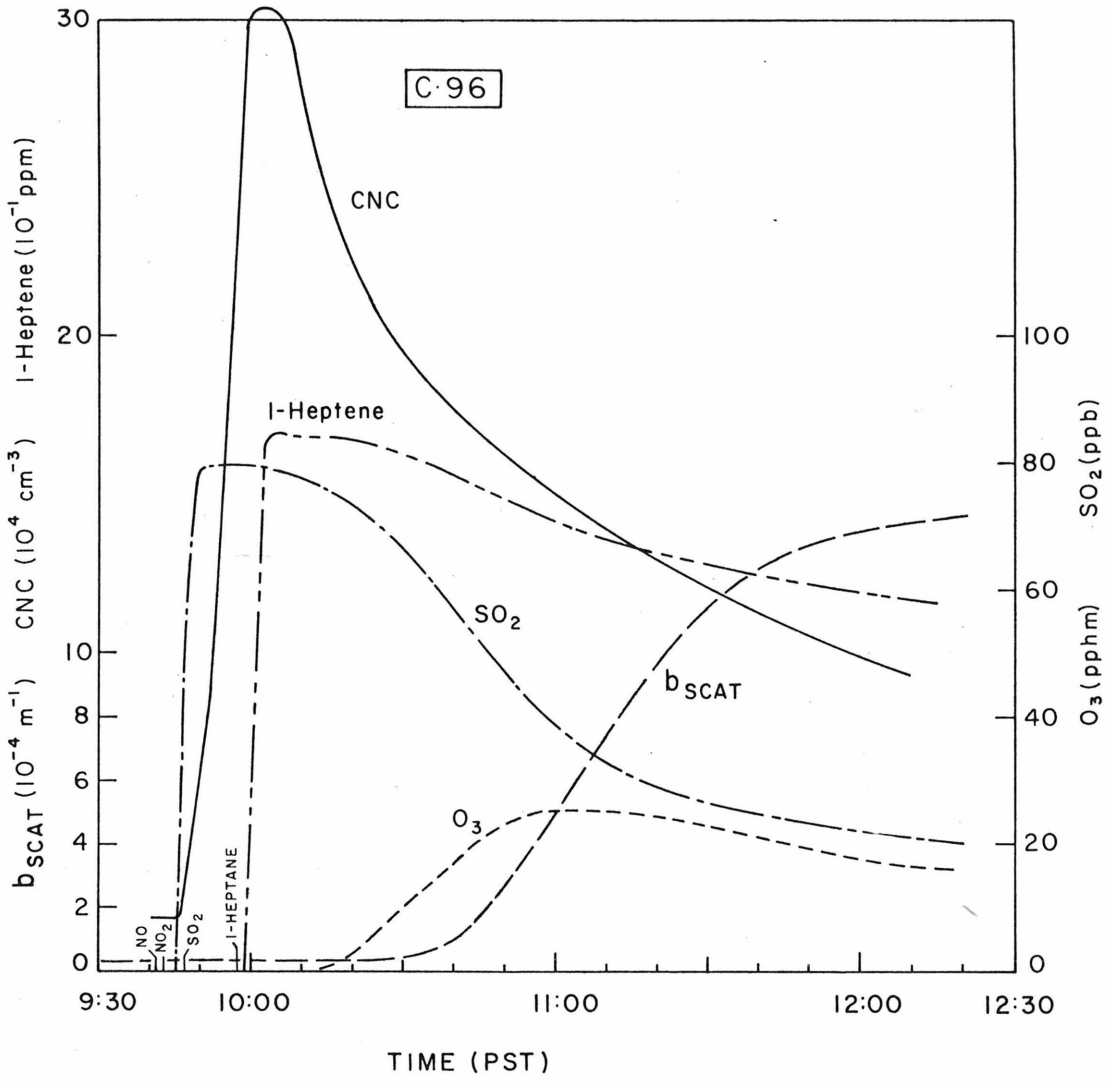

Figure 4.10 Concentration and Light Scattering Profiles for Experiment C.96. (Average of 14% RH and 38°C.)

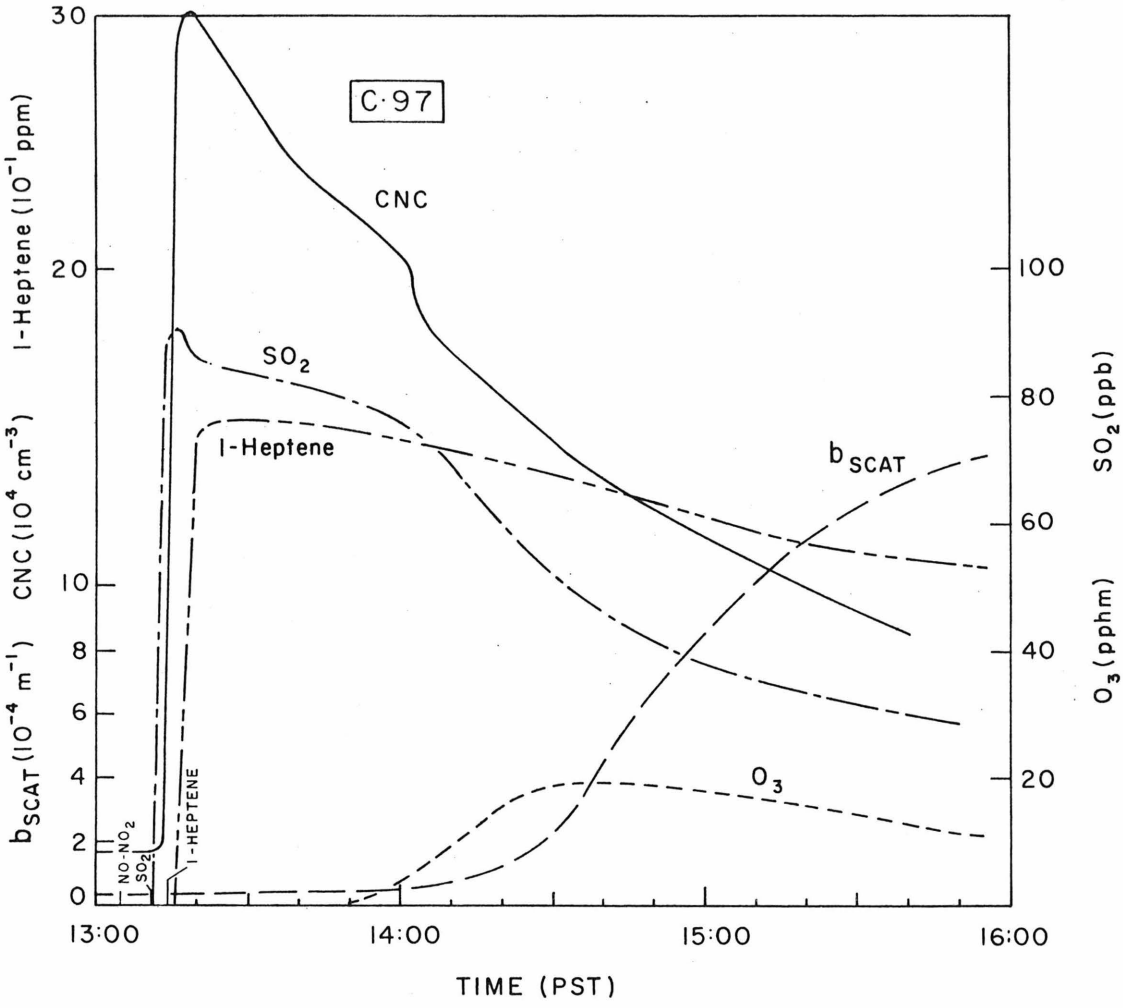

Figure 4.11 Concentration and Light Scattering Profiles for Experiment C.97. (Average of 16% RH and 36°C.)

with subsequent aerosol formation. During the first regime, new particles are being formed at a high rate from both SO_2 and 1-heptene; however, a sharp drop in new particle formation is observed during the second photochemical regime. The large decrease in new particle formation occurs just as the oxidation rates of both SO_2 and 1-heptene increased drastically. This observation indicates that a more condensable species is being formed during the second regime or that new surface is then providing a sufficient sink for the condensable species so that formation of new particles is no longer favored.

Figure 4.5 (experiment C.04) shows that there was some aerosol formation in the 1-heptene - NO_x system without SO_2, although the b_{scat} increase occurs later than in the system with SO_2 (and after the O_3 concentration has reached its maximum).

Another feature of these experiments was the near-first order decay of the SO_2 concentration just after the breaking point between the two regimes. This is illustrated for experiments C.95, C.96, and C.97 in Figures 4.12, 4.13, 4.14, respectively, where the log of the SO_2 concentration is plotted against time. The linear portion, indicating a first order decay in SO_2 concentration, extends for about an hour during each experiment.

4.4 EXPERIMENTS WITH OTHER HYDROCARBONS AND WITH AMBIENT AIR

Experiments also were run with NO, NO_2, SO_2, and the following hydrocarbons: cyclohexene, 2-methyl 2-butene, 2,3 dimethyl 2-butene, and 1,7 octadiene. Three experiments were run with only SO_2 added to ambient air. The starting conditions and other pertinent information are given in Table 4.2.

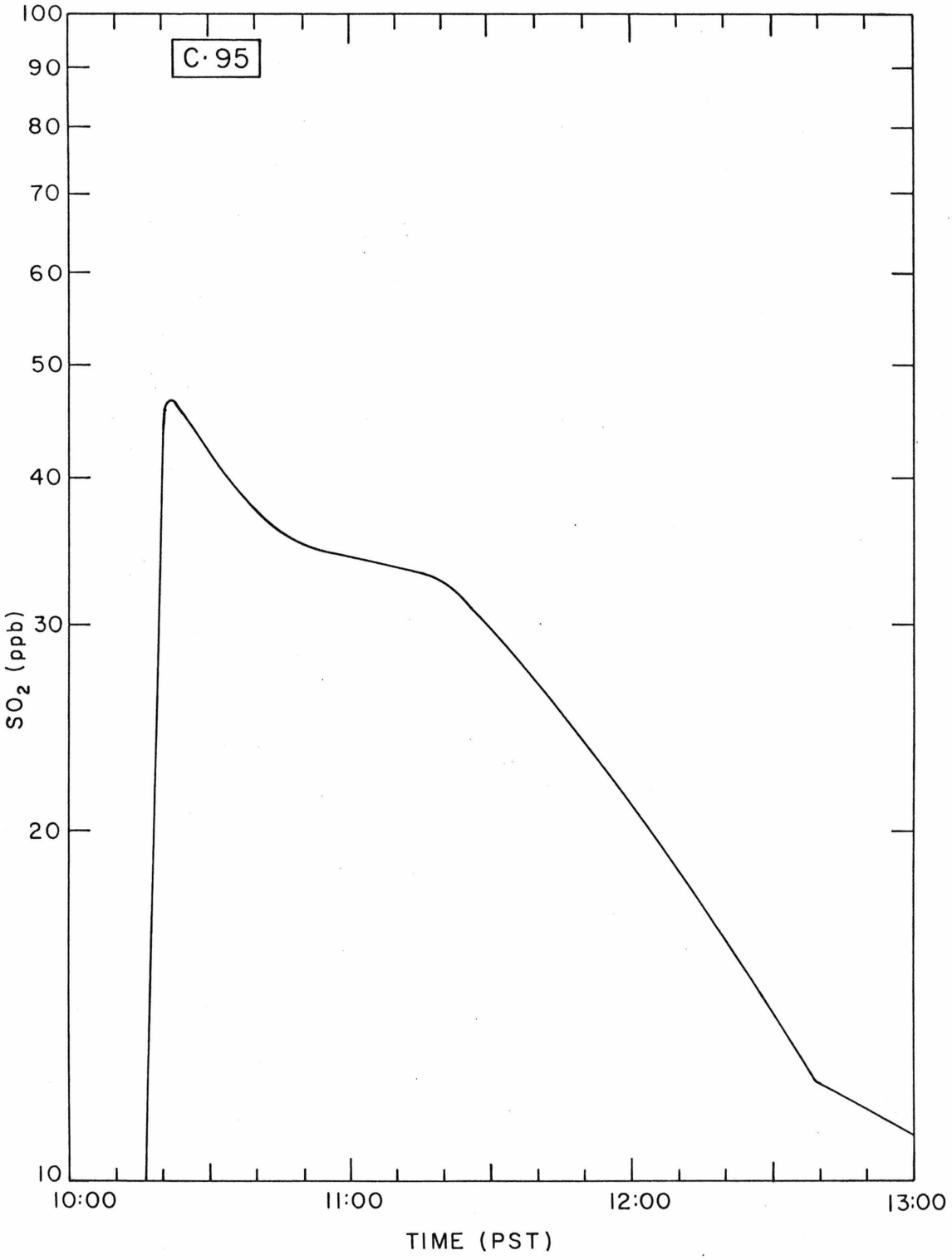

Figure 4.12 Concentration Profile for Experiment C.95 Showing the Near-First Order Decay of SO_2

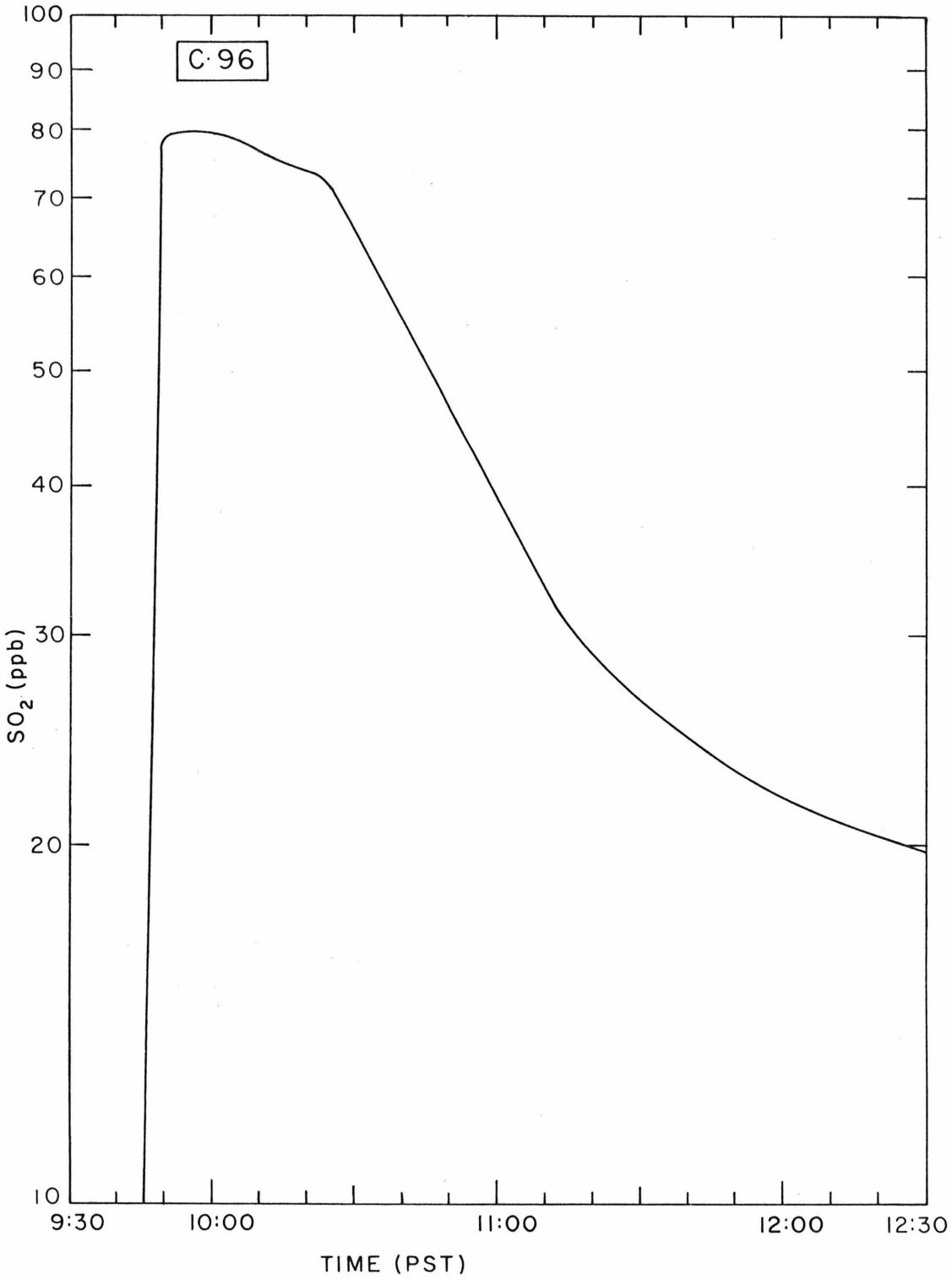

Figure 4.13 Concentration Profile for Experiment C.96 Showing the Near-First Order Decay of SO_2

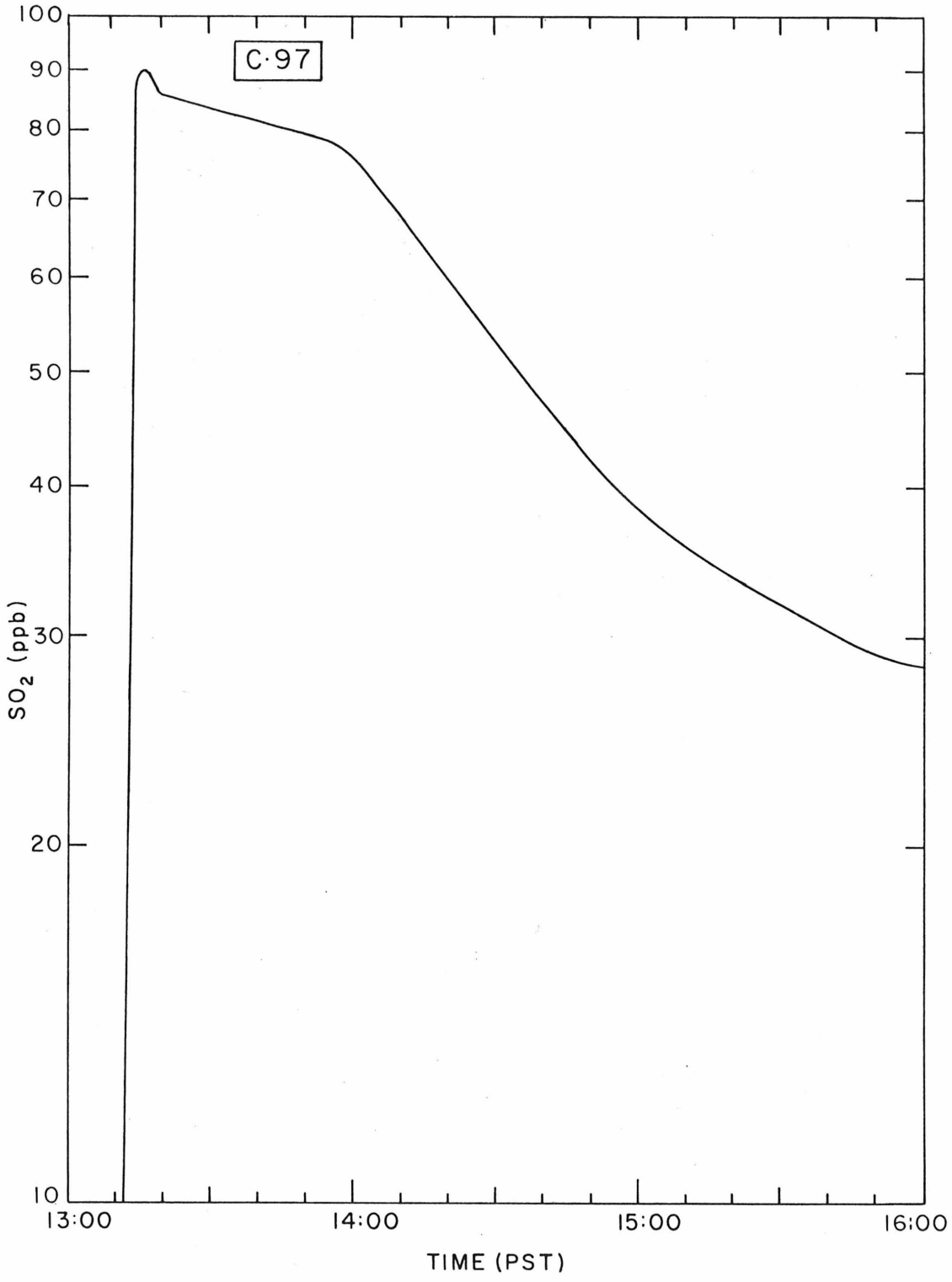

Figure 4.14 Concentration Profile for Experiment C.97 Showing the Near-First Order Decay of SO_2

The experiment with 2-methyl 2-butene (B.92) illustrates how little SO_2 is oxidized when there is only a small concentration of O_3 present ($[O_3] \lesssim 0.05$ ppm, because of cloud cover most of the day). There was no measurable change in the SO_2 concentration throughout the 1-3/4 hour experiment. Therefore, at low relative humidity and without appreciable photochemical activity, there is little oxidation of SO_2.

In experiment E.91 (2,3 dimethyl 2-butene), there was a large drop in the SO_2 concentration (about 11 ppb) within 2 minutes of the introduction of the hydrocarbon. However, there was little reaction of SO_2 throughout the rest of the experiment (about 4 ppb in 1 hour) and no change in b_{scat}. It is known that 2,3 dimethyl 2-butene reacts quickly in the presence of O_3, although it forms no organic aerosol (Grosjean, 1975). It is assumed that the product of SO_2 oxidation remains in the gas phase.

Experiments with cyclohexene (A.92) and 1,7 octadiene (F.91) show that SO_2 can be oxidized by such systems, but that the aerosol sulfur is overshadowed by the organic aerosol formed. In fact, the oxidation of SO_2 in F.91 stopped completely when the 1,7 octadiene concentration went to zero.

In experiments Z.91, Z.92, and Z.93, only SO_2 was added to unfiltered ambient air. As with all experiments with SO_2, more than 10^5/cc new particles were generated just after the SO_2 was added. Although SO_2 was oxidized at rates up to 11% $hour^{-1}$, there was actually a slight decline in b_{scat} during these 2-hour experiments. This was probably because of some wall losses and slight changes in the size distribution of the aerosol (possibly a result of heating in the bag).

4.5 AEROSOL FORMATION KINETICS

In this section a general reaction scheme is proposed for sulfur and carbon aerosol formation in a mixture of ozone, olefin, and sulfur dioxide (suggested in principle by Wilson, et al., 1974 and Grosjean, 1975). This scheme is then applied to the smog chamber studies described earlier in which NO, NO_2, SO_2, and 1-heptene were added to atmospheric air, which included existing particulate matter.

Many studies have shown that in a pure system, oxidation of SO_2 by some reactive intermediate of the O_3-olefin reaction can proceed at a substantial rate to produce aerosol sulfur (Groblicki and Nebel, 1971; Cox and Penkett, 1972; and McNelis, 1974). Other investigators have proposed the hydroxyl radical (Wood, et al., 1974) or the hydroperoxyl radical (Payne, et al., 1973) as a major contributor to the oxidation of SO_2 in the atmosphere. The homogeneous photooxidation of SO_2 is probably not an important mechanism in the presence of the above photochemical agents, especially in the light of the most recently measured values of the quantum yield (Sidebottom, et al., 1972; Friend, et al., 1973).

The oxidation of SO_2 in a system approximating atmospheric conditions, such as those in Los Angeles, has not been studied before. For example, starting a smog chamber experiment with O_3, an olefin, and SO_2 in particle-free air (Cox and Penkett, 1972; McNelis, 1974) limits the possible mechanisms. The data collected in this study were analyzed to determine the important mechanisms of aerosol sulfur formation.

4.51 General System

The proposed general reaction scheme is one involving the formation of a reactive intermediate (I) from the O_3 attack on the olefin (OL). This intermediate is then allowed to proceed to products via either unimolecular (i) or bimolecular (j) pathways:

$$O_3 + OL \xrightarrow{k} I \qquad \text{slow, the rate determining step}$$

$$I \xrightarrow{k_{1i}} P_{1ik} \qquad i = 1, N$$

$$I + R_j \xrightarrow{k_{2j}} P_{2jk} \qquad j = 1, M$$

This allows for N different unimolecular decompositions of I, and M different bimolecular reactions of I with species R_j. Each reaction can form a number of products, denoted by P_{1ik} and P_{2jk}. We are specifically interested in the products which lead to condensable species and subsequently to aerosol formation. Let CS_{1ik} and CS_{2jk} be the mass of condensable species from products P_{1ik} and P_{2jk}, respectively. And let α_{1ik} and α_{2jk} be the mass fraction of product P_{1ik} and P_{2jk} that lead to a condensable species via unimolecular (i) or biomolecular (j) reactions of the intermediate I. Then we have:

$$\sum_k CS_{1ik} = \sum_k \alpha_{1ik} P_{1ik} \qquad \text{for each } i = 1, N \qquad (4.2)$$

$$\sum_k CS_{2jk} = \sum_k \alpha_{2jk} P_{2jk} \qquad \text{for each } j = 1, M \qquad (4.3)$$

Also, let α be the fraction of the intermediate that reacted (via i or j) to form condensable species and let α_{1i} and α_{2j} be the mass average values for the different reaction pathways:

$$\alpha_{1i} = \frac{\sum_k \alpha_{1ik} P_{1ik}}{\sum_k P_{1ik}} \qquad \text{for each } i = 1, N \qquad (4.4)$$

$$\alpha_{2j} = \frac{\sum_k \alpha_{2jk} P_{2jk}}{\sum_k P_{2jk}} \qquad \text{for each } j = 1, M \qquad (4.5)$$

$$\alpha = \frac{\sum_k \alpha_{1i}\, k_{1i} + \sum_j \alpha_{2j}\, k_{2j}\, [R_j]}{\sum_i k_{1i} + \sum_j k_{2j}\, [R_j]} \qquad (4.6)$$

Now define the fraction of each condensable product that actually condenses as α_{1ic} or α_{2jc}. Thus, the overall mass average value is:

$$\alpha_c = \frac{\sum_i \alpha_{1i}\, \alpha_{1ic}\, k_{1i} + \sum_j \alpha_{2j}\, \alpha_{2jc}\, k_{2j}\, [R_j]}{\sum_i \alpha_{1i}\, k_{1i} + \sum_j \alpha_{2j}\, k_{2j}\, [R_j]} \qquad (4.7)$$

If we assume that the intermediate reaches a steady state concentration, then:

$$[I]_{ss} = \frac{k\, [O_3][OL]}{\sum_i k_{1i} + \sum_j k_{2j}\, [R_j]} \qquad (4.8)$$

The rate of formation of carbon species in the aerosol phase can thus be written at steady state as:

$$\frac{d[\text{aerosol carbon species}]}{dt} = \alpha\alpha_c \left\{ \sum_i k_{1i} + \sum_j k_{2j}[R_j] \right\} [I]_{ss} \quad (4.9)$$

$$= \alpha\, \alpha_c \quad k\, [O_3][OL]$$

But the loss of olefin from the gas phase can be written as:

$$-\frac{d[OL]}{dt} = k\, [O_3][OL] \quad (4.10)$$

Therefore, we are left with a general relationship between the olefin loss from the gas phase and the carbon species formed in the aerosol phase:

$$\frac{d[\text{aerosol carbon species}]}{dt} = \alpha\, \alpha_c \quad \left\{ -\frac{d[OL]}{dt} \right\} \quad (4.11)$$

This general mechanism assumes nothing about the nature of the reactive intermediate; it assumes only that its formation fits the O_3-olefin rate law and that there is competition for I between unimolecular and biomolecular reactions, some products of which we assume to proceed to condensable species and eventually aerosol formation.

There are two limiting cases of interest when the formation of I is the rate determining step. Specifically, if either the unimolecular or bimolecular pathway result in no aerosol formation, then α is reduced to an expression involving only the α_{1i}'s or the α_{2j}'s. However, if any k_{1i} or k_{2j} is small with respect to the formation rate of I, or if the rate of transfer of a condensable species from the gas phase

to the aerosol phase is slow, or if aerosol products are produced by reaction paths other than I, then the equations become much more complex.

4.52 1-Heptene, NO_x, SO_2 System

For the specific case of 1-heptene (H) and sulfur dioxide, the general kinetic equations are:

$$O_3 + H \xrightarrow{k} I \qquad \text{slow, the rate determining step}$$

$$I \xrightarrow{k_{1i}} P_{1ik} \qquad i = 1, N$$

$$I + SO_2 \xrightarrow{k_{21}} P_{21} + SO_3$$

$$I + R_j \xrightarrow{k_{2j}} P_{2jk} \qquad j = 2, M$$

where k_{21} is an effective rate constant, taking into account the possibility of other reactive intermediate formulations. If we assume that I reaches a steady state concentration, then:

$$[I]_{ss} = \frac{k\,[O_3]\,[H]}{\sum_i k_{1i} + k_{21}\,[SO_2] + \sum_j k_{2j}\,[R_j]} \tag{4.12}$$

The rate of formation of product P_{21} can thus be written at steady state as:

$$\frac{d[P_{21}]}{dt} = k_{21}\,[I]_{ss}[SO_2] \tag{4.13}$$

$$= \frac{k\,k_{21}\,[O_3]\,[H]\,[SO_2]}{\sum_i k_{1i} + k_{21}\,[SO_2] + \sum_j k_{2j}\,[R_j]}$$

Integration from time 0 to time T and assuming $[P_{21}] = 0$ at time 0 results in:

$$[P_{21}]_T = k\, k_{21} \int_o^T \frac{[O_3]\,[H]\,[SO_2]}{\sum_i k_{1i} + k_{21}\,[SO_2] + \sum_j k_{2j}\,[R_j]}\, dt \qquad (4.14)$$

With α_{21c} representing the fraction of condensable species resulting from P_{21} which actually condenses, the aerosol carbon concentration can be defined by:

$$[AC_{21}] = \alpha_{21}\,\alpha_{21c}\,[P_{21}] \qquad (4.15)$$

If other of the P_{nik}'s form aerosol species, we will have similar expressions. Thus, for the total aerosol carbon (TAC) at time T:

$$[TAC]_T = \sum_{i,k} [AC_{1ik}] + \sum_{j,k} [AC_{2jk}] \qquad (4.16)$$

$$= k\int_o^T \frac{\left\{\sum_i \alpha_{1i}\alpha_{1ic}k_{1i} + \alpha_{21}\alpha_{21c}k_{21}[SO_2] + \sum_j \alpha_{2j}\alpha_{2jc}k_{2j}[R_j]\right\}\,[O_3][H]dt}{\sum_i k_{1i} + k_{21}\,[SO_2] + \sum_j k_{2j}[R_j]}$$

To simplify the above expression, we make the following assumptions:

(1) There is little aerosol carbon formed in the 1-heptene, NO_x, system without SO_2, compared to the system with SO_2. The results of run C.04 described earlier (see Figure 4.5), as well as the work of Stevenson, et al. (1965), Wilson, et al.(1972), and O'Brien, et al. (1973) show that this is a good assumption at the concentration levels used in this study.

Thus,

$$\sum_i \alpha_{1i}\alpha_{1ic}k_{1i} + \sum_j \alpha_{2j}\alpha_{2jc}k_{2j}[R_j] \ll \alpha_{21}\alpha_{21c}k_{21}[SO_2]$$

(2) Little of the reactive intermediate, I, reacts with SO_2. Cox and Penkett (1972) have shown that there was no measurable difference in the variation with time of the O_3 and olefin concentrations, with and without SO_2. Thus,

$$k_{21}[SO_2] \ll \sum_i k_{1i} + \sum_j k_{2j}[R_j]$$

(3a) Little of the reactive intermediate reacts with R_j type species (i.e., most of the depletion of the reactive intermediate is via the unimolecular pathways):

$$\sum_j k_{2j}[R_j] \ll \sum_i k_{1i}$$

(3b) A less restrictive assumption can be made in place of (3a); that the R_j are present in sufficient concentration such that the concentration is not depleted by reaction with I:

$[R_j] \sim$ constant with time ($R_j = O_2$ is an example)

We are then left with the following expression to describe the aerosol carbon concentration at a given time T (using (3b), rather than (3a)):

$$[TAC]_T = \frac{k\, k_{21}}{\sum_i k_{1i} + \sum_j k_{2j}[R_j]} \int_o^T \alpha_{21}\alpha_{21c}[O_3][H][SO_2]dt \qquad (4.17)$$

Thus, if the assumptions that have been made previously are correct, we would expect the aerosol carbon to be a linear function of the integral of the product of the ozone, 1-heptene, and sulfur dioxide concentrations. This also assumes that α_{21} and α_{21c} are not functions of time.

The same type of analysis can be performed to determine the aerosol sulfur concentration at time T. A steady state concentration for I implies that:

$$\frac{d[SO_3]}{dt} = k_{21} [I]_{ss}[SO_2] \qquad (4.18)$$

Thus, making the same assumptions concerning the reactions of the intermediate ((1), (2), and (3b) above), integration from time 0 (no SO_3) to time T results in an expression for the concentration of aerosol sulfur:

$$[AS]_T = \frac{k\, k_{21}}{\sum_i k_{1i} + \sum_j k_{2j}\,[R_j]} \int_o^T \alpha_{SO_3}[O_3][H][SO_2]dt \qquad (4.19)$$

where α_{SO_3} represents the fraction of SO_3 formed which results in aerosol sulfur.

4.53 Results

The gas phase and aerosol phase measurements for experiments C.04, C.95, C.96, and C.97 were analyzed within the framework of the aerosol formation kinetic scheme developed in sections 4.51 and 4.52. Integrated forms (Equation 4.19) were used instead of differential forms (Equation 4.18) because we have continuous data for the gas phase species. The

data points which are shown in the figures of this section are computed for the midpoint of the aerosol samples taken during the experiments. Integrations were done using a planimeter.

The 1-heptene depletion rate can be used to measure the apparent O_3,1-heptene rate constant, assuming that 1-heptene only reacts with O_3 (as shown in Equation 4.10):

$$\frac{d[H]}{dt} = -k[O_3][H]$$

Integration from time 0 to time T results in:

$$[H]_o - [H]_T = k \int_o^T [O_3][H]dt \qquad (4.20)$$

Figure 4.15 shows the change in the 1-heptene concentration to be a linear function of the integral of the product of the O_3 and 1-heptene concentrations after a short induction period. A least squares fit to the linear section of the data yields the values of the O_3,1-heptene rate constant shown in Table 4.5. The average of the rate constants for these four experiments is 13.5×10^{-3} $ppm^{-1}min^{-1}$. This compares favorably with the literature value of $12 \times 10^{-3} ppm^{-1}min^{-1}$ (Cadle and Schadt, 1952), measured in a contaminant-free system. Although no other measurements have been made of the O_3-1-heptene rate constant, the Cadle and Schadt (1952) value for the O_3-1-hexene rate constant (15×10^{-3} ppm^{-1} min^{-1}) agrees well with the value recently determined by Japar, et al. (1974) of 16.1×10^{-3} ppm^{-1} min^{-1}.

The aerosol carbon and sulfur measurements will be used to evaluate the aerosol kinetic scheme via the relationships expressed in Equations 4.17 and 4.19. Figure 4.16 shows the aerosol carbon concentration,

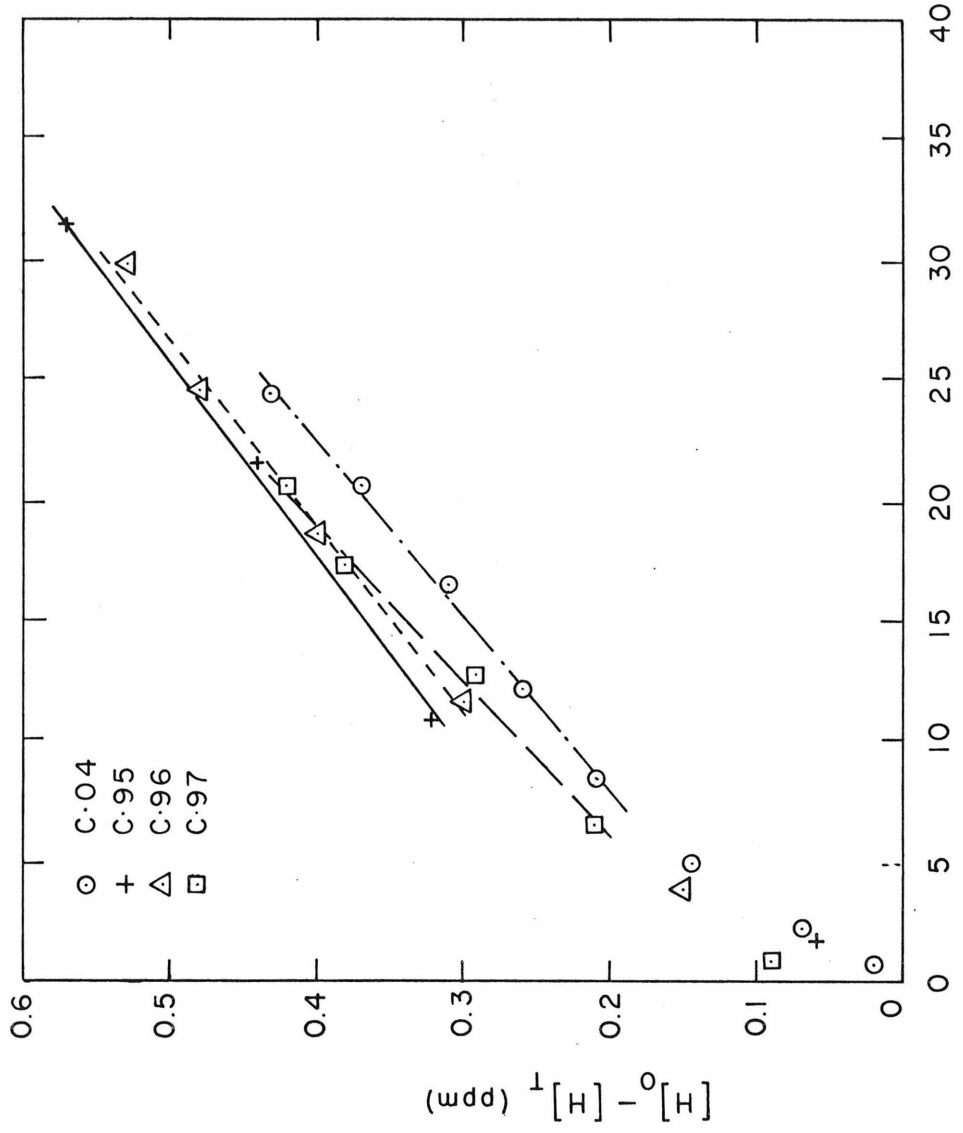

Figure 4.15 The Reaction of 1-Heptene during Experiments C.04, C.95, C.96, and C.97

TABLE 4.5

Reaction Rates for the 1-Heptene, NO, NO_2, SO_2 System

Quantity	Calculated by Equation	C.95	C.96	C.97	Average
$k(ppm^{-1}min^{-1})$	4.20	0.0122	0.0128	0.0154	0.0135*
$\frac{k\,\alpha_{21}\alpha_{21c}k_{21}}{\sum_i k_{1i} + \sum_j k_{2j}[R_j]}(ppm^{-2}min^{-1})$	4.17	0.0432	0.0423	0.0468	0.0441
$\frac{k\,\alpha_{SO_3}k_{21}}{\sum_i k_{1i} + \sum_j k_{2j}[R_j]}(ppm^{-2}min^{-1})$	4.19	0.0361	0.0435	0.0435	0.0410
$\alpha\,\alpha_c$	4.21	0.051	0.133	0.148	—
$\frac{\alpha_{21}\alpha_{21c}k_{21}}{\sum_i k_{1i} + \sum_j k_{2j}[R_j]}(ppm^{-1})$	4.22	2.48	3.75	3.33	3.19
$\frac{\alpha_{SO_3}k}{\alpha_{21}\alpha_{21c}}\ (ppm^{-1}min^{-1})$	4.23	0.0145	0.0116	0.0131	0.0131

*Includes value for C.04 of $k = 0.0136\ ppm^{-1}min^{-1}$.

as a function of the integrated product of the O_3, 1-heptene and SO_2 concentrations, for experiments C.95, C.96, and C.97. There is excellent linearity throughout all three experiments until the last sample or two in C.96 and C.97. The upward bend of the aerosol carbon concentration near the end of experiments C.96 and C.97 indicates that an aerosol carbon formation pathway, other than the one postulated in assumption (1) of section 4.52, is becoming significant. The slope of the relationship shown in Figure 4.16 is given in Table 4.5, using Equation 4.17. The linearity of the relationship indicates that, in the 1-heptene, NO, NO_2, SO_2 system, formation of most of the aerosol carbon is consistent with the reaction of SO_2 with a reactive intermediate of the O_3, 1-heptene reaction.

Based on the form of Equation 4.19, a plot of aerosol sulfur is shown in Figure 4.17. There was less than 2 $\mu gm/m^3$ of aerosol sulfur (as $SO_4^=$) in the first sample of each experiment. Therefore, the fast rise of the aerosol sulfur concentration at the beginning of each experiment is due to some mechanism of SO_2 oxidation other than the O_3-olefin reactive intermediate one. However, after this short induction period, there is a linear dependence of the aerosol sulfur concentration on the integral of the product of the O_3, 1-heptene, and SO_2 concentrations. The linear dependence is consistent with the assumptions made in section 4.52 concerning aerosol sulfur formation. The slope of this linear relationship is shown in Table 4.5 for the three 1-heptene experiments.

Integration of Equation 4.11 from time 0 to time T results in:

$$[TAC]_T - [TAC]_o = \alpha \alpha_c \left\{ [H]_o - [H]_T \right\} \qquad (4.21)$$

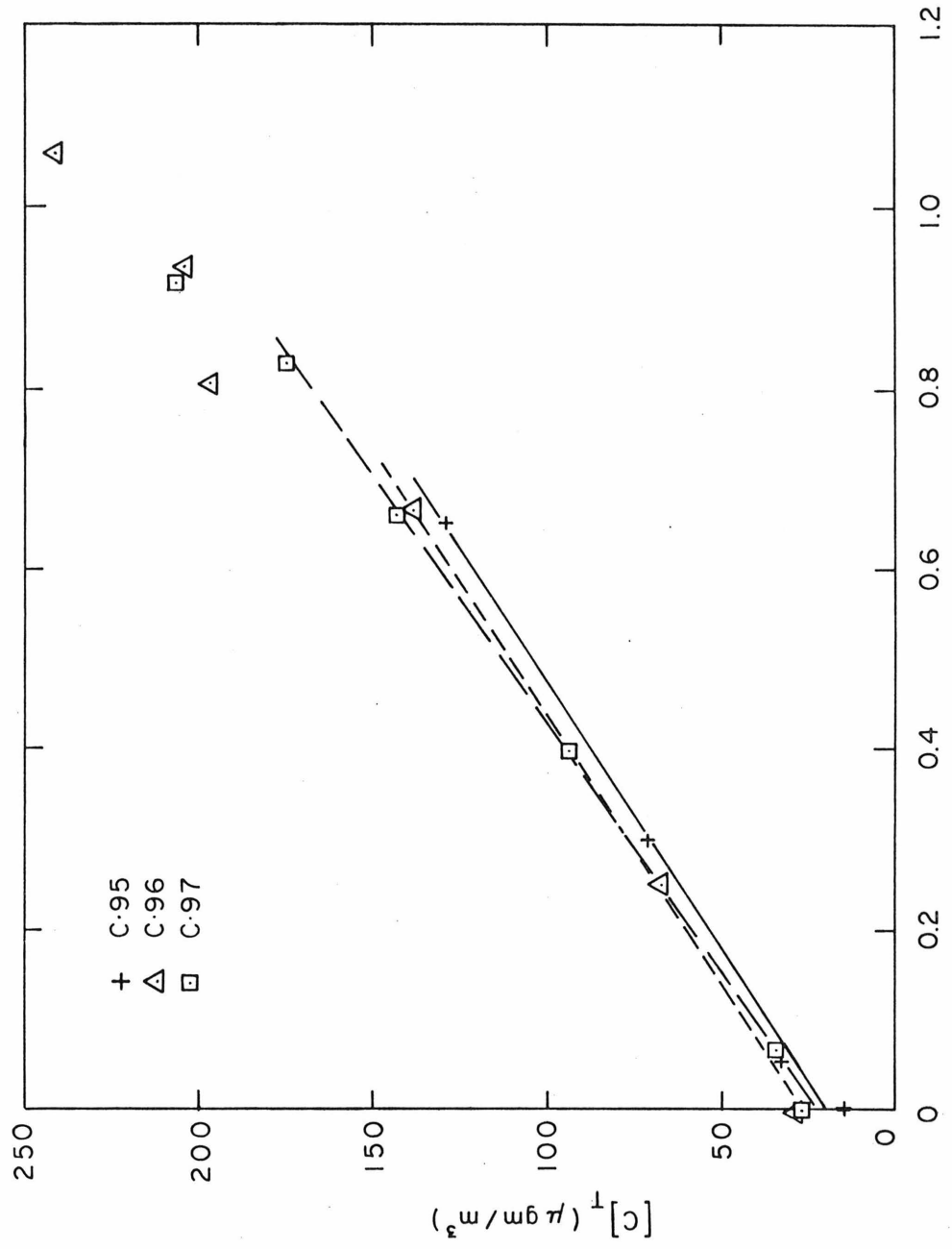

Figure 4.16 The Formation of Aerosol Carbon during Experiments C.95, C.96, and C.97

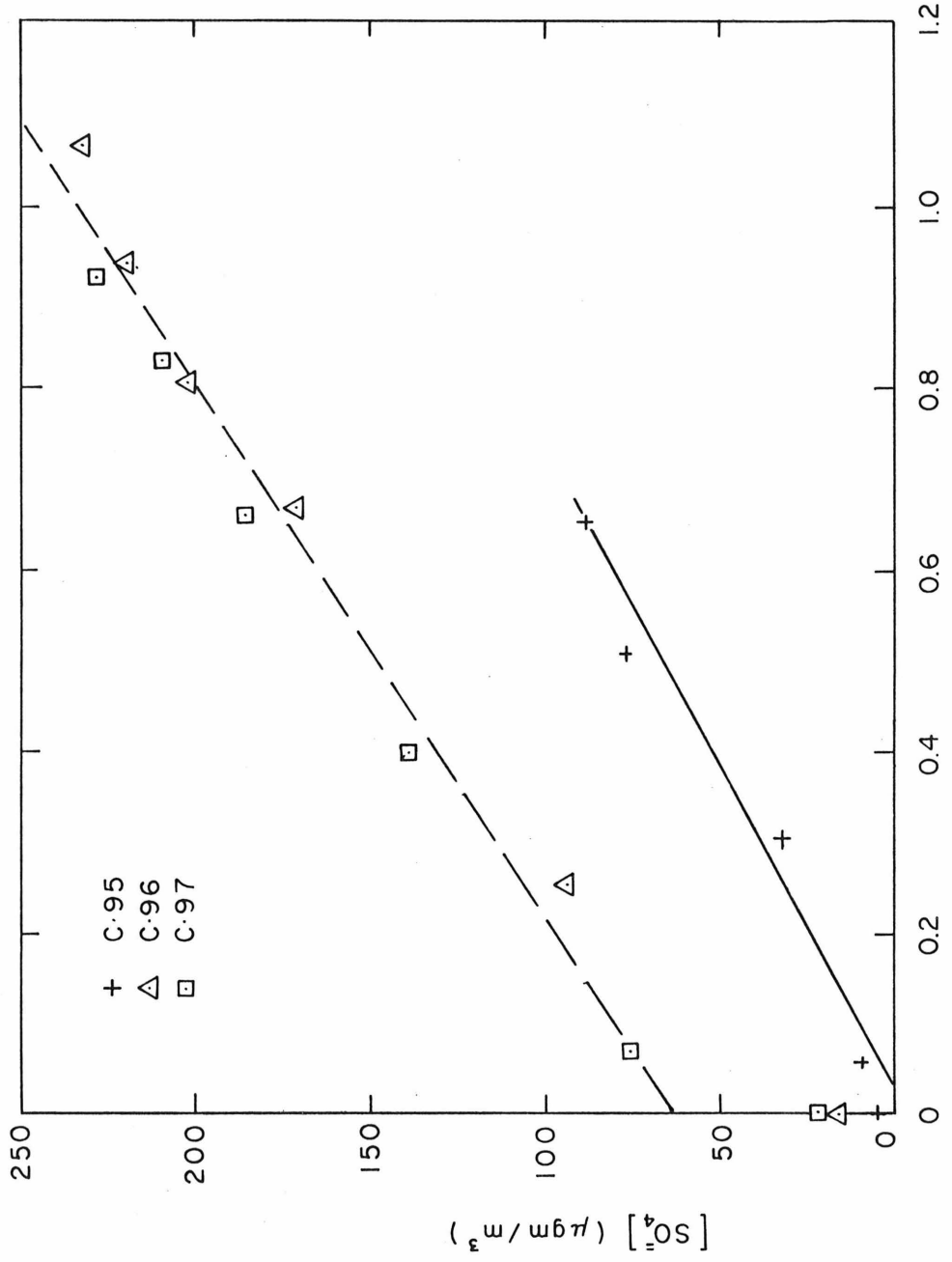

Figure 4.17 The Formation of Aerosol Sulfur during Experiments C.95, C.96, and C.97

Figure 4.18 shows the difference in the aerosol carbon concentration as a function of the 1-heptene reacted. The resulting values of $\alpha\,\alpha_c$ are shown in Table 4.5. Each experiment shows excellent linearity. The quantity $\alpha\,\alpha_c$ is the fraction of reacted 1-heptene that results in aerosol carbon. Because most of the aerosol carbon is formed in a reaction with SO_2, $\alpha\,\alpha_c$ depends upon the SO_2 concentration. We can use this fact to obtain additional information about the rate constant of the SO_2-reactive intermediate reaction, k_{21}. Substitution of Equations 4.17 and 4.20 into Equation 4.21 and rearrangement results in:

$$\frac{\alpha_{21}\alpha_{21c}k_{21}}{\sum_i k_{1i} + \sum_j k_{2j}[R_j]} = \alpha\,\alpha_c \frac{\int_o^T [O_3][H][SO_2]\,dt}{\int_o^T [O_3][H]\,dt} \qquad (4.22)$$

Calculated values for the left-hand side of Equation 4.22 are given in Table 4.5. Now, the value of the O_3, 1-heptene rate constant can be calculated, using the aerosol sulfur data:

$$\frac{\alpha_{SO_3}{}^k}{\alpha_{21}\alpha_{21c}} = \left\{ \frac{\alpha_{SO_3}{}^k k_{21}{}^k}{\sum_i k_{1i} + \sum_j k_{2j}[R_j]} \right\} \left\{ \frac{\alpha_{21}\alpha_{21c}k_{21}}{\sum_i k_{1i} + \sum_j k_{2j}[R_j]} \right\}^{-1} \qquad (4.23)$$

Since the values of $\alpha_{SO_3}{}^k/\alpha_{21}\alpha_{21c}$ are approximately the same as the calculated values of k, the ratio $\alpha_{SO_3}/\alpha_{21}\alpha_{21c}$ must be about 1.

The major problem in estimating the O_3, 1-heptene rate constant is that some of the concentrations may be depleted by reactions not taken into account in the analysis. Specifically, both

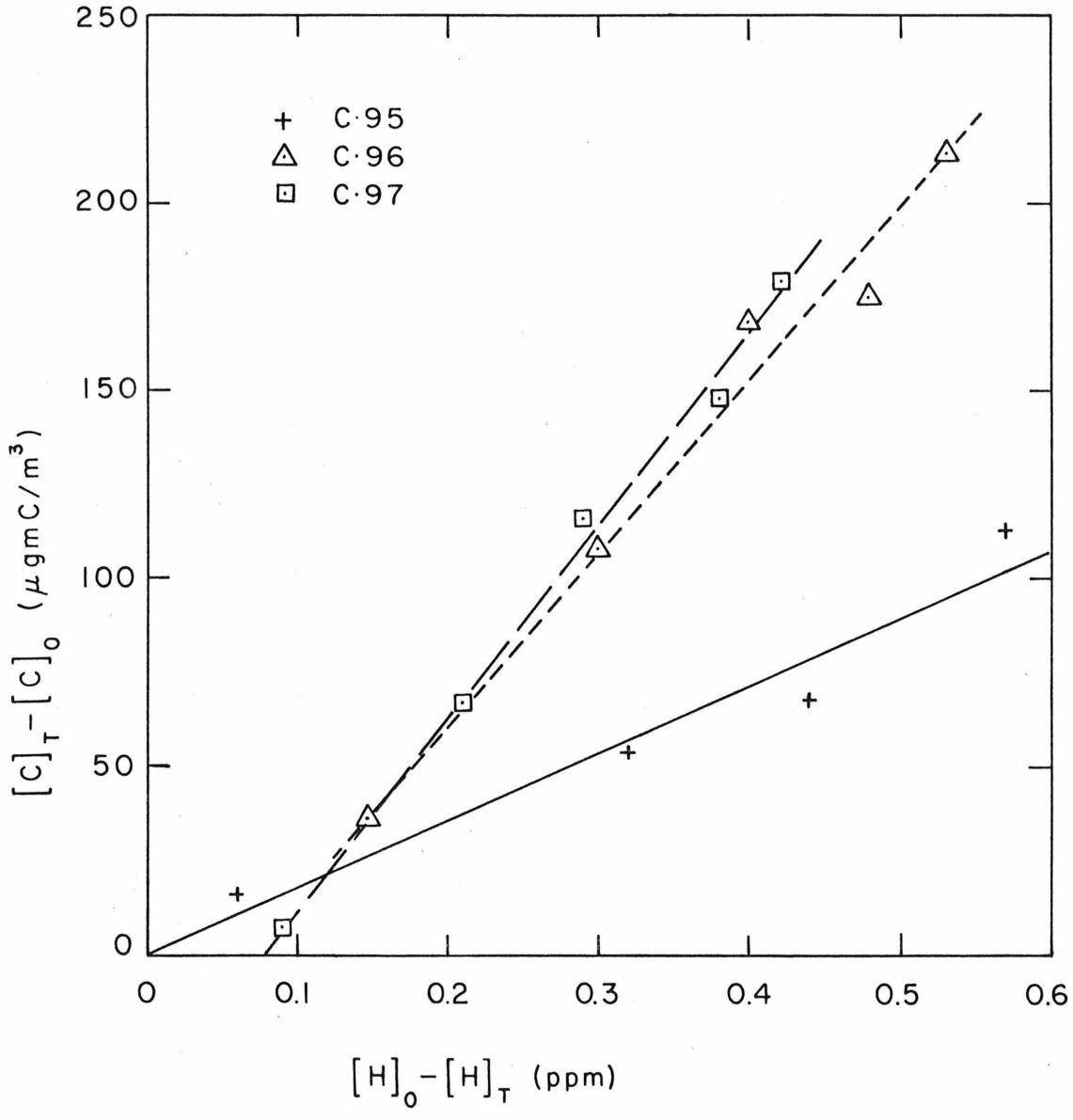

Figure 4.18 Formation of Aerosol Carbon as a Function of Reacted 1-Heptene during Experiments C.95, C.96, and C.97

the olefin and the SO_2 may react with other reactive species, such as O atoms, or OH and HO_2 radicals. Such depletion of the 1-heptene and SO_2 concentrations would result in a higher calculated value of the rate constant than the true value. In fact, this is the type of effect observed for the aerosol sulfur produced during the very early stages of the experiments (see Figure 4.17): there is a quick rise in the aerosol sulfur followed by a linear behavior during the remainder of the experiment. This effect is also observed in Figure 4.16, where the 1-heptene loss is faster at the beginning than it is throughout the rest of the experiment. However, since the O_3, 1-heptene rate constant determined from the linear section of the 1-heptene decay is the same as the literature value, the loss of 1-heptene is mainly from reaction with O_3 and not from other reactions with other species in the system. Linear behavior would not be expected throughout the rest of the experiment if other reactions were depleting significantly the 1-heptene.

Thus, the experimental results reported here for the system 1-heptene, NO, NO_2, and SO_2 in ambient air are consistent with a mechanism based on the reaction of SO_2 with a reactive intermediate of the O_3, 1-heptene reaction.

4.6 SULFUR SIZE DISTRIBUTION MEASUREMENTS

The distribution of particulate sulfur with respect to particle diameter was measured as a function of time during the 1-heptene experiments C.95, C.96, and C.97. The particle size fractionation was accom-

plished by a low pressure, single (round) jet, multi-stage cascade impactor (described in detail in Appendix C). Design and calibration of a low pressure impactor has been reported in the literature (Stern, et al., 1962; Parker and Buchholz, 1968; Buchholz, 1970; and Nelson, 1973). However, no investigator has reported mass or chemical size distribution data using such a device.

The stages of the low pressure impactor were constructed to fit the design of the "Battelle" impactor (Scientific Advances model no. CI-5). The low pressure impactor consisted of 4 stages and a restricting orifice upstream of the first stage (orifice diameter of 0.008 in.). The jet velocity in the last stage corresponded to a Mach number of 1/3, the pressure above the last stage was 81 mm Hg, and the flow rate was 220 cc/min. Small leaks downstream of the restricting orifice have a significant effect on the cut-off sizes of a low pressure impactor. Therefore, the pressure just above the last stage of the impactor was monitored to ensure proper operation. Following Marple (1970), the ratio of jet-to-plate distance to jet diameter was set at 1/2 and the jet Reynolds number for the last stage at 3000. The impactor was calibrated with polystyrene latex spheres of diameter 0.088 μm to 0.716 μm by counting the collected spheres with an electron microscope. The PSL calibration agreed well with the theoretically predicted size ranges (50% cut-off sizes): less than 0.09 μm, 0.09 μm to 0.20 μm, 0.20 μm to 0.37 μm, 0.37 μm to 0.86 μm, and greater than 0.86 μm, in diameter. The experimental efficiency curve for the 3rd stage shows good agreement with the theoretically predicted 50% cut-off value of

0.20 μm in diameter (Figure 4.19). Data for other stages are in Appendix C. The 4th stage (50% cut-off of 0.5 μm diameter) of the "Battelle" impactor (used for measurements in Section 5.1) also showed good agreement between the PSL-derived efficiency curve and the factory value. Thus, it is assumed that at these conditions (jet velocity less than 1/3 Mach, reduced pressure, and with hard PSL spheres), there is no significant bounce-off problem. Buchholz (1970b) found that bounce-off and wall losses were of little importance for submicron particles in a low pressure impactor.

The sulfur size distribution function can be determined from impactor data by assuming that there is a particle diameter below which the mass of sulfur can be neglected. The volume distribution function measured at West Covina on July 24, 1973, 1200-1400 PST (Hidy, et al., 1975) was used as representative of the mass distribution function below 0.09 μm (the 50% cut-off for the last stage of the low pressure impactor). A uniform distribution of the measured $SO_4^=$ concentration (16% of the total mass) results in 2% of the $SO_4^=$ less than 0.09 μm being below 0.02 μm, 9% below 0.03 μm, and 16% below 0.04 μm. In fact, even the extreme case of all the $SO_4^=$ being concentrated in the smallest range of particle diameter results in 2% of the less than 0.09 μm $SO_4^=$ being below 0.015 μm, and only 14% below 0.02 μm. Therefore, 0.02 μm has been used as a limit below which there is negligible sulfur.

A bar graph of the aerosol sulfur size distribution seemed inadequate for a complete representation of the aerosol sulfur in each size

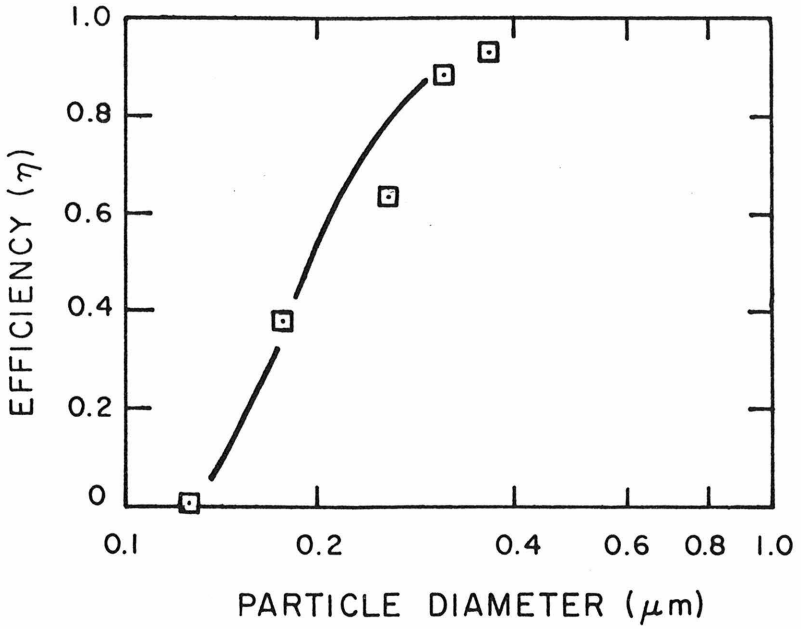

Figure 4.19 Experimental Efficiency Curve for Stage 3 of the Low Pressure Impactor

range. Therefore, continuous sulfur distributions have been estimated for each of the samples. A cumulative plot of the aerosol sulfur in all particles greater than a given diameter vs. that diameter was drawn and then differentiated to obtain a continuous aerosol sulfur distribution with respect to particle diameter. Such a procedure provides only qualitative information; the peak location and height can be changed fairly arbitrarily. Although both the measured bar graphs and the calculated continuous distribution show the same basic features, the continuous distribution exhibits gradual, rather than abrupt, changes in concentration level with particle diameter (for example, the decrease to zero of the sulfur distribution function as the particle diameter decreases below 0.03 μm). This procedure allows better visualization of the changing sulfur size distribution function. Proper redesign of the low pressure impactor will allow the observation of more detail in the sulfur size distribution function.

The sulfur cumulative and size distribution function vs. particle diameter plots are shown for bag experiments C.95, C.96, and C.97 in Figures 4.20, 4.21, and 4.22, respectively. All samples from a given experiment are shown on the cumulative particulate sulfur vs. particle diameter plot. Then, for each sample, both the measured bar and the calculated continuous sulfur size distribution function are shown. The sulfur size distribution development for each experiment is approximately the same: the first sample contains a small amount of particulate sulfur (all below 0.2 μm); then a bimodal distribution develops (one mode below 0.1 μm, the other between 0.2 and 0.4 μm);

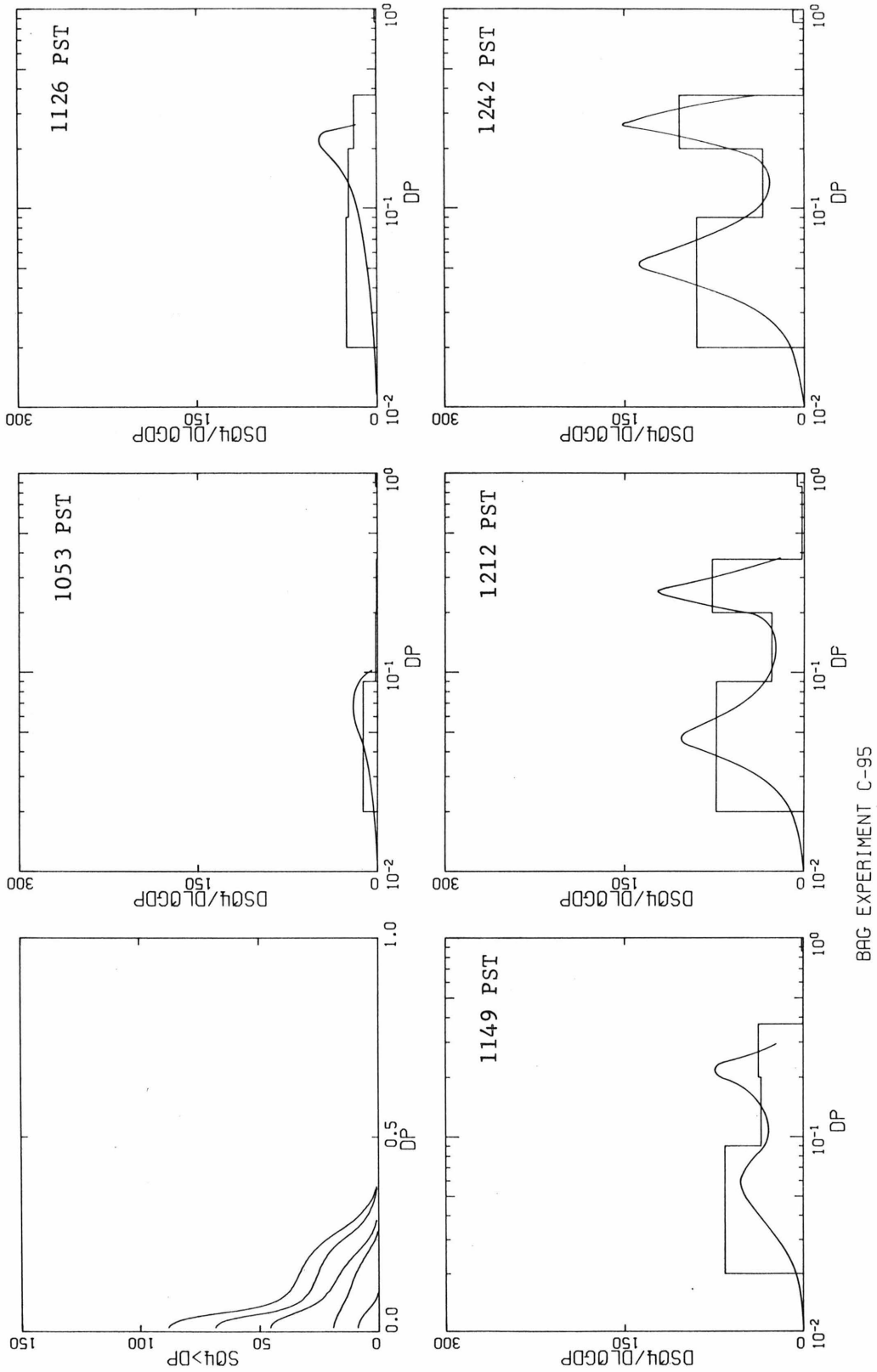

Figure 4.20 The Sulfur Size Distribution as a Function of Time during Experiment C.95

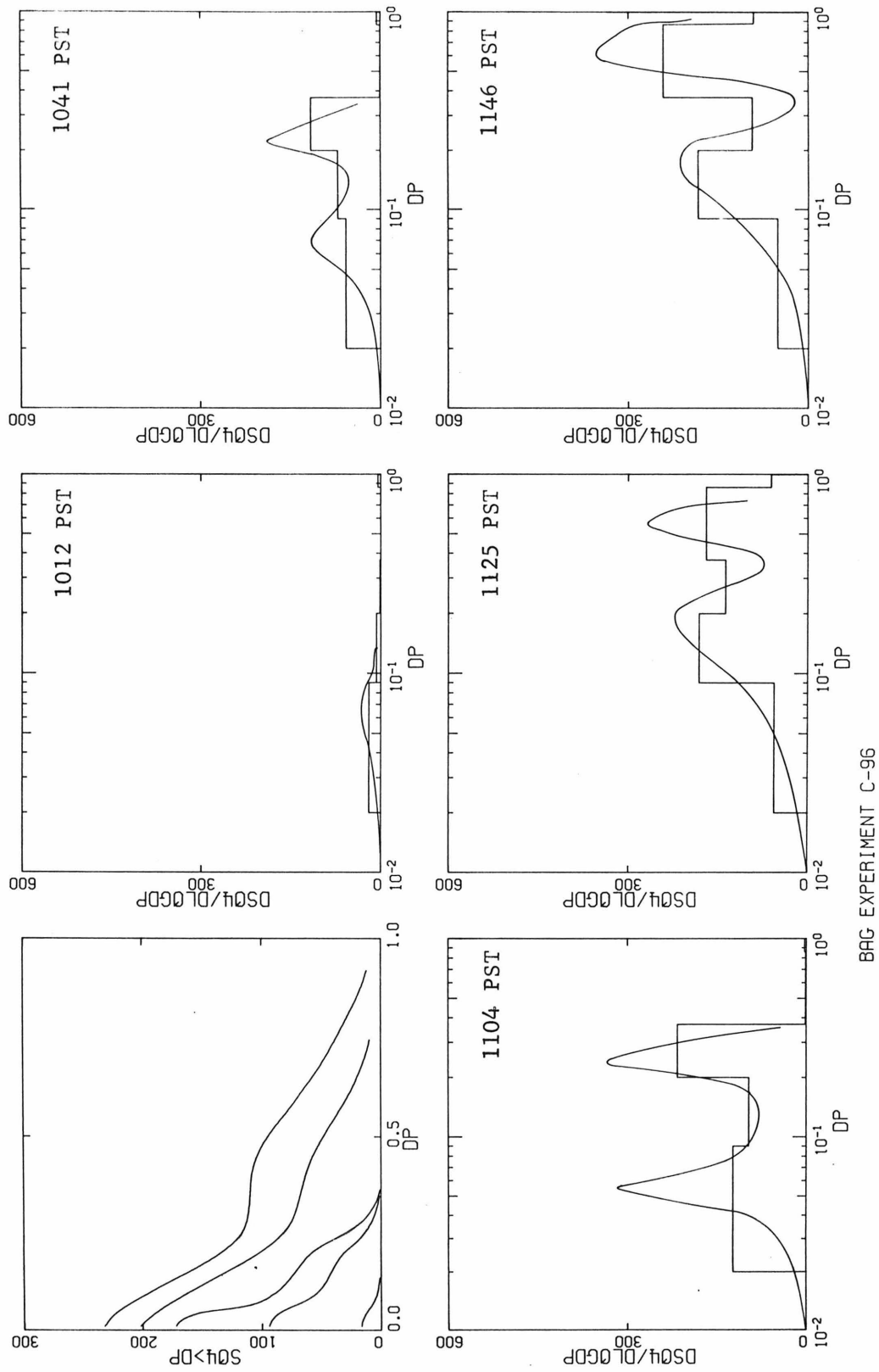

Figure 4.21 The Sulfur Size Distribution as a Function of Time during Experiment C.96

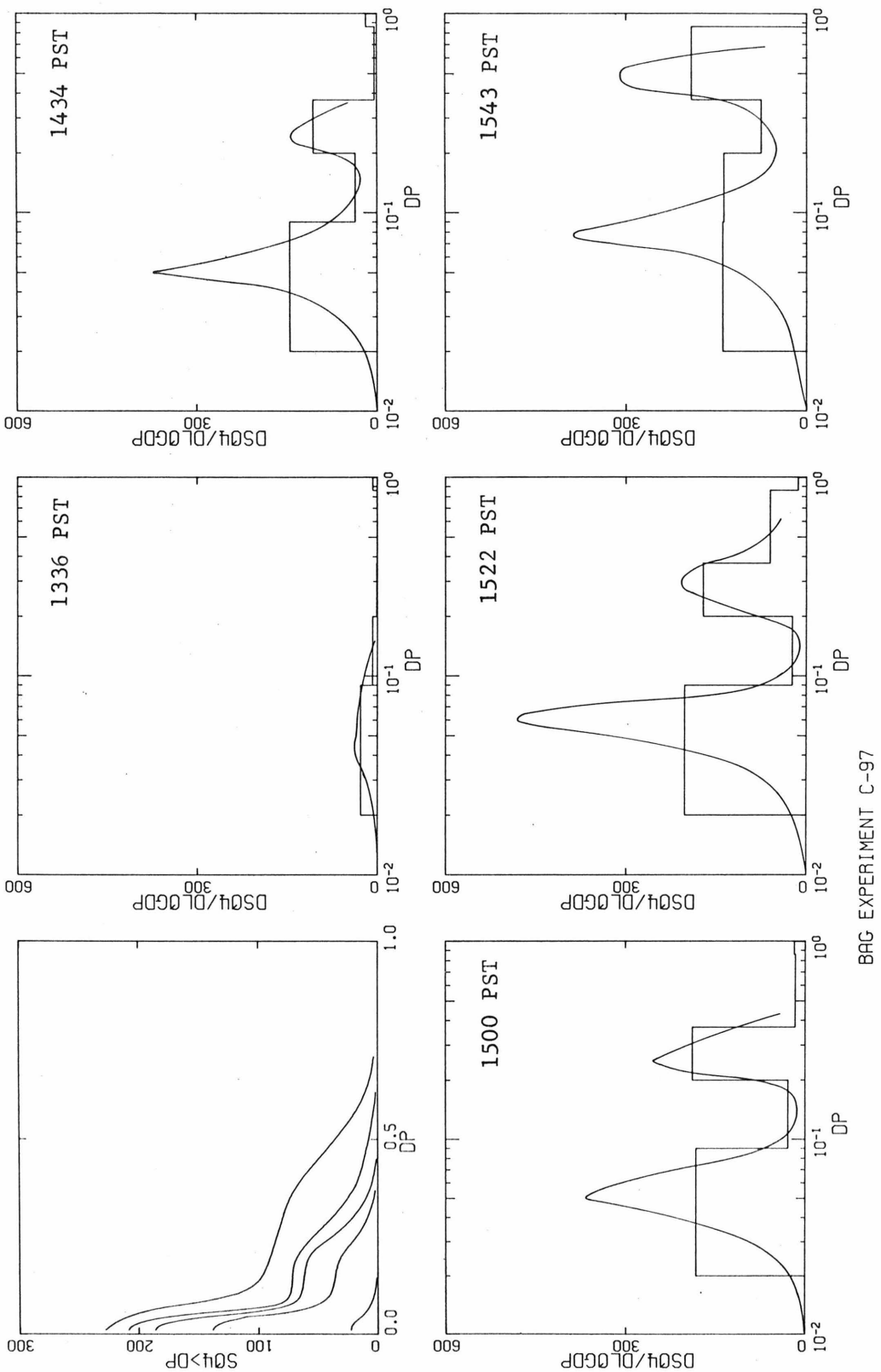

Figure 4.22 The Sulfur Size Distribution as a Function of Time during Experiment C.97

and then the two peaks grow to larger sizes by continued conversion from the gas phase. From direct comparison of the three experiments, it is evident that C.96 and C.97 resulted in the growth of sulfur to larger particle sizes than in C.95.

In section 4.5, we have shown that the formation of most of the aerosol carbon and aerosol sulfur can be explained by the reaction of SO_2 with a reactive intermediate of the O_3, 1-heptene reaction. Therefore, the aerosol sulfur is a linear function of the aerosol carbon (compare Equations 4.17 and 4.19). It was also found that the aerosol sulfur in the size range above 0.2 μm was a linear function of the total aerosol carbon (Figure 4.23). In fact, the ratio of the upper mode (> 0.2 μm) to total aerosol sulfur is 0.33 ± 0.07 throughout the three 1-heptene-SO_2 experiments. Thus, one third of the converted SO_2 appears in particles larger than 0.2 μm, and two thirds in particles smaller than 0.2 μm. In experiments with cyclohexene, cyclopentene, and 1,7 octadiene, Heisler (1975) has determined that the average critical size for aerosol carbon growth is 0.2 to 0.3 μm in diameter. This is an average taken over all of the carbon species forming aerosol from a given hydrocarbon. If a similar process is occurring in the case of 1-heptene, then it would be expected that most of the aerosol carbon is in particles greater than about 0.2 μm, thus coinciding with the upper mode in the sulfur size distribution. Calculations using the condensation nuclei concentrations from experiment C.95 indicate that the upper mode in the sulfur distribution cannot result from coagulation of particles of initial size 0.01 to 0.03 μm diameter.

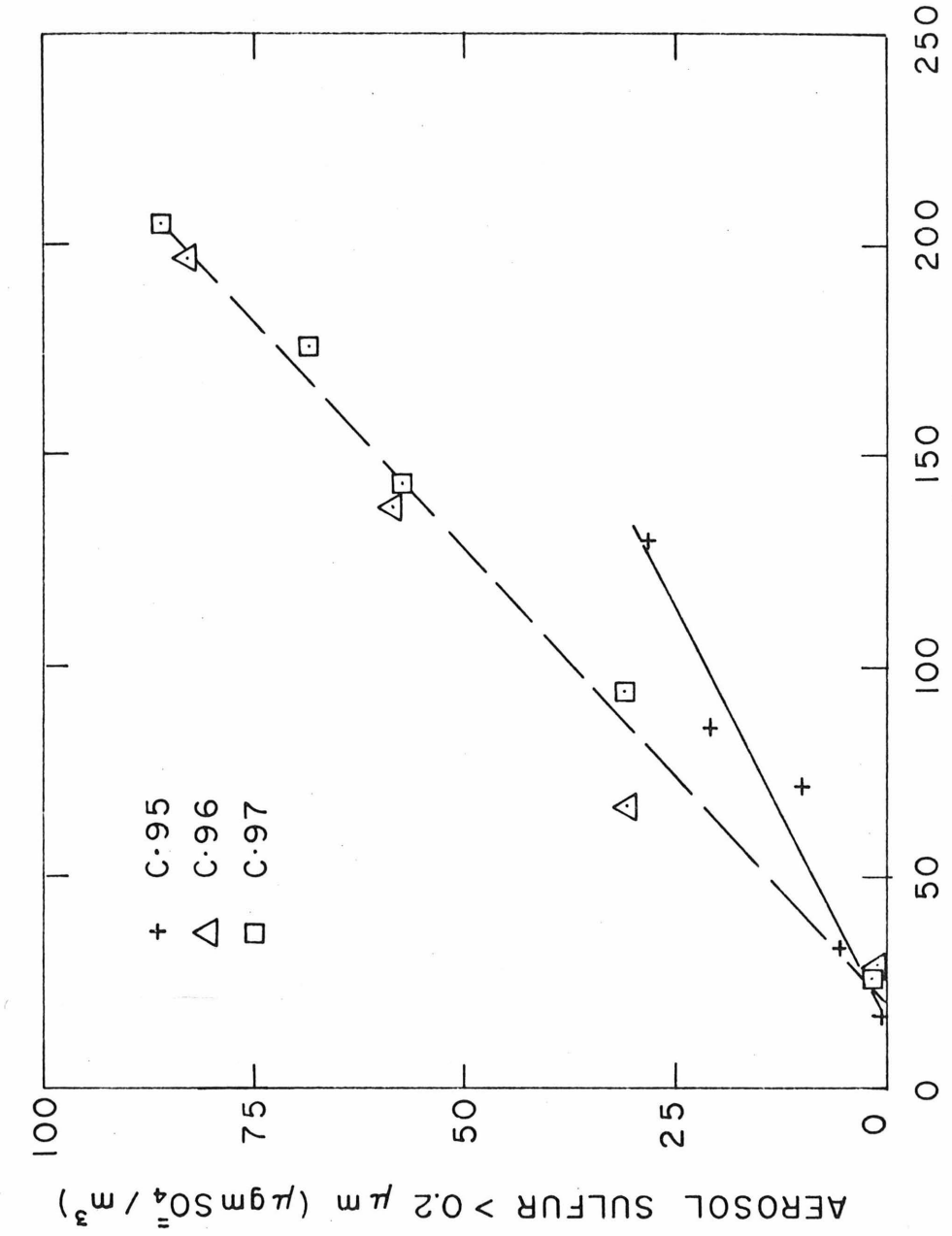

Figure 4.23 Aerosol Sulfur above 0.2 μm as a Function of Aerosol Carbon during Experiments C.95, C.96, and C.97

4.7 CONCLUSIONS

Smog chamber studies were carried out in a large Teflon bag irradiated with natural sunlight. Sulfur dioxide, nitrogen oxides, and various olefins were added to unfiltered, ambient air and allowed to react for up to 3 hours. The concentrations used were typical of average Los Angeles conditions, with the exception of the olefins. Olefin concentrations were about 100 times higher than individual ambient concentrations, although only two to five times higher than total olefin ambient concentrations. Sulfur mass balances during the experiments were excellent; measured gas and aerosol sulfur concentrations accounted for all of the initial SO_2 present.

A mechanism is proposed for aerosol sulfur and carbon formation in a system with 1-heptene, NO_x, and SO_2 added to unfiltered ambient air, irradiated by sunlight. The formation of condensable species of both carbon and sulfur is consistent with a reaction between SO_2 and a reactive intermediate of the O_3,1-heptene reaction. In fact, a drastic increase in the SO_2 oxidation rate occurred when the O_3 concentrations exceeded 0.05 ppm. Sulfur size distribution measurements as a function of time show a bimodal aerosol sulfur size distribution with a mode above and a mode below 0.2 μm . The concentration of aerosol sulfur in the upper mode is highly correlated with the total aerosol carbon and is believed to result from aerosol sulfur formation accompanying the formation of aerosol carbon. Figure 4.24 is a schematic summary of these gas-to particle conversion ideas.

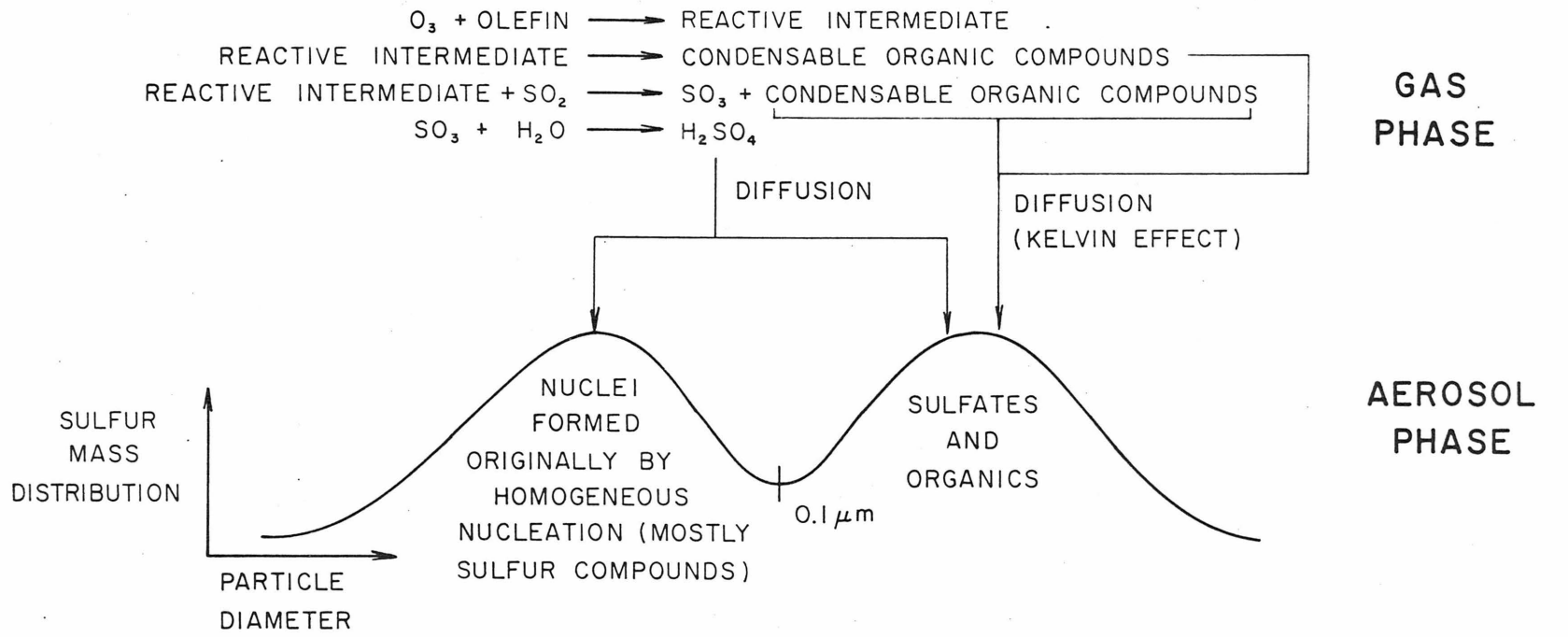

Figure 4.24 Schematic Diagram of Gas-to-Particle Conversion in the SO_2, Olefin, NO_x System. Only Limited Portions of the Proposed Scheme Have Been Experimentally Verified and the Diagram Should be Regarded as Tentative.

Large numbers of new particles were generated during the early stages of the experiments; however, no new particles were generated after the O_3 concentration exceeded about 0.05 ppm. Different mechanisms probably control the SO_2 oxidation for O_3 concentrations above and below 0.05 ppm.

CHAPTER 5

APPLICATIONS TO THE ATMOSPHERE

The distribution of sulfur species in the atmospheric aerosol as a function of particle size is extremely important because of possible detrimental effects on public health and visibility. Information about the sulfur size distribution as a function of reaction time provides a better understanding of sulfur aerosol formation.

The atmospheric size distribution of sulfur aerosol was measured at various locations in the Los Angeles basin. At a down wind receptor site (Pasadena), most of the aerosol sulfur was concentrated in the size range below 0.5 μm in diameter. However, at a site close to the major SO_2 stationary sources and at a site close to the coast, the aerosol sulfur was concentrated in larger particle sizes.

The sulfur size distribution measurements and the aerosol formation conclusions from the smog chamber studies are applied to the Los Angeles atmosphere. Estimates indicate that the SO_2 oxidation mechanism that was found to be dominant in the 1-heptene, NO_x, SO_2 smog chamber system can explain the atmospheric measurements of SO_2 reaction rates. However, the effect of compounds such as 1-heptene on the formation of carbon aerosol is estimated to be small.

The determination of the mechanism that controls SO_2 oxidation and the resulting formation of sulfur aerosol under photochemical conditions such as those in the Los Angeles atmosphere allow an evaluation of air quality control plans with respect to aerosol sulfur concentrations. Measurements of the distribution of sulfur aerosol with respect to

particle size at various times and locations throughout the Los Angeles basin allow an evaluation to be made of air quality control plans with respect to the detrimental health and visibility effects of sulfur aerosol in relation to particle size.

5.1 ATMOSPHERIC SULFUR SIZE DISTRIBUTION MEASUREMENTS

The size distribution of sulfur was measured at Pasadena in July, 1973; at California State University at Dominguez Hills in October, 1973; and at West Los Angeles in August, 1974, using a 5-stage single jet cascade impactor described in Appendix C (Scientific Advances, model no. CI-5). The samples were of 1 hour duration. The after filter and stages collect unit density particles of diameter (using the 50% cut-off sizes): less than 0.25 μm, 0.25 μm to 0.50 μm, 0.50 μm to 1.0 μm, 1.0 μm to 2.0 μm, 2.0 μm to 4.0 μm, and greater than 4.0 μm. By placing stainless steel strips in the impactor, sulfur measurements were made using the aerosol vaporization technique described in Chapter 2. Total filters were taken at the same time and analyzed by the vaporization technique. A complete listing of the atmospheric data may be found in Appendix A.

The sulfur size distributions taken in the Los Angeles basin can be classified by shape into two broad categories - those with a major portion of the aerosol sulfur mass below about 0.25 μm, and those with a major portion of the aerosol sulfur mass above about 0.50 μm. Figure 5.1 illustrates this classification. The differential sulfur mass distribution is shown as a function of particle diameter for four typical samples. The area under the curve in any particle size range

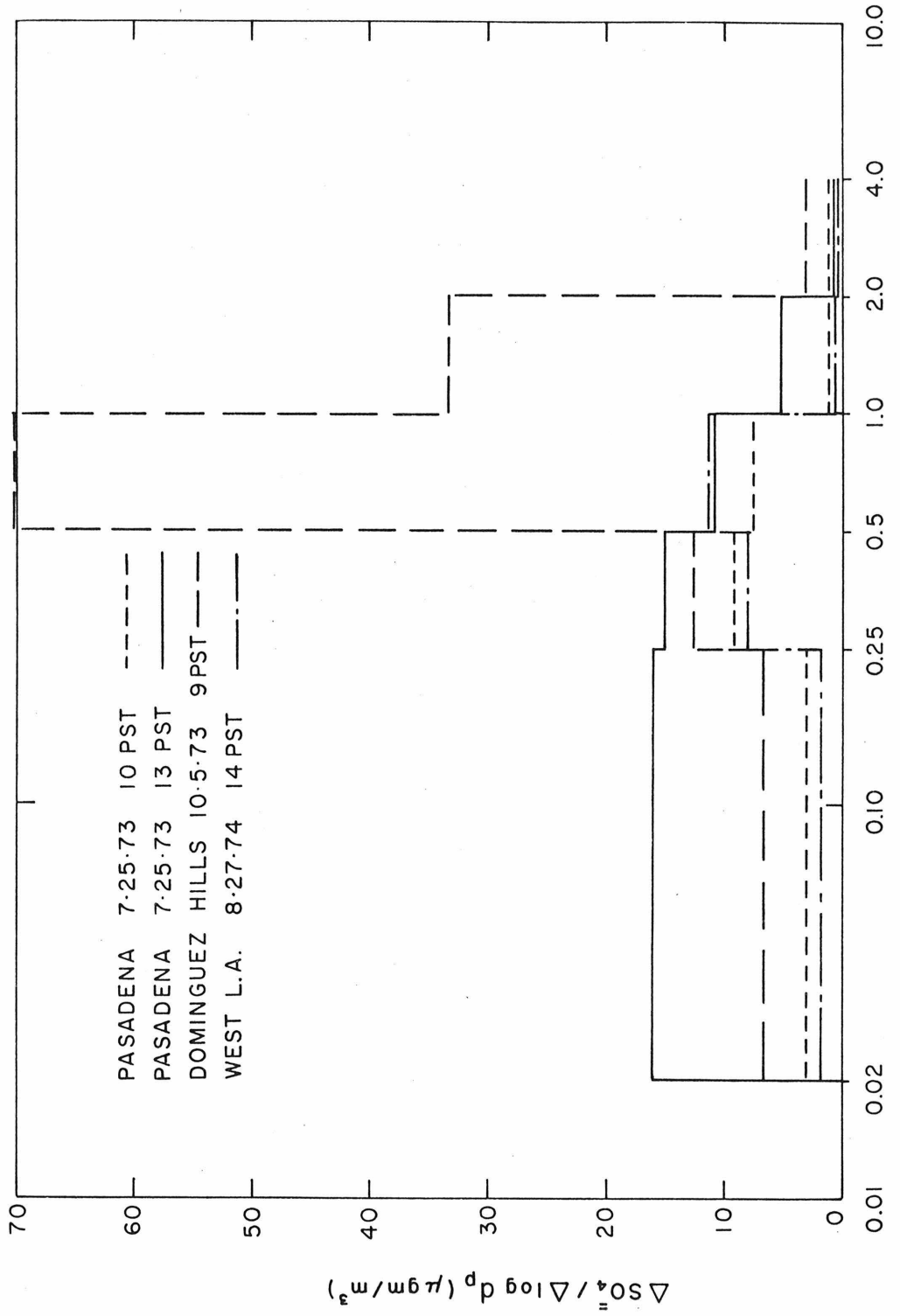

Figure 5.1 Sulfur Size Distributions at Various Locations in the Los Angeles Basin

is the mass of sulfur in that size range. A diameter of 0.02 μm was used for the lower cut-off of the after filter, as described in section 4.6. This figure shows that the sulfur size distribution function measured in the afternoon at a down wind receptor site is weighted toward the small particle sizes, while the other samples show a bias toward the larger particle sizes. This is demonstrated dramatically by the percent of the sulfur aerosol in the various size ranges for samples taken at Pasadena before and after 1200 PST (Table 5.1). An average of 24% of the aerosol sulfur was below 0.25 μm for the before 1200 PST samples; however, an average of 58% of the aerosol sulfur was below 0.25 μm for the after 1200 PST samples. The arrival time of the sea-breeze at Pasadena was about 1300 PST on both days. Figure 5.1 shows that the sulfur size distribution measurements at Dominguez Hills and West Los Angeles are similar in shape, with a peak in the distribution between 0.5 μm and 1.0 μm. The measurements made in the morning at Pasadena show a broader peak (centered at 0.5 μm) in the sulfur size distribution than either of the other two types of distributions.

Figure 5.2 shows the sulfur size distribution for two afternoon samples taken at Pasadena in March, 1975, using the low pressure impactor (discussed in Appendix C and used for the smog chamber experiments in section 4.6). The unit density particle diameter ranges for the after filter and the four stages are (using the 50% cut-off points): less than 0.09 μm, 0.09 μm to 0.20 μm, 0.20 μm to 0.37 μm, 0.37 μm to 0.86 μm, and greater than 0.86 μm. These measurements indicate that the double-peaked distributions found in the bag are found in the atmosphere.

TABLE 5.1

Average Percent Aerosol Sulfur in the Various Size Ranges
Morning and Afternoon Samples*

Particle diameter size range (μm)	Before 1200 samples	After 1200 samples
less than 0.25	24	58
0.25 to 0.50	32	19
0.50 to 1.0	35	16
greater than 1.0	9	7

*Samples taken July 25, 1973, and July 26, 1973, at Pasadena. Times are PST.

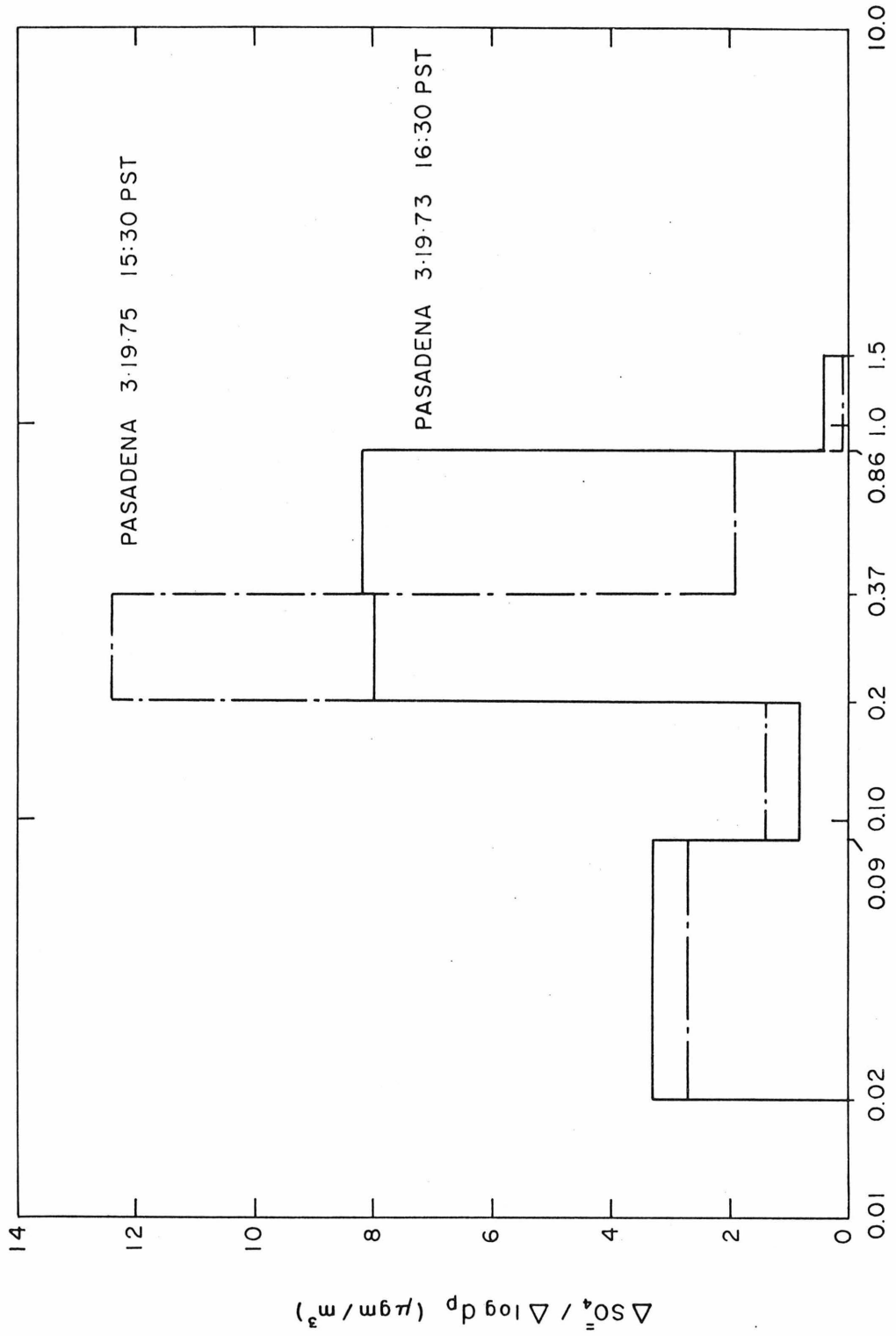

Figure 5.2 Sulfur Size Distributions at Pasadena using the Low Pressure Impactor

The concentration of sulfur mass in large particle sizes (0.5 μm diameter, and larger) is due to three major effects: a long residence time in the air, high relative humidity, and the generation of sulfur aerosols at the ocean surface. The morning samples at Pasadena had been at high humidity in the early morning and had long residence times (greater than 6 hours). The West Los Angeles measurements were taken within two miles of the coast and thus probably represent sea salt spray and natural background sources. The Dominguez Hills measurement was taken when the wind was carrying emissions from the local sulfuric acid plant to the sampling location. The samples shown in Figure 5.2 were taken on a smoggy spring day characterized by a mix of photochemistry and high relative humidity.

Sulfur size distribution measurements taken at Washington University in St. Louis, Missouri, on September 6, 1973, show distributions with greater than 90% of the sulfur aerosol below 0.5 μm in diameter (data listing in Appendix A).

Previous measurements of aerosol sulfur size distributions are in general agreement with the results reported here, although none have involved particle size discrimination below about 0.5 μm or time resolution of less than 2 hours (Roesler, et al., 1965; Ludwig, et al., 1968; Hidy, et al., 1975).

5.2 APPLICATIONS OF THE SMOG CHAMBER RESULTS TO THE ATMOSPHERE

The major test hydrocarbon used in the smog chamber studies, 1-heptene, has been measured in gasoline, diluted auto exhaust, and in the ambient atmosphere. Glasson and Tuesday (1970) found 1-heptene

in various gasolines at levels from 0.09 to 0.66 mole %. McEwen (1966) found 13 ppb 1-heptene in diluted automobile exhaust (2.27 ppm total hydrocarbons). Grosjean (1974) found 11 ppb 1-heptene in a week-long composite 8 to 10 A.M. sample taken at Pasadena in October, 1974.

The smog chamber studies discussed in Chapter 4 and the SO_2 oxidation rate constant estimates discussed in Chapter 3 determined that the fast rates of SO_2 oxidation in the Los Angeles atmosphere are a result of the photochemical involvement of O_3 and olefins in the oxidation. The pseudo-second order atmospheric rate constant for SO_2 oxidation determined in Chapter 3 was $k_2 = 0.73$ ppm^{-1} hr^{-1}. Neligan (1962) determined the average ratio of C_3-plus olefins to total hydrocarbons to be constant in Los Angeles. An estimate of 0.8 ppm olefins is made, using this constant ratio and measurements of the total hydrocarbon concentration for the samples used to estimate the rate constants in Chapter 3. This value agrees with the measurements of McEwen (1966): 0.7 ppm of total olefins in diluted automobile exhaust (2.27 ppm total hydrocarbons). Thus, an estimate of the atmospheric pseudo-third order rate constant for SO_2 oxidation is $k_3 = 0.73/0.8$ ppm^{-2} hr^{-1} = 0.9 ppm^{-2}hr^{-1} or $k_3 = 0.015$ ppm^{-2} min^{-1}. This can be compared with a similar value determined in the smog chamber experiments with 1-heptene; the pseudo-third order rate constant for oxidation of SO_2 is given in the second row of Table 4.5 as $k_3 = 0.044$ ppm^{-2} min^{-1}. Therefore, 1-heptene is about three times as effective in oxidizing SO_2 as the average C_3-plus olefin in the atmosphere. As indicated in Table 4.2, psuedo-first order oxidation rates in the smog chamber experiments with 1-heptene were from 20 to 100% hr^{-1}. Scaling these rates down by the atmospheric-olefins-

to-1-heptene-concentration-ratio and by the effectiveness ratio results in pseudo-first order oxidation rates of 3.5 to 17.5% hr^{-1}. This range is similar to the range of rates found in the atmosphere and determined in the smog chamber studies with just ambient air and SO_2.

The sulfur size distributions measured in the smog chamber experiments (section 4.6) showed aerosol sulfur growth in the size ranges found to be important in the atmospheric sulfur size distributions (section 5.1). The distributions measured in the chamber studies are consistent with the atmospheric distributions measured in Pasadena in the afternoon. However, the existence of a distinct double-peaked sulfur distribution in the atmosphere will have to be confirmed by further measurements with the low pressure impactor.

5.3 AIR QUALITY IMPLICATIONS OF THIS WORK

This work has combined laboratory and field study of sulfur aerosol formation in the Los Angeles atmosphere. This dual approach has produced laboratory studies which are closely linked to the results of the field studies. The major results of the combined study are:

(1) An aerosol vaporization technique was developed capable of measuring both total filter and cascade impactor aerosol samples for nanogram levels of sulfur.

(2) Sulfur dioxide is oxidized to form sulfur aerosol at a significant rate in the photochemically involved atmosphere of Los Angeles (about 9% hr^{-1}). Sulfur dioxide oxidation in a non-photochemically involved atmosphere such as St. Louis proceeds at a much slower rate (less than 2% hr^{-1}).

(3) The high rate of aerosol sulfur formation in a photochemical atmosphere and in smog chamber studies is dependent upon the presence of O_3 and olefins, as well as SO_2. In chamber experiments with 1-heptene and SO_2, the aerosol sulfur and the carbon formation is consistent with a reaction between SO_2 and a reactive intermediate of the O_3, 1-heptene reaction.

(4) The aerosol sulfur formed in smog chamber studies and in the Los Angeles basin is found predominantly in the size range most crucial for detrimental health effects and for visibility reduction - that from 0.1 μm to 1.0 μm in diameter.

(5) The present contribution of motor vehicles to aerosol sulfur air quality is minimal. The introduction of the catalytic converter on new automobiles will produce a small increase in aerosol sulfur concentrations at receptor sites; however, the catalytic converter will produce dramatic increases in aerosol sulfur concentrations near roadways.

The air quality implications of these findings are:

(i) Aerosol sulfur formed from air basin SO_2 emissions is more dominant in a photochemical atmosphere such as Los Angeles than in a non-photochemical atmosphere such as St. Louis.

(ii) Control of O_3 and/or olefin levels, as well as SO_2 levels, will improve aerosol sulfur air quality in a photochemical system such as Los Angeles.

(iii) Control of SO_2 levels will improve organic aerosol air quality in a photochemical system, although not on a substantial basis.

(iv) The catalytic converter will produce a dramatic increase in

aerosol sulfur concentrations near roadways, but will produce small effects at receptor sites. However, if general sulfur air quality were improved by (ii), the relative contribution of automobile catalytic converters to aerosol sulfur air quality would increase.

5.4 SUGGESTIONS FOR FURTHER RESEARCH

As mentioned in Chapter 1, aerosol sulfur air quality will continue to be an important topic of discussion and research. Therefore, the areas where further work is needed are: better aerosol sulfur analytical techniques; atmospheric rate constant determinations; the growth law for aerosol sulfur; and the effects of aerosol sulfur on human health.

A method of "continuous", on-line measurement of aerosol sulfur is necessary. The aerosol vaporization technique discussed in Chapter 2 has the potential to accomplish "continuous", on-line monitoring (possibly by using graphite or stainless steel filter materials). Also needed are techniques to measure separately the various aerosol sulfur species, such as H_2SO_4, $(NH_4)_2SO_4$, $ZnSO_4(NH_4)_2SO_4$, and $Fe_2(SO_4)_3$. Such information is critically needed in the study of the health effects of sulfur aerosol. Sulfur thermogram methods may be able to provide such information.

The technique used in Chapter 3 to determine the rate constant of SO_2 oxidation in the Los Angeles atmosphere should be applied to other data that presently exist in order to obtain a broader base of rate constant estimates (for example, the data in Hidy, et al., 1975).

Equipment is now available to measure the growth law for aerosol sulfur in a smog chamber study. The low pressure impactor described here should be redesigned to provide more size cuts in the range below 0.5 μm and to sample at a higher flow rate. Then, experiments similar to those discussed in Chapter 4 could be run, using an electrical mobility analyzer to measure the particle number distribution. These two series of measurements would provide sufficient information to determine the aerosol sulfur growth law, an input needed in any aerosol modeling scheme (Heisler, et al., 1973; Gartrell and Friedlander, 1975). More measurements of the atmospheric sulfur distribution need to be made using the low pressure impactor.

Further studies need to be conducted on health effects on humans. The relative detrimental health effects of various aerosol sulfur species need to be studied. The effects of humidity and the size distribution of the different sulfur species also need to be investigated. The most immediate problem is the assessment of possible health effects of catalytic converter emissions.

NOMENCLATURE

Arabic Notation (defining relation)

AC = aerosol carbon concentration; concentration of carbon-containing species in the aerosol, (4.15)

AS = aerosol sulfur concentration; concentration of sulfur-containing species in the aerosol, (4.19)

b_{scat} = aerosol light scattering coefficient, 10^{-4} m^{-1}

C = slip correction factor (C.2)

$\bar{C}$ = average concentration of general chemical species, ppm.

CNC = condensation nuclei count, particles/cc.

CO = carbon monoxide concentration, ppm.

d_p = particle diameter, μm

D_j = jet diameter, cm.

f = aerosol sulfur to total sulfur ratio for automobile emissions = $(W'_{S_T} - W'_{SO_2})/W'_{S_T}$

g = sulfur dioxide to total sulfur ratio = SO_2/S_T

H = 1-heptene concentration, ppm (Chapter 4)

H, $\bar{H}$ = mixing height, m (Chapter 3)

I = concentration of the reactive intermediate product of the O_3-olefin reaction, ppm

k = pseudo-first order rate constant for SO_2 decay, hr^{-1} (Chapter 3)

k = rate constant of the O_3-olefin reaction, ppm^{-1} hr^{-1} (Chapter 4)

k_1 = pseudo-third order rate constant, ppm^{-2} hr^{-1} (3.11)

k_2 = pseudo-second order rate constant, ppm^{-1} hr^{-1} (3.12)

k'_2 = pseudo-second order rate constant, ppm^{-1} hr^{-1} (3.13)

k_c = fixed, non-photochemical reaction rate, ppm/hr (3.13)

k_{ii} = rate constant of unimolecular reactions of I, min^{-1}

k_{2j} = rate constant of bimolecular reactions of I, ppm^{-1} min^{-1}

K_x, K_y, K_z = eddy diffusivities in the x, y, z directions

NO = nitric oxide concentration, ppm

NO_2 = nitrogen dioxide concentration, ppm

NO_x = nitrogen oxides concentration, ppm NO_2

OL = olefin concentration, ppm

O_3 = ozone concentration, ppm or pphm

P_{1ik} = concentration of product in unimolecular reactions of I

P_{2jk} = concentration of product in bimolecular reactions of I

Q = volumetric flow rate, ℓ/min

R_j = concentration of reactant in bimolecular reactions of I

Re = jet Reynolds number = $4Q_p/\pi\mu D_j$

SO_2, $\overline{SO_2}$ = sulfur dioxide concentration, ppm or $\mu gm\ SO_2/m^3$

$SO_4^=$ = sulfate concentration, $\mu gm\ SO_4^=/m^3$

S_T = total sulfur concentration = $SO_2 + 2AS/3$, $\mu gm\ SO_2/m^3$

Stk = Stokes number = $C V_j d_p^2 \rho_p/9\mu D_j$

T = time interval

t = time

TAC = total aerosol carbon species concentration, (4.16)

$\bar{u}$ = average wind velocity in the x-direction, m/sec

V_j = gas velocity at jet exit, cm/sec

v_a = aerosol sulfur deposition velocity, cm/sec

v_g = gaseous SO_2 deposition velocity, cm/sec

W_{SO_2} = area source emissions of SO_2, $\mu gm\ SO_2/m^2$-hr

W'_{SO_2} = area source emissions of SO_2 from the automobile, μgm SO_2/m^2-hr

W_{S_T} = area source emissions of S_T, μgm SO_2/m^2-hr

W'_{S_T} = area source emissions of S_T from the automobile, μgm SO_2/m^2-hr

x = direction of mean wind

y = direction perpendicular to mean wind and parallel to ground

z = vertical direction

Greek Notation (defining relation)

α = fraction of I that reacts to form condensable species

α_c = fraction of α which actually condenses

η = efficiency of particle collection

λ = mean free path of air, μm

μ = viscosity of air, gm-cm/sec

π = pi

ρ = gas density, gm/cm^3

ρ_p = particle density, gm/cm^3

ψ = impaction parameter (C.1)

ψ_{50} = value of the impaction parameter at an efficiency of 50%

REFERENCES

Alshuller, A. P., and J. Bufalini: Photochemical Aspects of Air Pollution: A Review, Photochemistry and Photobiology, 4:97 (1965).

Alshuller, A. P., and J. Bufalini: Photochemical Aspects of Air Pollution: A Review, Environ. Sci. Technol., 5:39 (1971).

Angell, J. K., D. H. Pack, L. Machta, C. R. Dickson, and W. H. Hoecker: Three-Dimensional Air Trajectories Determined from Tetroon Flights in the Planetary Boundary Layer of the Los Angeles Basin, J. Appl. Meteorology, 11:451 (1972).

Appel, B. R., and J. J. Wesolowski: Selection of Filter Media for Particulate Sampling with a Lundgren Impactor, AIHL Report No. 125, Air Industrial Hygiene Laboratory, State of California Department of Public Health, Berkeley, California, 1972.

Blumenthal, D. L., T. B. Smith, S. C. Marsh, P. S. McMurry, K. R. Lamb, and P. Owens: Three-Dimensional Pollutant Gradient Study, 1973 Program, vol. II:Data Summary, ARB Project ARB-2-1245, Meteorology Research, Inc., Altadena, California, 1975.

Buchholz, H.: An Underpressure Cascade Impactor, Staub-Reinhalt Luft, 30: no. 4, 17 (1970a).

Buchholz, H.: On the Separation of Airborne Matter by Inertia Effect in the Submicronic Range, Staub-Reinhalt Luft, 30: no. 5, 15 (1970b).

Bufalini, Marijon: Oxidation of Sulfur Dioxide in Polluted Atmospheres: A Review, Environ. Sci. Technol., 5:685 (1971).

Cadle, R. D., and C. Schadt: Kinetics of the Gas Phase Reaction of Olefins with Ozone, J. Am. Chem. Soc., 74:6002 (1952).

Caffe, S. T., and R. W. Gerstle: Emissions from Coal-Fired Power Plants: A Comprehensive Summary, Public Health Service Publication No. 999-AP-35, 1967.

California Air Resources Board Staff Report: Sources and Effects of Sulfates in the Atmosphere, presented at special meeting on Sulfates from Oxidation Catalyst Equipped Motor Vehicles, Sacramento, California, March 6, 1975.

Calvert, J. G.: Interaction of Air Pollutants, United States Senate, Proceedings of the Conference on Health Effects of Air Pollutants, Assembly of Life Sciences, National Academy of Sciences - National Research Council, October 3-5, 1973.

Chamberlain, A. C.: Transport of Lycopodium Spores and Other Small Particles to Rough Surfaces, Proc. Royal Soc. (A) London, 290:236 (1966).

Cheng, R. T., M. Corn, and J. O. Frohliger: Contribution to the Reaction Kinetics of Water Soluble Aerosols and SO_2 in Air at ppm Concentrations, Atmos. Environ., 5:987 (1971).

Clark, W. E.: Measurements of Aerosols Produced by the Photochemical Oxidation of SO_2 in Air, Ph. D. Thesis, University of Minnesota, Minneapolis, August, 1972.

Cox, R. A., and S. A. Penkett: The Photo-oxidation of SO_2 in Sunlight, Atmos. Environ., 4:425 (1970).

Cox, R. A., and S. A. Penkett: Aerosol Formation from Sulphur Dioxide in the Presence of Ozone and Olefinic Hydrocarbons, J. Chem. Soc., Faraday Trans. I, 68:1735 (1972).

Demerjian, K. L., J. A. Kerr, and J. G. Calvert: The Mechanism of Photochemical Smog Formation, in J. N. Pitts and R. L. Metcalf (eds.), "Advances in Environmental Science and Technology," vol. 4, John Wiley and Sons, New York, 1974.

Demore, W. B., J. C. Romanovsky, M. Feldstein, W. J. Hamming, and P. K. Mueller: Comparison of Oxidant Calibration Procedures, a report of the Ad Hoc Oxidant Measurement Committee of the California Air Resources Board, February 3, 1975.

Du Pont Technical Information Bulletin T-3E (Chemical Properties), T-5A (Optical Properties), and T-6B (Weatherability) on Teflon FEP Hydrocarbon Film, 1966.

Eriksson, E.: The Yearly Circulation of Chloride and Sulfur in Nature: Meteorological, Geochemical, and Pedological Implications, Part II, Tellus, 12:69 (1960).

Finklea, J. F., et al.: Health Consequences of Sulfur Oxides: Summary and Conclusions Based Upon CHESS Studies of 1970-1971, in "Health Consequences of Sulfur Oxides: A Report from CHESS, 1970-1971," U. S. Environmental Protection Agecny, No. EPA-650/1-74.004, Research Triangle Park, North Carolina, May, 1974.

Forrest, J., J. H. Klein, and L. Newman: Sulfur Isotope Ratios of Some Power Plant Flue Gases: A Method for Collecting Sulfur Oxide, J. Appl. Chem. Biotechnol., 23:855 (1973).

Forrest, J., and L. Newman, Brookhaven National Laboratory, personal communication, August, 1974.

Friend, J. P.: The Global Sulfur Cycle, in S. I. Rasool (ed.), "Chemistry of the Lower Atmosphere," Plenum Press, New York, 1973.

Gartrell, F. E., F. W. Thomas, and S. B. Carpenter: Atmospheric Oxidation of SO_2 in Coal-Burning Power Plant Plumes, Am. Ind. Hygiene J., 24:113 (1963).

Gartrell, G., Jr., and S. K. Friedlander: Relating Particulate Pollution to Sources: The 1972 California Aerosol Characterization Study, Atmos. Environ., 9:279 (1975).

Georgii, H. W.: Contribution to the Atmospheric Sulfur Budget, J. Geophys. Res., 75:2365 (1970).

Gerhard, E. R., and H. T. Johnstone: Photochemical Oxidation of SO_2 in Air, Ind. Eng. Chem., 47:972 (1955).

Glasson, W. A., and C. S. Tuesday: Hydrocarbon Reactivity and the Kinetics of the Atmospheric Photooxidation of Nitric Oxide, J. Air Pollut. Control Assoc., 20:239 (1970).

Groblicki, P. J., and G. J. Nebel: The Photochemical Formation of Aerosols in Urban Atmospheres, in C. S. Tuesday (ed.), "Chemical Reactions in Urban Atmospheres," Elsevier, New York, 1971.

Grosjean, D.: The Role of Ozone in the Formation of Organic Aerosols, California Institute of Technology, to be published, 1975.

Grosjean, D., California Institute of Technology, private communication on sample taken in October, 1974.

Grosjean, D.: Solvent Extraction and Organic Carbon Determination in Atmospheric Particulate Matter, Anal. Chem., 47:797 (1975).

Grosjean, D., and S. K. Friedlander: Gas-Particle Distribution Factors for Organic and Other Pollutants in the Los Angeles Atmosphere, paper no. 74-154 presented at the 67th Annual Meeting of the Air Pollution Control Association, Denver, Colorado, June 9-13, 1974.

Haagen-Smit, A. J.: Chemistry and Physiology of Los Angeles Smog, Ind. Eng. Chem., 44:1342 (1952).

Haldane, J. S., and J. G. Priestley: "Respiration," Oxford, 1935.

Harkins, J., and S. W. Nicksic: Role of Hydrocarbon Photooxidation Rates in the Atmospheric Oxidation of Sulfur Dioxide, ACS, Div. of Petroleum Chem., preprints vol. 10, no. 2, April, 1965.

Harkins, J., and S. W. Nicksic: Studies on the Role of SO_2 in Visibility Reduction, J. Air Pollut. Control Assoc., 15:218 (1965).

Heisler, S. L., California Institute of Technology, private communication, 1975.

Heisler, S. L., S. K. Friedlander, and R. B. Husar: The Relationship of Smog Aerosol Size and Chemical Element Distributions to Source Characteristics," Atmos. Environ., 7:633 (1973).

Hidy, G. M., et al.: Characterization of Aerosols in California, Final Report, Rockwell International Science Center report SC 524.25FR, Thousand Oaks, California, 1975.

Husar, J. D., R. B. Husar, W. E. Wilson, J. L. Durham, W. Shepard, J. Anderson, and S. Gregg: Aircraft Sampling and Analysis of Particulate Sulfur from Large Plumes, to be published, 1975.

Japar, S. M., C. H. Wu, and N. Niki: Rate Constants for the Reaction of Ozone with Olefins in the Gas Phase, J. Phys. Chem., 78:2318 (1974).

Johnstone, H. F., and D. R. Coughanowr: Absorption of Sulfur Dioxide from Air-Oxidation in Drops Containing Dissolved Catalyst, Ind. Eng. Chem., 50:1169 (1958).

Johnstone, H. F., and A. J. Moll: Formation of H_2SO_4 in Fogs, Ind. Eng. Chem., 52:861 (1960).

Junge, C. E.: "Air Chemistry and Radioactivity," Academic Press, New York, 1963.

Junge, C. E., and T. G. Ryan: Study of the SO_2 Oxidation in Solution and Its Role in Atmospheric Chemistry, Quart. J. Roy. Met. Soc., 84:46 (1958).

Katz, M.: Photoelectric Determination of Atmospheric Sulfur Dioxide, Anal. Chem., 22:1040 (1950).

Katz, M.: Photochemical Aspects of Atmospheric Pollutants, Can. J. Chem. Eng., 48:3 (1970).

Kellogg, W. W., R. D. Cadle, E. R. Allen, A. L. Lazrus, and E. A. Martell: The Sulfur Cycle, Science, 175: 587 (1972).

Knights, R. L.: Computer Controlled Fast Cydic Scan Mass Spectrometric Thermal Analysis II. Inorganic Air Pollutants, Ph. D. Thesis, University of Washington, Seattle, 1973.

Lamb, R. G.: Note on the Application of K-Theory to Diffusion Problems Involving Nonlinear Chemical Reactions, Atmos. Environ., 7:257 (1973).

Leahy, D., R. Siegel, P. Klotz, and L. Newman: The Separation and Characterization of Sulfate Aerosol, Atmos. Environ., 9:219 (1975).

Lee, R. E., and J. Wagman: A Sampling Anomaly in the Determination of Atmospheric Sulfate Concentration, Am. Ind. Hyg. Assoc. J., 27:266 (1966).

Lees, L., et al.: Smog: A Report to the People, Environmental Quality Laboratory, California Institute of Technology, Pasadena, 1972.

Los Angeles County Air Pollution Control District (LAAPCD): 1974 Profile of Air Pollution Control, Los Angeles, California, 1974.

Los Angeles County Air Pollution Control District (LAAPCD): Emissions and Air Quality Data, Los Angeles, California, 1973.

Ludwig, F. L., and E. Robinson: Variations in the Size Distributions of Sulfur-Containing Compounds in Urban Aerosols, Atmos. Environ., 2:13 (1968).

McEwen, D. J.: Automobile Exhaust Hydrocarbon Analysis by Gas Chromatography, Anal. Chem., 38:1047 (1966).

McNelis, D. N.: Aerosol Formation from Gas-Phase Reactions of Ozone and Olefin in the Presence of Sulfur Dioxide, EPA-650/4-74-034, Ph. D. Thesis, University of North Carolina, August, 1974.

Maddalone, R. F., G. L. McClure, and P. W. West: Determination of Sulfate by Thermal Reduction of Perimidylammonium Sulfate, Anal. Chem., 47:316 (1975).

Manowitz, B., et al.: The Atmospheric Diagnostics Program at Brookhaven National Laboratories: Second Status Report, BNL 50206, 1970.

Manowitz, B., et al.: The Atmospheric Diagnostics Program at Brookhaven National Laboratories: Fourth Status Report, BNL 50361, 1973.

Marple, V. A.: A Fundamental Study of Inertial Impactors, Ph. D. Thesis, University of Minnesota, Minneapolis, December, 1970.

May, K. R.: The Cascade Impactor: An Instrument for Sampling Coarse Aerosols, J. Sci. Instr., 22:187 (1945).

Miller, M. S., S. K. Friedlander, and G. M. Hidy: A Chemical Element Balance for the Pasadena Aerosol, J. Colloid. Interface Sci., 39:165 (1972).

Mudgett, P. S., L. W. Richards, and J. R. Roehrig: A New Technique to Measure Sulfuric Acid in the Atmosphere, in R. K. Stevens and W. F. Herget (eds.), "Analytical Measurements Applied to Air Pollution Measurements," Ann Arbor Science Publishers, Inc., Ann Arbor, Michigan, 1974.

Neiburger, M., and J. G. Edinger: Summary Report on Meteorology of the Los Angeles Basin with Particular Respect to the "Smog" Problem, Southern California Air Pollution Foundation Report No. 1, Los Angeles, California, 1954.

Neligan, R. E.: Hydrocarbons in the Los Angeles Atmosphere, Arch. Environ. Health, 5:581 (1962).

Nelson, P. A.: A High Pressure Drop Cascade Impactor for Sizing Particles Between 10 Microns and 0.03 Microns in Diameter, paper no. 73-AP-26 presented at the Pacific Northwest International Section, Air Pollution Control Association, Seattle, Washington, November 28-30, 1973.

Novakov, T., S. G. Chang, and A. B. Harker: Sulfates as Pollution Particulates: Catalytic Formation on Carbon (Soot) Particles, Science, 186:259 (1974).

O'Brien, R. J., J. H. Gabtree, J. R. Holmes, M. C. Hoggan, and A. H. Bockian: Organic Photochemical Aerosol, Part I: Environmental Chamber Experiments, submitted for publication in Environ. Sci. Technol. (1973).

Okita, T.: Filter Method for the Determination of Trace Quantities of Amines, Mercaptans, and Organic Sulphides in the Atmosphere, Atmos. Environ., 4:93 (1970).

Ostroff, A. G., and R. T. Sanderson: Thermal Stability of Some Metal Sulphates, J. Norg. Nuclear Chem., 9:45 (1959).

Parker, G. W., and H. Buchholz: Size Classification of Submicron Particles by a Low-Pressure Cascade Impactor, ORNL-4226, Oak Ridge National Laboratory, Oak Ridge, Tennessee, June, 1968.

Payne, W. A., L. J. Stief, and D. D. Davis: A Kinetics Study of the Reaction of HO_2 with SO_2 and NO, J. Am. Chem. Soc., 95:7614 (1973).

Pierson, W. R., R. H. Hammerle, and J. T. Kummer: Sulfuric Acid Aerosol Emissions from Catalyst-Equipped Engines, SAE paper no. 740287 presented at the Automotive Engineering Congress, Detroit, Michigan, February 25 - March 1, 1974.

Prager, M. J., E. R. Stephens, and W. E. Scott: Aerosol Formation from Gaseous Air Pollutants, Ind. Eng. Chem., 52:521 (1960).

Renzetti, N. A., and G. Doyle: The Chemical Nature of the Particulate in Irradiated Automobile Exhaust, J. Air Pollut. Control Assoc., 8:293 (1959).

Roberts, Paul T., and Sheldon K. Friedlander: Conversion of SO_2 to Sulfur Particulate in the Los Angeles Atmosphere, Environ. Health Perspectives, April, 1975, p. 103. Presented at the Symposia Impact of Mobile Emissions Controls, Durham, North Carolina, April 16-19, 1974.

Roberts, P. J. W., P. M. Roth, and C. L. Nelson: "Contaminant Emissions in the Los Angeles Basin," Appendix A, Systems Applications, Inc., Beverly Hills, California, 1971.

Robinson, E., and R. C. Robbins: "Sources, Abundance, and Fate of Gaseous Atmospheric Pollutants," SRI Report no. 6755, Stanford Research Institute, Menlo Park, California, 1968.

Roesler, J. F., H. J. R. Stevenson, and J. S. Nader: Size Distribution of Sulfate Aerosols in the Ambient Air, J. Air Pollut. Control Assoc., 15:576 (1965).

Scaringelli, F. P., and K. A. Rehme: Determinations of Atmospheric Concentrations of Sulfuric Acid by Spectrophotometry, Coulometry, and Flame Photometry, Anal. Chem.,41:707 (1969).

Schutzle, D.: Computer Controlled High Resolution Mass Spectrometric Analysis of Air Pollutants, Ph. D. Thesis, University of Washington, Seattle, 1972.

Scott, D. J.: "Gas Chromatographic Detectors," John Wiley and Sons, New York, 1974.

Shepherd, J. G.: Measurements of the Direct Deposition of Sulphur Dioxide onto Grass and Water by the Profile Method, Atmos. Environ., 8:69 (1974).

Sidebottom, H. W., C. C. Badock, G. E. Jackson, J. G. Calvert, G. W. Reinhardt, and E. K. Damon: Photooxidation of Sulfur Dioxide, Environ. Sci. Technol., 6:72 (1972).

Smith, J. P., and P. Urone: Static Studies of Sulfur Dioxide Reactions: Effects of NO_2, C_3H_6, and H_2O, Environ. Sci. Technol., 8:742 (1974).

Stephens, E. R., and M. A. Price: Comparison of Synthetic and Smog Aerosols, J. Colloid Interface Sci., 39:272 (1972).

Stern, S. C., H. W. Zeller, and A. I. Schekman: Collection Efficiency of Jet Impactors at Reduced Pressures, Ind. Eng. Chem. Fundamentals, 1:273 (1962).

Stevenson, H. J. R., D. E. Sanderson, and A. P. Altshuller: Formation of Photochemical Aerosols, Int. J. Air Wat. Poll., 9:367 (1965).

Study of Critical Environmental Problems: "Man's Impact on the Global Environment," MIT Press, Cambridge, Massachusetts, 1970.

Tokiwa, Y., B. R. Appel, S. Wall, and J. J. Wesolowski: Evaluation of Sulfate Data in the Los Angeles Metropolitan Area, California Department of Health, Air and Industrial Hygiene Laboratory, Berkeley, California, September 15, 1974.

Urone, Paul, and William H. Schroeder: SO_2 in the Atmosphere: A Wealth of Monitoring Data, but Few Reaction Rate Studies, Environ. Sci. Technol., 3:436 (1969).

U. S. Bureau of Mines, Department of Interior: "Motor Gasolines: Summer 1973," 1974.

Wagman, J., R. E. Lee, Jr., and C. J. Axt: Influence of Some Atmospheric Variables on the Concentration and Particle Size Distribution of Sulfate in Urban Air, Atmos. Environ., 1:479 (1967).

Weber, Erich: Contribution to the Residence Time of SO_2 in a Polluted Atmosphere, J. Geophys. Res., 75:2909 (1970).

Wendlandt, W. W., and T. M. Southern: An Apparatus for Simultaneous Gas Evolution Analysis and Mass Spectrometric Analysis, Anal. Chim. Acta, 32:405 (1965).

White, W. H., R. B. Husar, and S. K. Friedlander: A Study of Los Angeles Smog Aerosol Dynamics by Air Trajectory Analysis, paper no. 73-111 presented at the 66th Annual Meeting of the Air Pollution Control Assoc., Chicago, Illinois, June 24-28, 1973.

White, W. H., and P. T. Roberts: The Nature and Origins of Visibility-Reducing Aerosols in Los Angeles, paper no. 75-28.6 presented at the 68th Annual Meeting of the Air Pollution Control Assoc., Boston, Massachusetts, June 15-20, 1975.

Wilson, W. E., Jr., M. C. Dodge, D. N. McNelis, and J. Overton: SO_2 Oxidation Mechanism in Olefin-NO_x-SO_2 Smog, Div. Env. Chem. paper no. 20, presented at the 167th ACS Meeting, Los Angeles, California, March 31 - April 5, 1974.

Wilson, W. E., and A. Levy: A Study of Sulfur Dioxide in Photochemical Smog I. Effect of SO_2 and Water Vapor Concentration in the 1-Butene/NO_x/SO_2 System, J. Air Pollut. Control Assoc., 20:385 (1970).

Wilson, W. E., Jr., A. Levy, and D. B. Wimmer: A Study of Sulfur Dioxide in Photochemical Smog II. Effect of Sulfur Dioxide on Oxidant Formation in Photochemical Smog, J. Air Pollut. Control Assoc., 22:27 (1972).

Winer, A. M., J. W. Peters, J. P. Smith, and J. N. Pitts, Jr.: Response of Chemiluminescent NO-NO_2 Analyzers to Other Nitrogen-Containing Compounds, Environ. Sci. Technol., 8:1118 (1974).

Wood, W. P., A. W. Castleman, Jr., and I. N. Tang: Mechanisms of Aerosol Formation from SO_2, paper no. 74-153 presented at the 67th Annual Meeting of the Air Pollution Control Assoc., Denver, Colorado, June 9-13, 1974.

APPENDIX A

ATMOSPHERIC AND SMOG CHAMBER AEROSOL DATA

A complete listing of both atmospheric and smog chamber aerosol chemical data is available in this Appendix. Table A.1 is a computer listing of total filter data for Pasadena, Dominguez Hills, West Los Angeles and St. Louis, Missouri (Washington University). This table also includes SO_2 concentration data for the same samples. Errors in the aerosol sulfur concentrations are estimated from replicate analysis, plus errors in the flow rate, etc. Table A.2 contains the atmospheric sulfur size distribution data for Pasadena, Dominguez Hills, West Los Angeles, and St. Louis, Missouri (Washington University). Table A.3 is a listing of the sulfur size distribution data for smog chamber experiments C.95, C.96, and C.97. Table A.4 is a computer listing of smog chamber total filter sulfur data. Table A.5 is a listing of smog chamber total filter carbon data. Table A.6 is a listing of dry and wet sulfur deposition measurements made at Pasadena and Dominguez Hills.

TABLE A.1

ATMOSPHERIC DATA: AEROSOL SULFUR TOTAL FILTERS

ALL CONCENTRATIONS IN MICROGRAMS/CUBIC METER

DATE TIME	SO4	SO4 SIGMA	SO4 AS SO2	SO4,2 SIGMA	SO2 AVG	SO2 SIGMA	SO2/ST	SO2/ST3 SIGMA
7103 8.0	59.23	13.82	39.48	9.21	10.00	13.25	0.20	0.04
7103 9.0	50.52	11.85	33.67	7.90	28.00	13.25	0.45	0.06
710310.0	38.67	9.04	25.78	6.03	51.00	13.25	0.66	0.05
710311.5	19.76	4.58	13.17	3.05	88.00	13.25	0.87	0.03
710313.0	20.28	4.73	13.52	3.15	118.00	13.25	0.90	0.02
710314.0	21.88	5.12	14.58	3.41	97.00	13.25	0.87	0.03
710315.0	24.42	5.71	16.28	3.81	42.00	13.25	0.72	0.06
710316.0	37.64	8.80	25.09	5.87	44.00	13.25	0.64	0.06
710318.5	15.93	3.68	10.62	2.45	18.00	13.25	0.63	0.11
712310.0	50.00	11.37	33.33	7.58	50.00	13.25	0.60	0.05
712312.0	32.00	7.27	21.33	4.85	44.79	13.25	0.68	0.06
712314.0	45.00	10.23	29.99	6.82	59.72	13.25	0.67	0.05
712316.5	24.00	5.43	16.00	3.62	53.75	13.25	0.77	0.05
7253 9.0	8.64	2.19	5.76	1.46	31.06	5.30	0.84	0.03
725310.0	10.68	2.64	7.12	1.76	47.77	5.30	0.87	0.03
725311.0	9.21	2.26	6.14	1.50	28.66	5.30	0.82	0.04
725312.0	24.35	5.91	16.23	3.94	28.66	5.30	0.64	0.04
725313.0	27.72	6.74	18.48	4.49	31.06	5.30	0.63	0.04
725314.0	34.10	8.24	22.73	5.49	35.83	5.30	0.61	0.04
725315.0	24.35	5.78	16.23	3.85	47.77	5.30	0.75	0.04
725316.0	18.51	4.37	12.34	2.91	35.83	5.30	0.74	0.04
726310.0	14.60	3.71	9.73	2.47	17.92	5.30	0.65	0.06
726311.0	14.51	3.66	9.67	2.44	28.37	5.30	0.75	0.04
726312.0	18.15	4.44	12.10	2.96	43.00	5.30	0.78	0.04
726313.0	13.25	3.30	8.83	2.20	34.63	5.30	0.80	0.04
726314.0	13.18	3.20	8.79	2.14	22.69	5.30	0.72	0.05
726315.0	14.55	3.52	9.70	2.35	35.83	5.30	0.79	0.04
726317.5	16.19	3.85	10.79	2.56	101.50	5.30	0.90	0.02
PA-110.5	35.79	7.59	23.86	5.06	34.71	7.95	0.59	0.04
PA-211.5	48.26	6.65	32.17	4.43	29.94	7.95	0.48	0.04
PA-312.5	68.50	8.59	45.66	5.73	47.96	7.95	0.51	0.03
PA-413.5	31.37	4.72	20.91	3.15	62.94	7.95	0.75	0.03

TABLE A.1 (CONTINUED)

DATE TIME	SO4	SO4 SIGMA	SO4 AS SO2	SO4,2 SIGMA	SO2 AVG	SO2 SIGMA	SO2/ST	SO2/ST SIGMA
PA-514.5	38.87	9.42	25.91	6.28	84.14	7.95	0.76	0.04
PA-615.5	32.66	5.88	21.77	3.92	80.82	7.95	0.79	0.03
PA-716.5	18.47	6.27	12.31	4.18	45.05	7.95	0.79	0.05
PAS1 9.0	15.44	4.83	10.29	3.22	10.60	7.95	0.51	0.10
PAS211.0	13.47	4.07	8.98	2.71	29.15	7.95	0.76	0.06
PAS312.5	18.20	5.23	12.13	3.48	9.27	7.95	0.43	0.10
PAS414.0	8.06	1.17	5.37	0.78	8.48	7.95	0.61	0.14
PAS5NITE	12.67	1.19	8.45	0.79	0.0	0.0	0.0	0.0
AT W-01	27.93	4.64	18.61	3.09	85.25	7.95	0.82	0.02
AT W-02	13.31	5.52	8.87	3.68	99.69	7.95	0.92	0.03
AT W-03	3.11	1.07	2.07	0.72	98.87	7.95	0.98	0.01
AT W-04	24.80	3.31	16.53	2.21	75.84	7.95	0.82	0.02
AT W-05	23.83	3.92	15.89	2.62	169.33	7.95	0.91	0.01
AT W-06	6.85	0.90	4.56	0.60	75.31	7.95	0.94	0.01
AT W-07	40.50	7.81	26.99	5.21	229.54	7.95	0.89	0.02
AT W-08	36.53	7.32	24.35	4.88	139.65	7.95	0.85	0.02
AT W-09	32.48	3.75	21.65	2.50	161.65	7.95	0.88	0.01
AT W-10	37.75	4.85	25.16	3.23	101.63	7.95	0.80	0.02
AT W-11	3.45	0.47	2.30	0.32	81.78	7.95	0.97	0.00
AT W-12	2.20	0.48	1.47	0.32	43.99	7.95	0.97	0.01
AT W-13	7.29	1.01	4.86	0.68	158.20	7.95	0.97	0.00
AT W-14	3.65	0.41	2.43	0.28	120.31	7.95	0.98	0.00
AT W-15	4.29	0.67	2.86	0.45	62.54	7.95	0.96	0.01
3174 2.0	1.16	0.48	0.77	0.32	107.59	8.00	0.99	0.00
3174 6.0	8.03	1.73	5.35	1.15	103.62	8.00	0.95	0.01
3174 9.0	4.54	0.65	3.02	0.43	77.51	8.00	0.96	0.01
317411.0	2.02	0.72	1.35	0.48	151.05	8.00	0.99	0.00
317413.0	2.13	0.73	1.42	0.49	76.59	8.00	0.98	0.01
317415.0	1.53	0.69	1.02	0.46	51.54	8.00	0.98	0.01
317417.0	4.77	1.10	3.18	0.74	54.86	8.00	0.95	0.01
317419.0	2.36	1.20	1.58	0.80	44.12	8.00	0.97	0.02
317422.0	4.07	0.54	2.71	0.36	204.85	8.00	0.99	0.00

TABLE A.2

Atmospheric Data: Sulfur Size Distributions*

	Times (PST)							
	Start	Stop	1	2	3	4	5	Total Filter
Pasadena								
7-12-73	1100	1300	0.1	0.1	1.2	10.1	6.8	32.0
	1300	1500	0.1	0.6	0.2	2.7	8.6	45.0
	1500	1800	0.0	0.0	0.1	2.0	1.9	24.0
7-25-73	0830	0927	0.2	0.2	0.4	1.8	3.5	8.6
	0930	1027	—	1.2	0.6	2.4	3.3	10.7
	1030	1126	0.2	0.4	0.3	2.3	2.7	9.2
	1130	1227	0.4	0.4	0.6	3.4	4.3	24.4
	1230	1328	0.3	0.2	1.6	3.3	4.5	27.7
	1330	1423	0.8	0.4	1.0	3.4	6.6	34.1
	1430	1528	0.3	0.2	0.8	5.3	5.3	24.4
	1530	1630	0.4	0.5	0.7	3.3	3.8	18.5
7-26-73	0938	1032	0.4	0.4	0.5	6.9	6.0	14.6
	1038	1132	0.3-	—	0.5	7.9	2.6	14.5
	1136	1244	0.2	0.2	0.7	6.9	6.0	18.2
	1343	1430	—	0.2	0.2	1.9	2.0	13.2
	1436	1537	0.2	0.2	0.1	2.4	5.3	14.6
	1538	1834	—	0.1	0.2	2.2	3.3	16.2
West Los Angeles								
8-27-74	1311	1418	0.0	0.0	0.1	3.4	2.4	7.9
	1428	1515	0.0	0.0	0.0	3.0	2.5	10.5
	1526	1620	0.0	0.0	0.0	3.1	1.2	9.7

TABLE A.2 (continued)

	Times (PST) Start	Stop	1	2	3	4	5	Total Filter
Dominguez Hills								
10-4-73	0910	1021	1.2	1.0	0.6	4.8	1.5	24.8
	1026	1125	1.5	0.1	1.8	2.8	8.4	23.8
	1129	1400	0.4	0.1	0.1	3.7	2.1	6.8
10-5-73	0837	0939	1.6	0.9	10.0	21.2	3.8	40.5
	0943	1107	0.3	0.4	2.0	14.2	6.4	36.5
	1112	1217	0.3	0.1	1.7	13.7	8.9	32.5
	1221	1525	0.5	0.5	1.1	7.2	3.2	37.8
10-11-73	0939	1100	0.1	0.2	0.3	1.6	2.0	2.2
	1104	1204	0.1	0.1	0.2	1.0	6.9	7.3
	1210	1403	0.3	0.1	0.1	0.9	1.2	3.6
	1407	1510	0.1	0.0	0.0	0.3	2.4	4.3
St. Louis								
9-6-73	0007	0821	0.1	0.0	0.0	0.1	1.8	2.8
	0826	1004	0.1	0.1	0.1	0.1	5.7	24.3
	1010	1200	0.1	0.1	0.1	0.1	6.2	16.6
	1204	1525	0.0	0.0	0.0	0.0	1.6	7.6
	1600	1803	0.1	0.1	0.1	0.1	1.9	9.0
	1807	0113	0.0	0.0	0.0	0.1	1.6	4.6

*Values are μgm $SO_4^=/m^3$. Fifty percent cut-off diameters are: stage 1, 4.0 μm; stage 2, 2.0 μm; stage 3, 1.0 μm; stage 4, 0.5 μm; stage 5, 0.25 μm.

TABLE A.3

Smog Chamber Data: Aerosol Sulfur Size Distributions*†

Experiment no.	Sample no.	Stage 1	Stage 2	Stage 3	Stage 4	Total filter	Calculated total filter
C.95	1	0.1	0.0	0.3	0.6	5.7	8.9
	2	0.2	0.1	5.0	8.1	9.4	19.1
	3	0.1	0.0	9.8	12.2	31.2	45.5
	4	0.4	0.7	20.5	9.4	77.4	68.7
	5	0.6	0.1	27.8	11.9	86.4	88.3
C.96	1	0.3	0.1	0.5	2.6	3.4	16.4
	2	0.4	0.2	30.9	24.7	87.2	93.8
	3	0.2	0.5	57.8	33.2	179.2	171.8
	4	4.0	62.0	36.5	62.9	202.7	201.6
	5	21.2	88.5	24.8	63.5	235.5	220.2
	6	---------- samples lost ----------					232.2
C.97	1	0.5	0.2	0.4	2.8	9.5	22.5
	2	---------- samples lost ----------					76.1
	3	1.2	1.4	28.2	12.5	143.0	138.3
	4	1.2	6.0	50.2	9.8	194.2	186.2
	5	0.9	21.9	45.7	8.0	234.6	208.7
	6	0.9	70.0	20.0	47.5	230.4	228.2

*concentrations expressed as μgm $SO_4^{=}/m^3$

†50% cut-off diameters: stage 1, 0.86 μm; stage 2, 0.37 μm; stage 3, 0.20 μm; stage 4, 0.09 μm

TABLE A.4

SMOG CHAMBER DATA: AEROSOL SULFUR TOTAL FILTERS

ALL CONCENTRATIONS IN MICROGRAMS/CUBIC METER

SAMPLE TIME	SO4	SO4 SIGMA	SO4 AS SO2	SO4,2 SIGMA	SO2 AVG	SO2 SIGMA	SO2/ST	SO2/ST SIGMA
B011038	5.70	2.09	3.80	1.39	93.10	7.95	0.96	0.01
B021114	9.41	3.58	6.27	2.39	80.05	7.95	0.93	0.02
B031141	31.08	7.95	20.72	5.30	62.47	7.95	0.75	0.04
B041202	77.18	20.97	51.45	13.97	46.95	7.95	0.48	0.04
B051228	86.21	13.27	57.47	8.85	33.86	7.95	0.37	0.02
B061000	3.43	1.19	2.28	0.80	199.84	7.95	0.99	0.00
B071029	87.20	11.08	58.12	7.39	148.22	7.95	0.72	0.02
B081056	179.21	21.44	119.45	14.29	96.16	7.95	0.45	0.02
B091116	202.73	29.46	135.13	19.64	76.31	7.95	0.36	0.01
B101136	235.53	38.09	156.99	25.39	63.91	7.95	0.29	0.01
B111201	228.68	32.42	152.42	21.61	55.88	7.95	0.27	0.01
B121321	9.54	2.04	6.36	1.36	211.60	7.95	0.97	0.01
B131354	44.14	8.47	29.42	5.65	175.95	7.95	0.86	0.02
B141423	142.95	21.00	95.28	14.00	134.41	7.95	0.59	0.02
B151449	194.20	50.67	129.45	33.77	102.47	7.95	0.44	0.03
B161515	234.57	32.22	156.35	21.47	87.53	7.95	0.36	0.01
B171533	230.41	45.53	153.58	30.35	78.49	7.95	0.34	0.02

TABLE A.5

Smog Chamber Data: Aerosol Carbon Total Filters

Experiment no.	Sample no.	Sampling Time (PST) Start	Stop	Total Aerosol Carbon (μgm C/m^3)
C.95	1	1038	1108	17.1
C.95	2	1115	1137	33.5
C.95	3	1141	1158	70.9
C.95	4	1202	1223	85.1
C.95	5	1228	1256	128.8
C.96	1	1000	1025	29.5
C.96	2	1029	1052	66.9
C.96	3	1056	1112	137.7
C.96	4	1117	1133	197.3
C.96	5	1137	1155	204.2
C.96	6	1201	1226	242.0
C.97	1	1321	1351	26.5
C.97	2	1355	1419	33.8
C.97	3	1423	1444	93.9
C.97	4	1449	1510	142.5
C.97	5	1515	1530	174.8
C.97	6	1533	1553	205.5

TABLE A.6

Aerosol Phase and Gas Phase Sulfur Deposition

Location		Pasadena	Pasadena	Pasadena	Dominguez Hills	Dominguez Hills
Begin	Date Time (PST)	6·14·73 0915	10·9·73 0745	5·11·74 1000	10·3·73 0858	10·9·73 0917
End	Date Time (PST)	6·15·73 01015	10·11·73 1420	5·12·74 1020	10·5·73 1156	10·12·73 0732
Dry Flux (μgm $SO_4^=/cm^2$-day)*		0.08	0.04	0.32	--	0.11
Aerosol Sulfur (μgm $SO_4^=/m^3$)		--	9.5	38.0	--	--
Aerosol Sulfur Deposition Velocity, v_a (cm/sec)		--	0.05	0.08	--	--
Wet Flux (μgm SO_2/cm^2-day)†		--	2.0	0.32	2.6	2.4
Sulfur Dioxide (μgm SO_2/m^3)		--	48	6	67	--
SO_2 Deposition Velocity (cm/sec)		--	0.8	0.6	0.5	--

*Sulfur collected on stainless steel strips

†Sulfur collected in purified water

APPENDIX B

AIR TRAJECTORIES

This Appendix contains the air trajectories calculated by Warren H. White as described in Section 3.2. They are for arrival at Caltech at the midpoint of each aerosol sample time. Only the trajectories which showed direct transport from the coast are included.

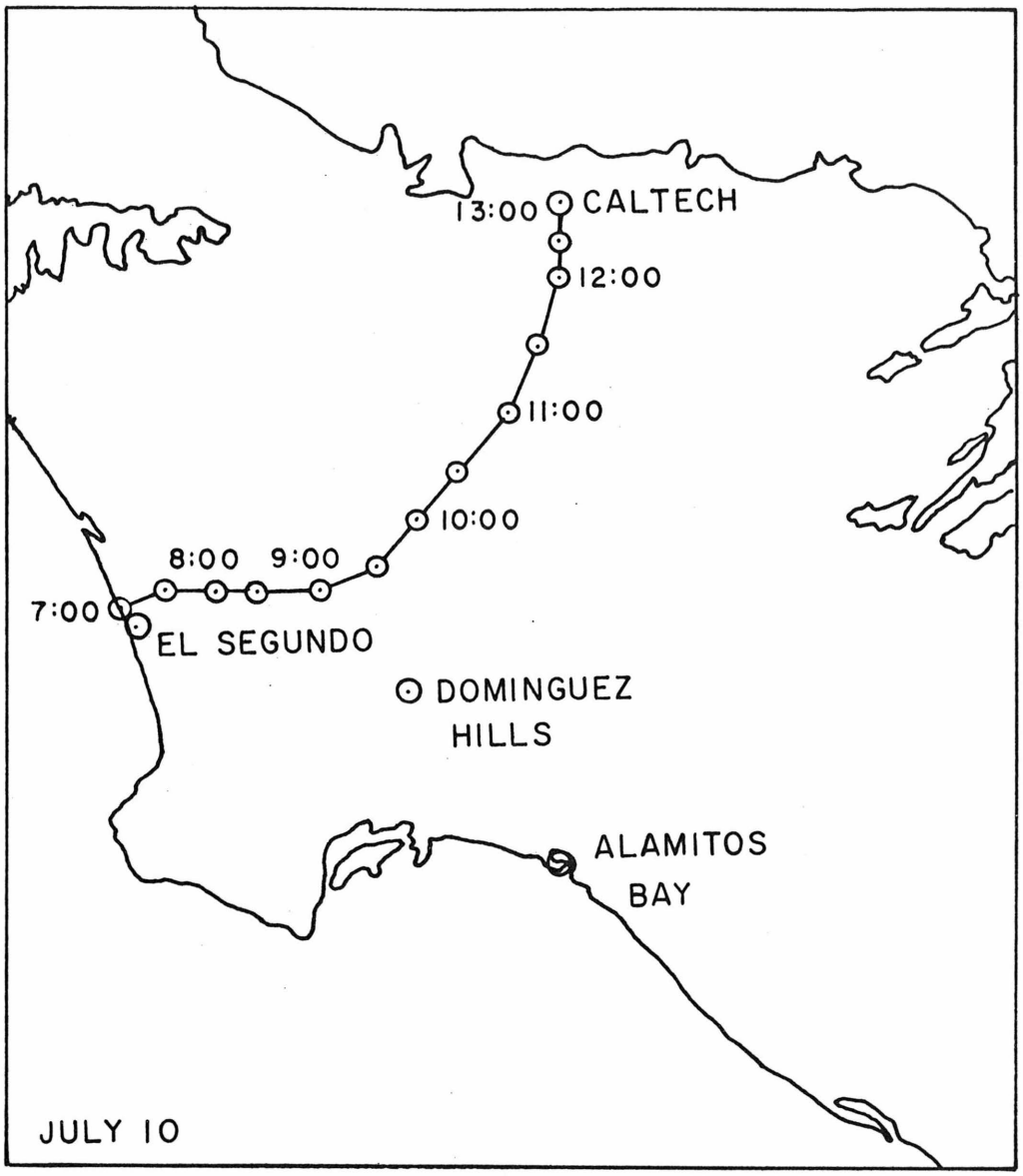

Figure B.1 Trajectory for 1300 PST Arrival at Caltech, July 10, 1973

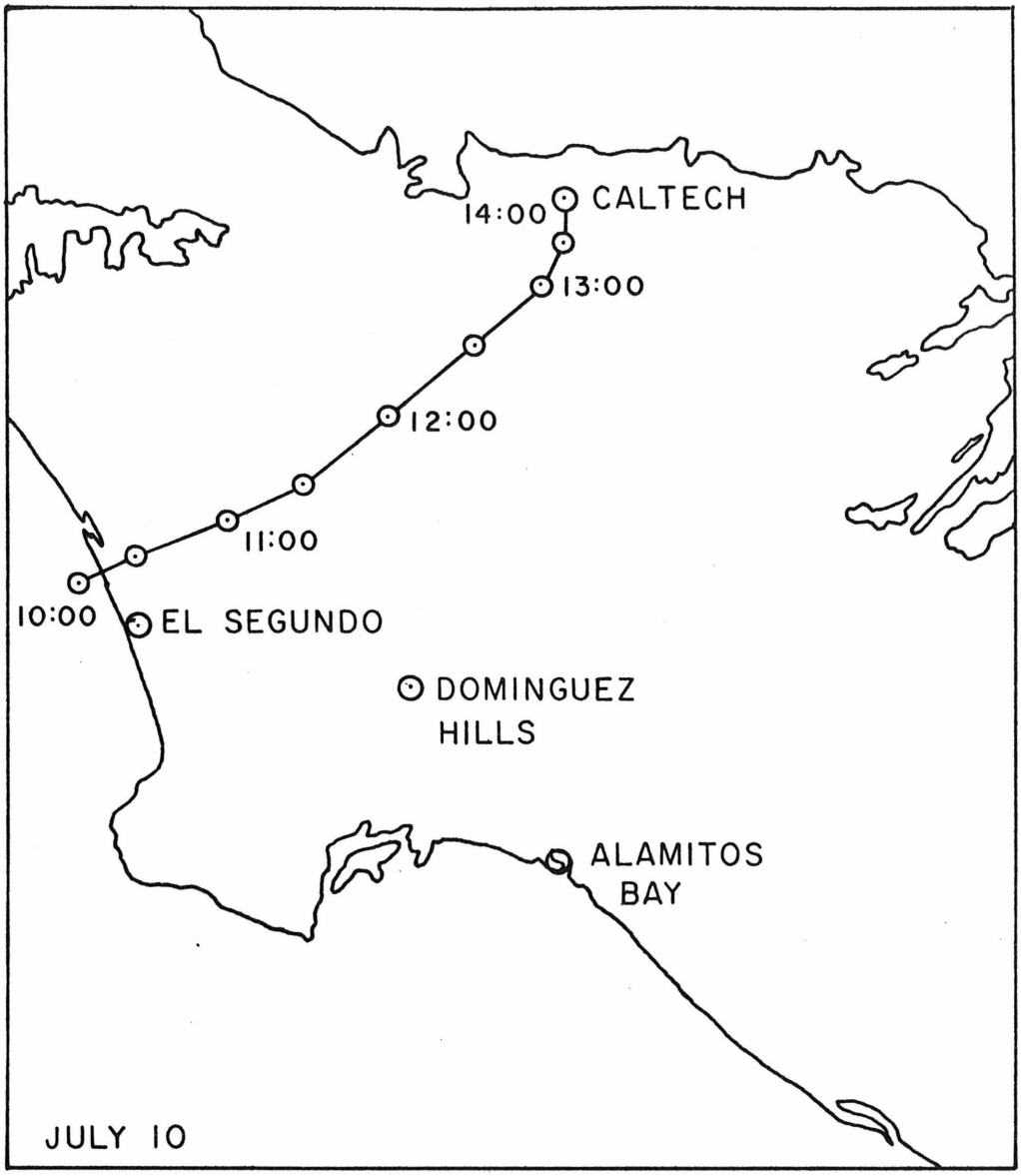

Figure B.2 Trajectory for 1400 PST Arrival at Caltech, July 10, 1973

Figure B.3 Trajectory for 1500 PST Arrival at Caltech, July 10, 1973

Figure B.4 Trajectory for 1600 PST Arrival at Caltech, July 10, 1973

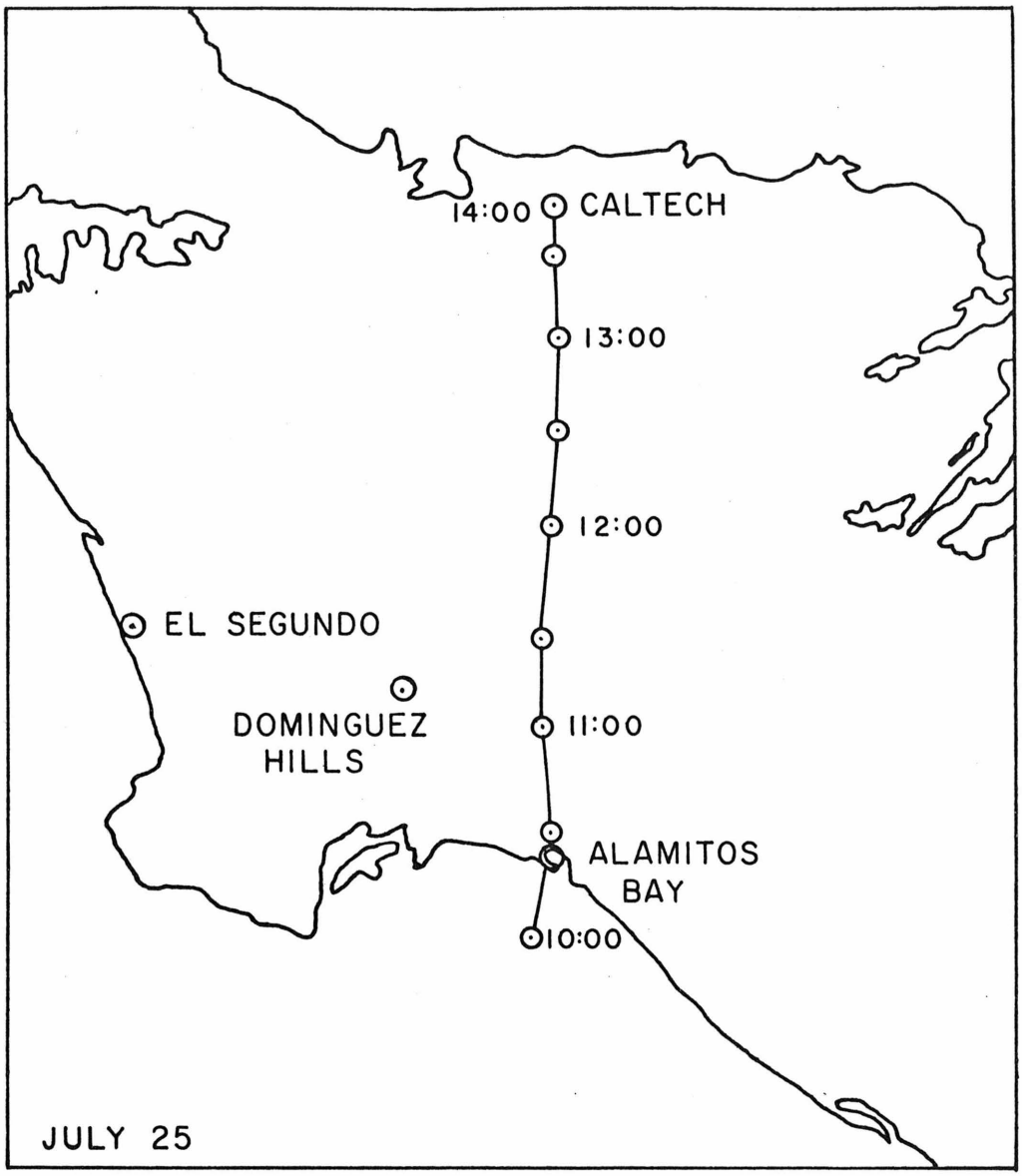

Figure B.5 Trajectory for 1400 PST Arrival at Caltech, July 25, 1973

Figure B.6 Trajectory for 1500 PST Arrival at Caltech, July 25, 1973

Figure B.7 Trajectory for 1600 PST Arrival at Caltech, July 25, 1973

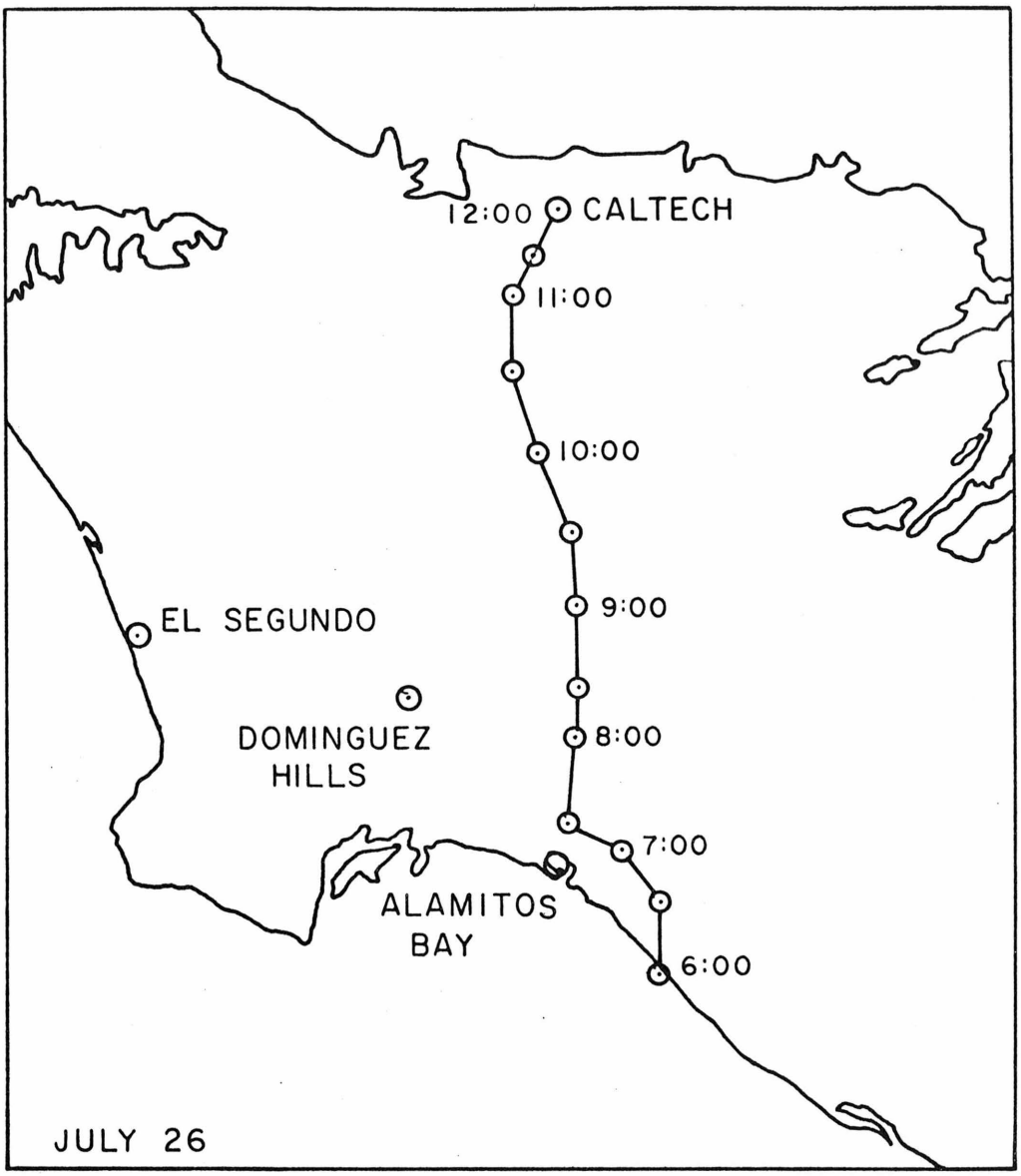

Figure B.8 Trajectory for 1200 PST Arrival at Caltech, July 26, 1973

Figure B.9 Trajectory for 1300 PST Arrival at Caltech, July 26, 1973

Figure B.10 Trajectory for 1400 PST Arrival at Caltech, July 26, 1973

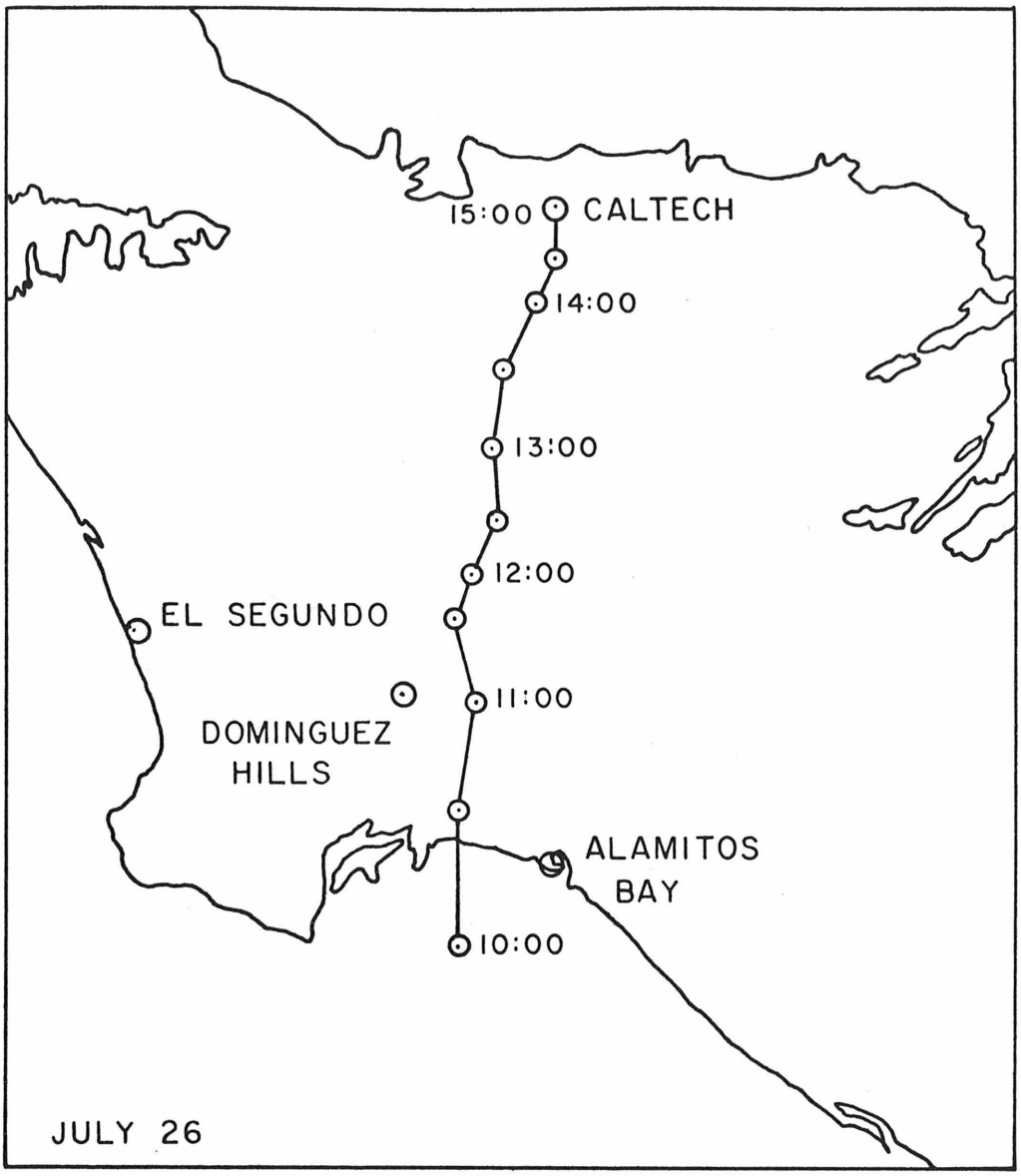

Figure B.11 Trajectory for 1500 PST Arrival at Caltech, July 26, 1973

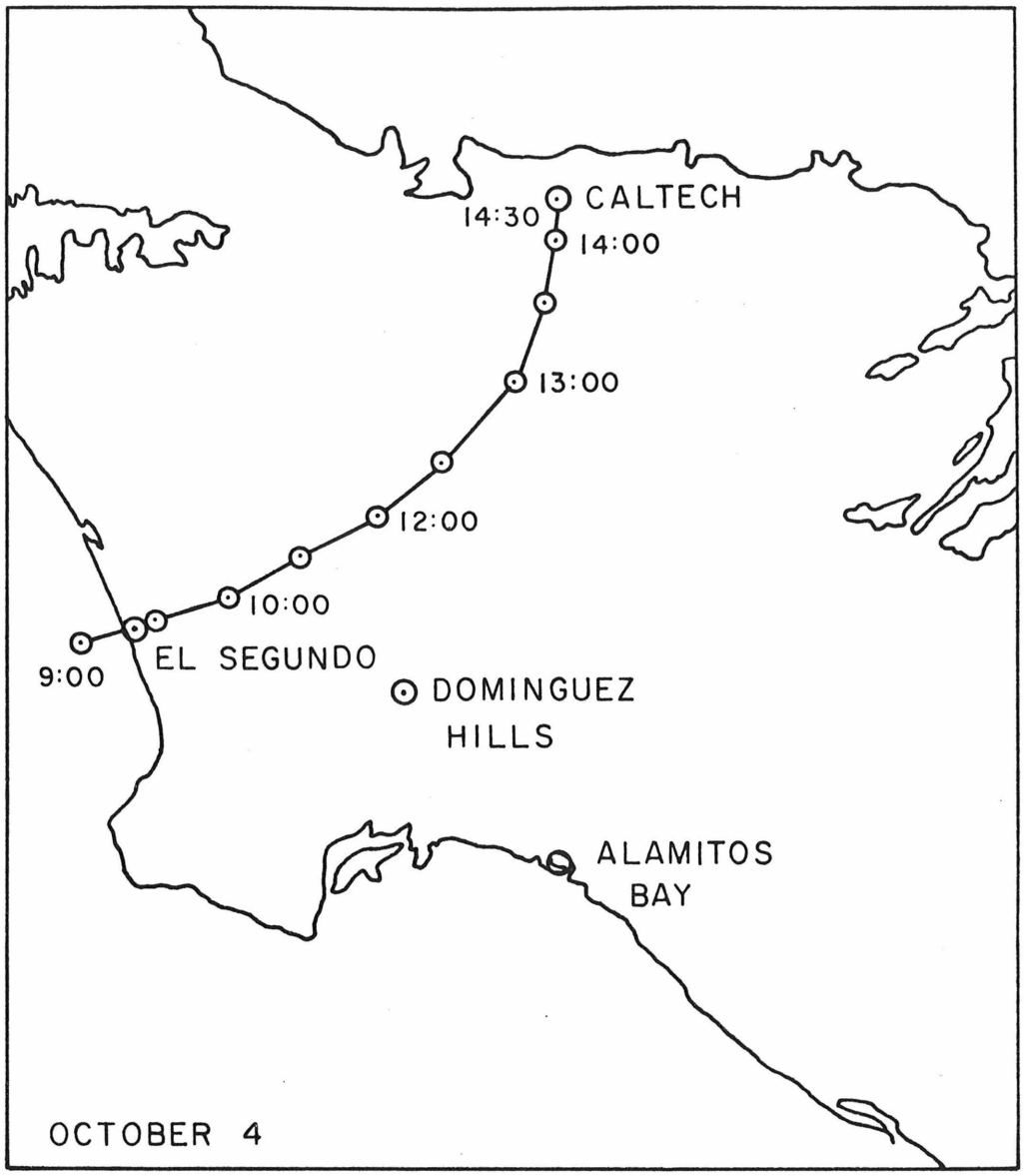

Figure B.12 Trajectory for 1430 PST Arrival at Caltech, October 4, 1973

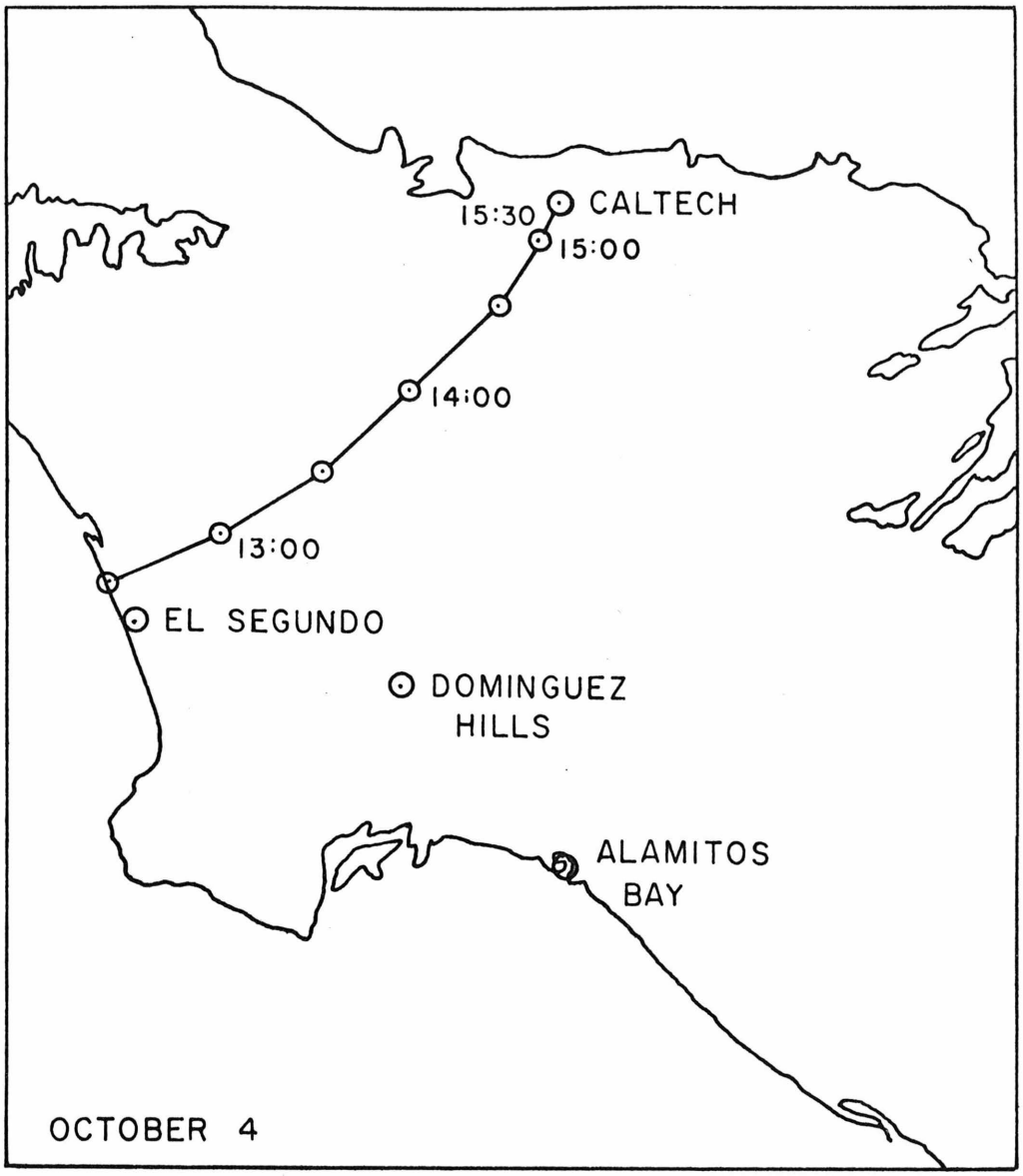

Figure B.13 Trajectory for 1530 PST Arrival at Caltech, October 4, 1973

Figure B.14 Trajectory for 1630 PST Arrival at Caltech, October 4, 1973

APPENDIX C

DESIGN AND CALIBRATION OF A LOW PRESSURE IMPACTOR

Many cascade impactors have been reported in the literature since the original study of May (1945). However, the smallest particle diameter that can be collected is about 0.25 μm (sonic velocity at the jet exit and 1 atmosphere upstream pressure). Stern, et al. (1962) and more recent investigators have used the slip correction factor to advantage by operating a cascade impactor at reduced pressure, thus allowing collection of particles smaller than 0.25 μm diameter. However, no investigator has used the low pressure impactor for atmospheric chemical analysis. Each investigator has only reported the design and calibration procedure and results. In the process of designing and constructing a low pressure cascade impactor, we observed the extreme sensitivity of the impactor cut-off sizes to the pressure at each stage. If there were small leaks in the impactor system (greater than 1 mm Hg), the cut-off size would change dramatically. Therefore, the pressure just upstream of the last stage of the impactor was monitored to ensure proper operation.

C.1 IMPACTOR DESIGN

Using impaction theory, the particle collection efficiency can be calculated from the particle diameter (d_p), the particle velocity (V), the particle density (ρ), the jet diameter (D_j), the gas viscosity (μ), and the geometry of the device (May, 1945). The efficiency (η) can be

represented by the impaction parameter (ψ), which can be written as:

$$\psi = \frac{C\rho V d_p^2}{18\ \mu D_j} \qquad (C.1)$$

Where C is the Cunningham slip correction factor, expressed as a function of particle diameter and the mean free path of the gas (λ):

$$C = 1 + 2\lambda/d_p[1.23 + 0.41\ \exp(-0.44d_p/\lambda)] \qquad (C.2)$$

At a fixed flow rate, the collection efficiency of a given stage depends on the particle diameter, assuming that there is no re-entrainment or bounce-off. It is common to use that particle size which is separated with an efficiency of 50% as a measure of the impactor stage performance. This particle size is called the 50% cut-off size, or d_{50}. The 50% cut-off size is associated with a value of the impaction parameter, ψ_{50}. Thus, Equation C.1 can be rewritten by replacing the jet velocity by the flow rate (Q, at STP, but then corrected to the lower pressure p) divided by the cross-sectional area of the jet:

$$\psi_{50} = \frac{2C\rho Q d_{50}^2}{9\mu D_j^3 \pi p} \qquad (C.3)$$

For jet velocity less than 1/3 Mach, the pressure (p) can be set equal to the pressure at the entrance side of the jet, since under these conditions the gas can be assumed to be incompressible. For impactor stages of similar geometric design, ψ_{50} is considered to be constant.

Values of ψ_{50} reported in the literature vary over a wide range, depending on the stage geometry in an unknown way. Therefore, a value

of ψ_{50} was determined from data on the 5-stage "Battelle" Impactor (Scientific Advances model CI-5). For stages 1 through 4 (jet velocities less than 1/3 Mach), the parameters needed for Equation C.3 were measured and the corresponding ψ_{50}'s were calculated (using the manufacturer's specified 50% cut-off sizes of 4.0, 2.0, 1.0, and 0.5 μm, respectively. The d_{50} for stage 4 was verified in Section C.2). The average 50% impaction parameter was 0.091 ± 0.012. Because the low pressure impactor had the same geometry as the "Battelle" Impactor, this value of ψ_{50} was used to calculate the 50% cut-off particle sizes for each of the stages. Data for the low pressure impactor are shown in Table C.1 for unit density, spherical particles.

C.2 EXPERIMENTAL VERIFICATION OF CUT-OFF SIZES

The impactor was calibrated with polystyrene latex spheres (density of 1.05 gm/cc) of diameter 0.088 μm to 0.716 μm by counting the collected spheres on successive stages with an electron microscope. The stage efficiency for a particular particle size was therefore the number collected on that stage, divided by the number on that stage plus all following stages. Because viewing the particles that passed through the last stage was not possible, we obtained no quantitative data for the efficiency of stage 4. However, since it operates in the same flow regime as the other stages, agreement between experiment and theory should be similar. A photograph of atmospheric particles collected on stage 4 shows many particles of diameter about 0.1 μm (Figure C.1). Figure C.2 shows the experimental efficiency curves for stages 2 and 3 of the low pressure impactor and stage 4 of the

TABLE C.1

Low Pressure Impactor Data*

Stage	D_j jet diameter (cm)	S jet-to-plate distance (cm)	S/D_j	p pressure (mm Hg)	d_{50}+ 50% cut-off (μm)
1	0.180	0.066	0.44	94	0.86
2	0.140	0.076	0.55	94	0.37
3	0.099	0.051	0.51	92	0.20
4	0.070	0.041	0.51	81	0.09

*Flow rate = 220 cc/min; restricting oriface diameter of 0.008 inch, length of 2. in; no after filter; atmospheric pressure = 755 mm Hg.

+for unit density spheres.

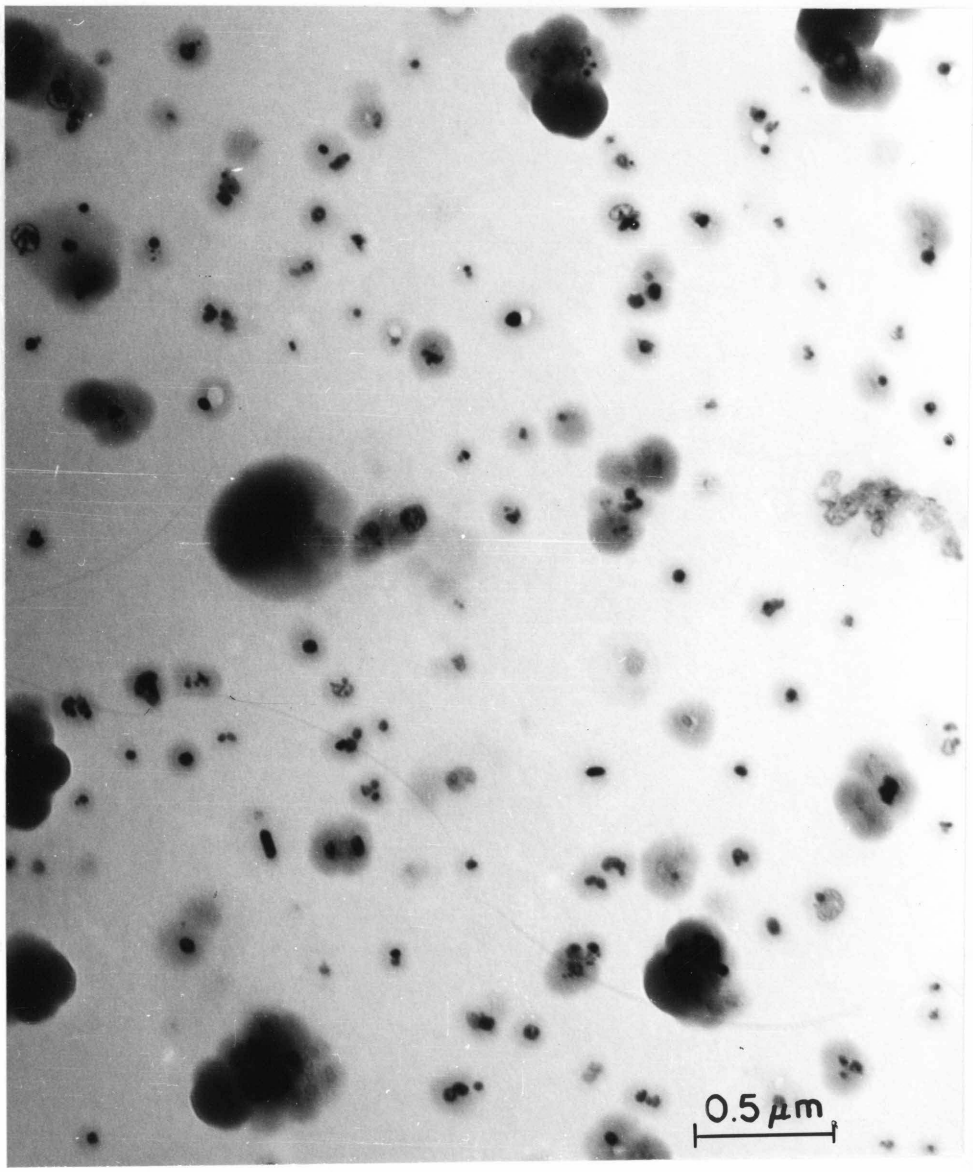

Figure C.1 Photograph of Atmospheric Particles Collected on Stage 4 of the Low Pressure Impactor (run without stages 2 and 3). Particle Diameters from 0.09 to 0.86 µm.

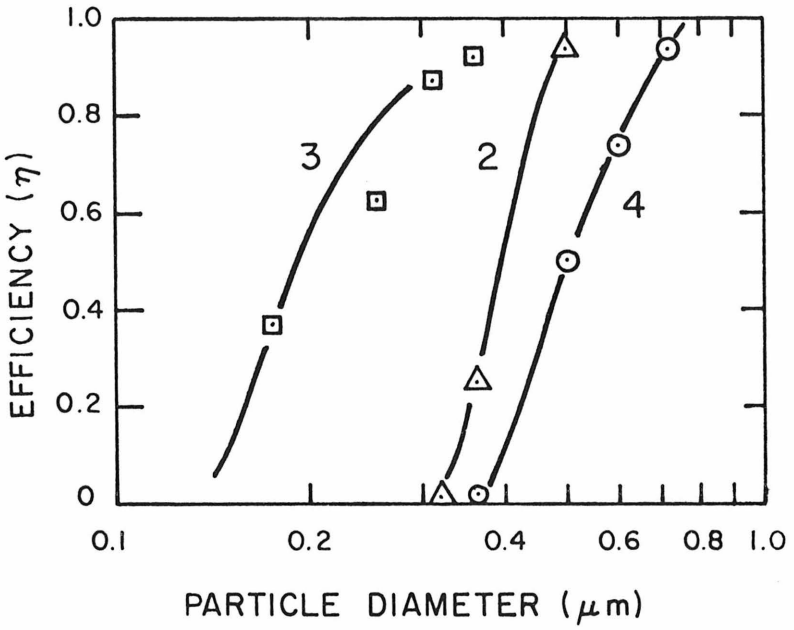

Figure C.2 Experimental Efficiency Curves for Stages 2 and 3 of the Low Pressure Impactor and Stage 4 of the "Battelle" Impactor

"Battelle" Impactor. The 50% cut-off values agree with those predicted theoretically by Equation C.3.

C.3 CONCLUSIONS AND RECOMMENDATIONS

A low pressure cascade impactor has been designed to collect particles of unit density down to 0.09 μm in diameter. The theoretically predicted 50% cut-off sizes have been experimentally verified using polystyrene latex spheres.

Use of this low pressure impactor (in Sections 4.6 and 5.1) has shown that a significant fraction of the aerosol sulfur is collected on stage 4 or passes through the impactor. Therefore, it is recommended that another impactor be designed to obtain better size resolution below 0.20 μm in particle diameter, using the design procedure discussed in Section C.2.

APPENDIX D

COMPUTER PROGRAMS

A listing of the computer programs is included in this Appendix. The programs and their function are:

GRACER: Calculates the automotive sulfur injected into a specified trajectory as a function of position along the trajectory.

LYNN: Calculates the pseudo-first order rate constant of SO_2 loss for a specified trajectory (using Equation 3.8).

LYNND: Calculates the pseudo-second order rate constant of SO_2 loss (first order in both SO_2 and O_3 concentration) for a specified trajectory (using Equation 3.12 and 3.8).

LDR: Calculates the variation of the pseudo-first order rate constant due to changes in the SO_2/S_T ratio at Pasadena and at the beginning of the trajectory.

LDR2: Calculates the variation of the pseudo-second order rate constant due to changes in the SO_2/S_T ratio at Pasadena and at the beginning of the trajectory.

SVR: Calculates the pseudo-first order rate constant with a fixed rate when the O_3 concentration is below 0.05 ppm (using Equation 3.13 and 3.8).

SCUBED: Calculates the aerosol sulfur and SO_2 concentrations and the SO_2/S_T ratio, plus errors, for direct analysis of total filters using the technique described in Chapter 2.

SQUARD: Calculates the aerosol sulfur and SO_2 concentration and the SO_2/S_T ratio, plus errors, for extraction analysis of total filters using the technique described in Chapter 2.

SMOOTH3: Draws both bar graph and calculated continuous sulfur size distributions for the low pressure impactor data.